Theses and Dissertations (ETD)　　　　　　　College of Graduate Health Sciences

12-2012

Anti-apoptotic MCL-1 Localizes to the Mitochondrial Matrix and Couples Mitochondrial Fusion to Respiration

Rhonda Perciavalle
University of Tennessee Health Science Center

Anti-apoptotic MCL-1 Localizes to the Mitochondrial Matrix and Couples Mitochondrial Fusion to Respiration

Abstract

MCL-1, an anti-apoptotic BCL-2 family member that is essential for the survival of multiple cell lineages, is also among the most highly amplified genes in cancer. Although MCL-1 is known to oppose cell death, precisely how it functions to promote survival of normal and malignant cells is poorly understood. Here, I report that different forms of MCL-1 reside in distinct mitochondrial locations and exhibit separable functions. On the outer mitochondrial membrane, a MCL-1 isoform acts like other anti-apoptotic BCL-2 molecules to antagonize apoptosis, whereas an amino-terminally truncated isoform of MCL-1 that is imported into the mitochondrial matrix is necessary to facilitate normal mitochondrial fusion, ATP production, membrane potential, respiration, cristae ultrastructure, and maintenance of oligomeric ATP synthase. My results provide insight into how MCL-1's surprisingly diverse salutary functions may control the survival of both normal and cancer cells.

Document Type

Dissertation

Degree Name

Doctor of Philosophy (PhD)

Program

Biomedical Sciences

Research Advisor

Joseph T. Opferman, Ph.D.

Keywords

Apoptosis, Cancer, Cell Death, MCL-1, Metabolism, Mitochondria

Subject Categories

Medical Genetics | Medical Sciences | Medicine and Health Sciences

Anti-apoptotic MCL-1 Localizes to the Mitochondrial Matrix and Couples Mitochondrial Fusion to Respiration

A Dissertation
Presented for
The Graduate Studies Council
The University of Tennessee
Health Science Center

In Partial Fulfillment
Of the Requirements for the Degree
Doctor of Philosophy
From The University of Tennessee

By
Rhonda Perciavalle
December 2012

DEDICATION

This dissertation is dedicated to my dear friend Josh Fielder and to every child at St. Jude fighting cancer, whose courage and strength inspire me to make the world a better place.

ACKNOWLEDGEMENTS

ABSTRACT

MCL-1, an anti-apoptotic BCL-2 family member that is essential for the survival of multiple cell lineages, is also among the most highly amplified genes in cancer. Although MCL-1 is known to oppose cell death, precisely how it functions to promote survival of normal and malignant cells is poorly understood. Here, I report that different forms of MCL-1 reside in distinct mitochondrial locations and exhibit separable functions. On the outer mitochondrial membrane, a MCL-1 isoform acts like other anti-apoptotic BCL-2 molecules to antagonize apoptosis, whereas an amino-terminally truncated isoform of MCL-1 that is imported into the mitochondrial matrix is necessary to facilitate normal mitochondrial fusion, ATP production, membrane potential, respiration, cristae ultrastructure, and maintenance of oligomeric ATP synthase. My results provide insight into how MCL-1's surprisingly diverse salutary functions may control the survival of both normal and cancer cells.

TABLE OF CONTENTS

LIST OF FIGURES

LIST OF ABBREVIATIONS

ß-TCRP	Beta-transducin repeat containing E3 ubiquitin protein ligase
Δ	Delta
µl	Microliter
µM	Micromolar
A1	BCL-2-related protein A1
ADP	Adenosine diphosphate
AKT	Protein kinase B
ALL	Acute lymphoblastic leukemia
AML	Acute myelogenous leukemia
APAF1	Apoptotic protease activating factor 1
ATP	Adenosine triphosphate
BAD	BCL-2 antagonist of cell death
BAK	BCL-2 antagonist/killer
BAX	BCL-2-associated x protein
BCL-2	B cell lymphoma 2
BCL-W	BCL-2-like protein 2
BCL-X	BCL-2-like protein 1
BCL-X$_L$	BCL-2-related gene, long isoform
BH	BCL-2 homology
BH3	BCL-2 homology 3
BID	BH3-interacting-domain death agonist
BIM	BCL-2-interacting mediator of cell death
BN-PAGE	Blue native polyacrylamide gel electrophoresis
BSA	Bovine serum albumin
CJ	Cristae junction
CLL	Chronic lymphocytic leukemia
CLP	Common lymphoid progenitor
ClpXP	Protease specificity-enhancing factor
CM	Cristae membrane
CML	Chronic myelogenous leukemia
CMP	Common myeloid progenitor
CNS	Central nervous system
CoA	Coenzyme A
CoQ	Cytochrome c oxidoreductase
C-terminal	Carboxyl-terminal
DCIP	2,6-dichlorophenolindophenol
DMEM	Dulbecco's modified eagle medium
DMSO	Dimethyl sulfoxide
DNA	Deoxyribonucleic acid
DRP1	Dynamin-related protein
dsRED	Discosoma sp. red fluorescent protein
DTT	Dithiothreitol
E	Embryonic day

EDTA	Ethylene diaminetetraacetic acid
EGTA	Ethylene glycol bis-(2-amino-ethylether)-N, N, N', N′-tetraacetic
ER	Endoplasmic reticulum
ETC	Electron transport chain
FADD	FAS-associated death domain
FBS	Fetal bovine serum
FBW7	F-box and WD repeat domain containing 7, E3 ubiquitin protein ligase
FCCP	Carbonylcyanide-p-trifluoromethoxyphenylhydrazone
GFP	Green fluorescent protein
GMP	Granulocyte monocyte progenitor
GSK-3	Glycogen synthase kinase 3
HBSS	Hank's balanced saline solution
HECT	Homologous to the E6-AP carboxyl terminus
HEPES	4-(2-hydroxyethyl)-1-piperazineethanesulfonic acid
HM	Heavy membrane
HSC	Hematopoietic stem cell
IBM	Inner boundry membrane
IF1	Inhibitory factor 1
IgG	Immunoglobulin G
IL	Interleukin
IMM	Inner mitochondrial membrane
IMS	Inner membrane space
JAK	Janus kinase
JNK	c-Jun N-terminal kinases
kD	Kilodalton
LON	Lon peptidase
MAP	Mitogen-activated protein
MCL-1	Myeloid cell leukemia 1
MEF	Mouse embryonic fibroblast
MFN	Mitofusin
MgCl2	Magnesium chloride
MIB	Mitochondrial isolation buffer
MnSOD	Manganese superoxide dismutase
Mx1	Interferon-induced GTP-binding protein
NAD+	Nicotinamide adenine dinucleotide
NADPH	Nicotinamide adenine dinucleotide phosphate
NK	Natural Killer
PDH	Pyruvate dehydrogenase
PEST	Proline, glutamine, serine, and threonine
PI	Propidium Iodide
PI3K	Phosphoinositide 3 kinase
PMS	Phenazine methosulphate
PMSF	phenylmethanesulfonylfluoride
PUMA	P53-upregulated modulator of apoptosis
PVDF	Polyvinylidene fluoride

RNA	Ribonucleic acid
RNAi	Ribonucleic acid interference
ROS	Reactive oxygen species
SCF	Stem cell factor
SDS-PAGE	Sodium dodecyl sulfate polyacrylamide gel electrophoresis
Ser	Serine
STAT	Signal transducer and activator of transcription
SV40	Simian virus 40
TIM	Translocase of inner membrane
TOM	Translocase of outer membrane
TNF	Tumor Necrosis Factor
TPA	12-O-tetradecanoylphorbol-13-acetate
USP9X	Ubiquitin specific peptidase 9, X-linked
UV	Ultraviolet

CHAPTER 1. INTRODUCTION

The BCL-2 Family Proteins and Apoptosis

Apoptosis is an essential genetic program required in the regulation of development and maintenance of homeostasis of animals. Dysregulation of apoptosis can lead to a variety of human pathologies, including cancer, neurodegenerative, and autoimmune diseases (Cory and Adams, 2002). Two programs that regulate apoptosis merge to induce the activation of caspases, which are proteases responsible for the demise of a cell. The extrinsic pathway involves the ligation of death receptors on the surface of the cell. The death receptors (members of the tumor necrosis factor receptor superfamily) contain an intracellular death domain that recruits and activates Caspase-8 (Youle and Strasser, 2008). Caspase-8 is recruited through the adaptor protein Fas-associated death domain (FADD), resulting in subsequent activation of effector caspases, such as Caspase-3 (Youle and Strasser, 2008).

In many cell types, the extrinsic pathway for cell death does not involve BCL-2 family members or mitochondrial outer membrane permeabilization. The intrinsic cell death pathway, however, is regulated by BCL-2 family members and focuses much of its effort at the level of the mitochondria (Chipuk et al., 2010). It consists of both pro and anti-apoptotic members that share a homology within four conserved regions called BCL-2 homology domains (BH), which correspond to α-helical segments (Danial and Korsmeyer, 2004; Opferman, 2008) (**Fig. 1.1**). Anti-apoptotic BCL-2 family members (such as BCL-2, BCL-X$_L$, BCL-W, MCL-1, and A1) share all four BH domains and possess a hydrophobic binding pocket that binds the BH3 domain of other family members (**Fig. 1.1**). The pro-apoptotic BCL-2 family members can be subdivided into two groups, the multidomain pro-apoptotic effectors (such as BAX and BAK) which have three BH domains and the BH3-only molecules (such as BID, BAD, BIM, PUMA, NOXA, etc.) which reside upstream of BAX/BAK activation (Cheng et al., 2001) (**Fig. 1.1**). Death signals activate and/or induce the BH3-only molecules through either transcriptional regulation or post-translational modification (Chipuk et al., 2010). The activated BH3 only proteins subsequently promote BAX and BAK oligomerization; a process antagonized by anti-apoptotic BCL-2 family members (Cheng et al., 2001) (**Fig. 1.2**). Activation and oligomerization of BAX/BAK results in mitochondrial outer membrane permeabilization (MOMP) that releases a variety of apoptogenic proteins, such as cytochrome *c,* from the mitochondrial intermembrane space (Goldstein et al., 2000) (**Fig. 1.2**). Cytochrome *c* then binds to APAF-1, changing its conformation so that it can recruit Caspase-9. Once Caspase-9 is bound to APAF-1 it can activate itself. The active Caspase-9 then cleaves the effector caspases, such as Caspase-3, resulting in the orderly demise of a cell (Opferman and Korsmeyer, 2003) (**Fig. 1.2**).
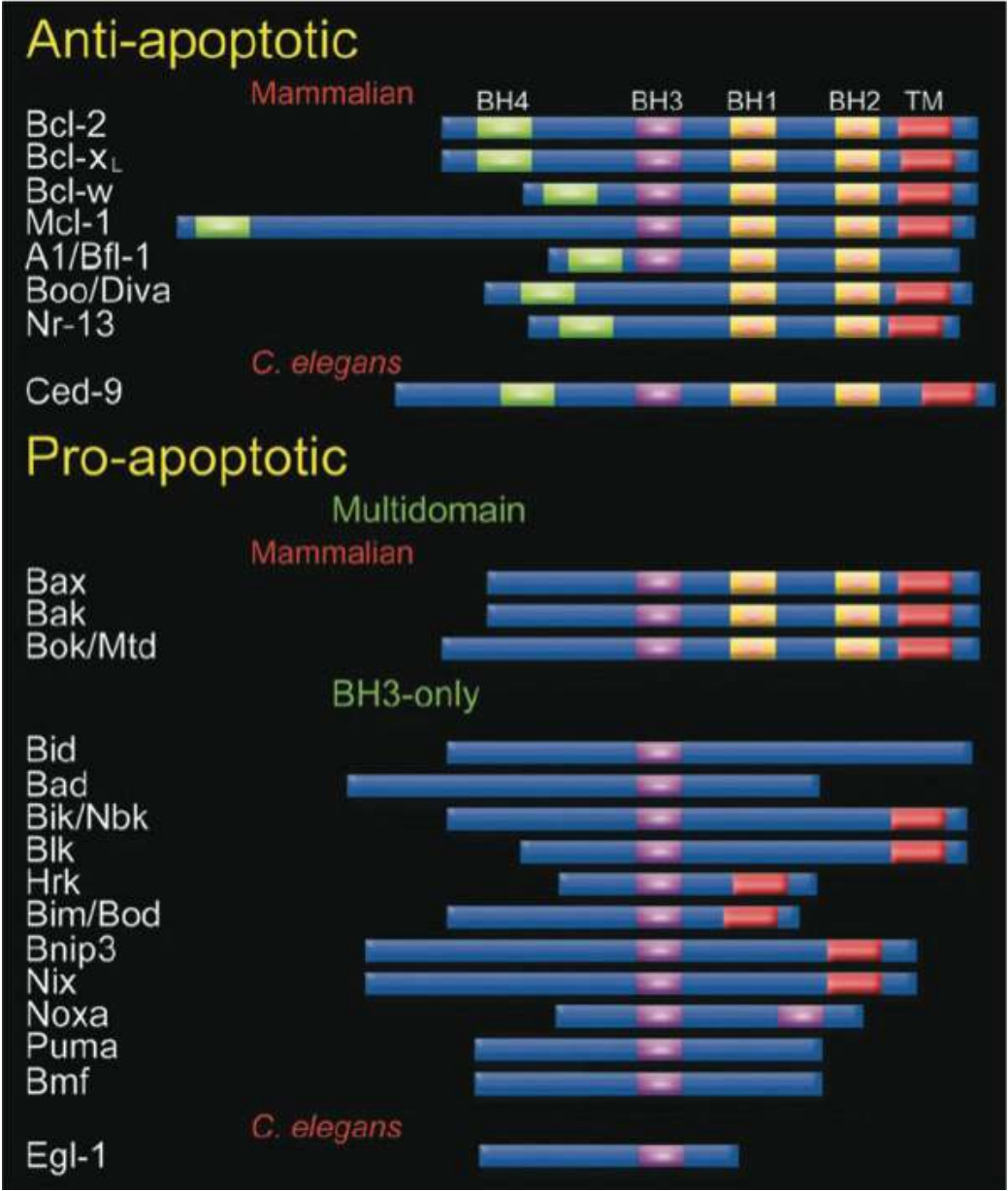
Figure 1.1.   The BCL-2 Family
Reprinted by permission from Macmillan Publishers Ltd: Opferman, J.T., and
Korsmeyer, S.J. (2003). Apoptosis in the development and maintenance of the immune
system. Nat Immunol *4*, 410-415.
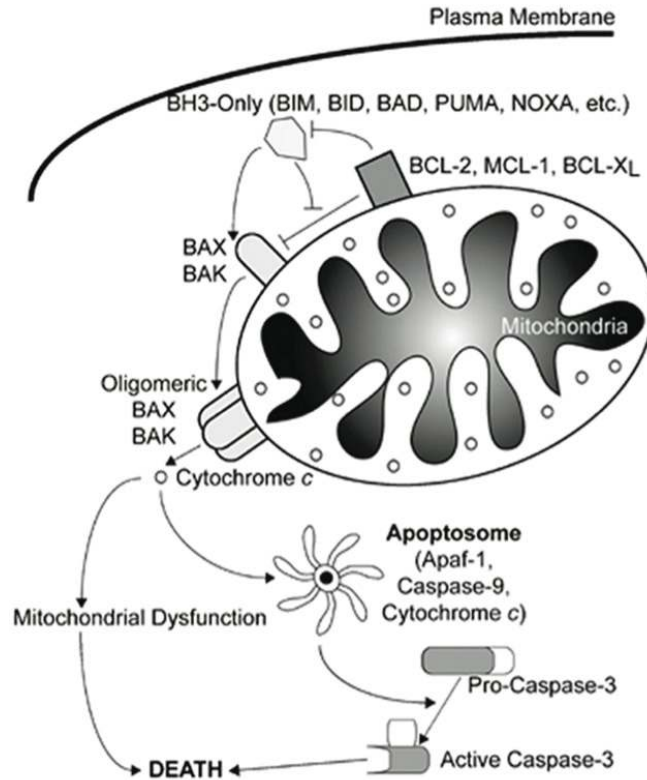
Figure 1.2.   BCL-2 Family Mediated Apoptosis
The BCL-2 family integrates death signals from a variety of sources and regulates
mitochondria-dependent apoptosis. BH3-only family members act as sentinels for many
death stimuli and can be regulated by transcriptional and post-translational mechanisms,
allowing rapid response to changing cellular conditions. They can be directly sequestered
by antiapoptotic BCL-2 family members (e.g. BCL-2, BCL-X$_L$, MCL-1, etc.). Upon
sufficient activation, BH3-only family members can mediate the activation of the
multidomain proapoptotics BAX and BAK either by a 'hit and run' interaction or by
relieving antiapoptotic antagonism of BAX and BAK allowing oligomerization. Upon
BAX and BAK oligomerization, the mitochondrial outer membrane is permeabilized
releasing a variety of apoptogenic substrates from the mitochondrial intermembrane
space, such as cytochrome c, into the cytosol. Released cytochrome c can complex with
APAF1 and Pro-Caspase-9 to form the apoptosome, which catalyzes Caspase-9
activation. Activated Caspase-9 can then trigger the activation of a downstream caspase
cascade leading to cell death. Reprinted by permission from Macmillan Publishers Ltd:
Opferman, J.T. (2008). Apoptosis in the development of the immune system. Cell Death
Differ *15*, 234-242.

Anti-apoptotic MCL-1

Mcl-1 was initially identified as an early-induced gene during TPA induced differentiation in a human myeloid leukemia cell line (ML-1) (Kozopas et al., 1993). MCL-1 shares sequence homology to BCL-2 in the carboxy-terminal region where it contains three amphipathic alpha-helical segments; however, its amino-terminal region is poorly conserved (Kozopas et al., 1993). The amino-terminus of MCL-1 is much longer than that of any other anti-apoptotic BCL-2 family member and contains two PEST sequences (Kozopas et al., 1993). In addition, at the carboxy-terminal end, it possesses a membrane spanning domain consisting of 20 hydrophobic amino acids, flanked by charged residues similar to BCL-2 (Kozopas et al., 1993). Deletion of either the amino- or carboxy-terminus of MCL-1 does not disrupt its ability to bind pro-apoptotic molecules (Day et al., 2005).

During murine embryogenesis, MCL-1 expression is rapidly induced after fertilization and peaks during the 2-cell through 8-cell stages and then decreases in blastocysts (Sano et al., 2000). MCL-1 is expressed in human epithelial cells of the skin, gastrointestinal tract, and pulmonary tissues, in cardiomyocytes, skeletal muscle, hematopoietic cells, lymphocytes, uterus, adrenal cortex, sympathetic ganglia, pancreatic islets, and hepatocytes (Krajewski et al., 1995). MCL-1 expression is also regulated by growth factor signaling. Both mature lymphocytes and immature progenitors increase MCL-1 expression in response to IL-7 stimulation (Opferman et al., 2003). Hematopoietic stem cells also increase *Mcl-1* mRNA after exposure to stem cell factor (SCF) and IL-6 (Opferman et al., 2005). Conversely, withdrawal from IL-3 in BAF/3 cells results in decreased MCL-1 expression (Maurer et al., 2006).

MCL-1 is predominantly localized to the mitochondrial membrane, with some distribution also detectable in ER membranes (Germain and Duronio, 2007; Yang et al., 1995). Membrane association of MCL-1 depends on the presence of its hydrophobic carboxy-terminus which serves as a transmembrane domain (Yang et al., 1995). The amino-terminus of MCL-1 also regulates its association with mitochondrial membranes; however, the underlying mechanism is unclear (Germain and Duronio, 2007). Additionally, several reports claim that MCL-1 is localized both to the mitochondria and the nucleus, where it interacts with PCNA and inhibits cells from progressing through S-phase (Fujise et al., 2000).

MCL-1 Anti-apoptotic Function

In-vitro binding assays with recombinant anti-apoptotic BCL-2 family members and peptides corresponding to the BH3 domains of pro-apoptotic molecules demonstrate that MCL-1 selectively binds pro-apoptotic family members (Chen et al., 2005b). MCL-1 displays selective binding for pro-apoptotic molecules BIM, PUMA, NOXA, and BAK but does not interact with BAD (Chen et al., 2005b; Opferman et al., 2003). Interestingly, *in-vitro* competitive binding assays indicate that MCL-1 and A1 are the only anti-apoptotic family members with the ability to interact with NOXA (Chen et al.,

2005b). Moreover, BAK selectively interacts with MCL-1 and BCL-X but not BCL-2 (Chen et al., 2005b). The interaction between MCL-1 and BAK has also been confirmed by co-immunoprecipitation of proteins derived from mitochondria (Willis et al., 2005). Another report indicated that MCL-1 interacts with BAX, where it protects hematopoietic cells from apoptosis under a variety of death stimuli including etoposide, UV irradiation, and growth factor withdrawal (Zhou et al., 1997).

MCL-1 and Cell Survival

BCL-2 family members play specific roles in regulating homeostasis during various stages of hematopoiesis (**Fig. 1.3**). The roles of anti-apoptotic BCL-2 family members during hematopoiesis have been identified through loss of function studies. *Bcl-2*-deletion results in viable mice that display an increase in apoptosis of mature B and T lymphocytes after 3 weeks of age (Veis et al., 1993). *Bcl-X$_L$*-deficient embryos die at embryonic day 13 due to neuronal and erythroid defects (Motoyama et al., 1995). Conditional deletion of *Bcl-X$_L$* in the erythroid lineage results in severe anemia and reduces the number of red blood cells significantly, indicating that BCL-X$_L$ is important during erythropoiesis (Wagner et al., 2000).

MCL-1 is unique among pro-survival BCL-2 molecules in that it is essential for early (E3.5) embryonic development and also has a critical role during multiple stages of hematopoiesis and lymphopoiesis (Rinkenberger et al., 2000) (**Fig. 1.3**). Conditional deletion of *Mcl-1* during early thymocyte development, using Lck-Cre, results in no viable, mature, deleted T cells (Opferman et al., 2003). Additionally, deletion of *Mcl-1* during early B cell development, using CD19-Cre, results in death at the pro-B stage (Opferman et al., 2003). This suggests that MCL-1 is critical for the development of lymphocytes. Furthermore, MCL-1 is also required for the maintenance of mature lymphocytes (Dzhagalov et al., 2008; Opferman et al., 2003).

MCL-1 is also essential during the early stages of hematopoiesis (**Fig. 1.3**). Inducible deletion of *Mcl-1* in hematopoietic lineages results in rapid hematopoietic failure (Opferman et al., 2005). The earliest populations lost are the hematopoietic stem cells (HSCs), common myeloid progenitors (CMPs), and common lymphoid progenitors (CLPs) (Opferman et al., 2005). Moreover, during myelopoiesis, MCL-1 is required for the differentiation of granulocyte precursors to mature neutrophils (Dzhagalov et al., 2007; Steimer et al., 2009). In contrast, deletion of *Mcl-1* in the myeloid lineage does not block the development of mature macrophages but is important for survival during effector function (Dzhagalov et al., 2007; Steimer et al., 2009). These data underscore an essential role for MCL-1 in promoting the survival and differentiation of many hematopoietic lineages.

In addition to hematopoiesis, MCL-1 is also required during the development of the central nervous system (CNS) (Arbour et al., 2008). Conditional deletion of *Mcl-1* in the forebrain results in embryonic lethality at day 15, whereas, deleting *Mcl-1* earlier in CNS development results in lethality at embryonic day 12.5 (Arbour et al., 2008).
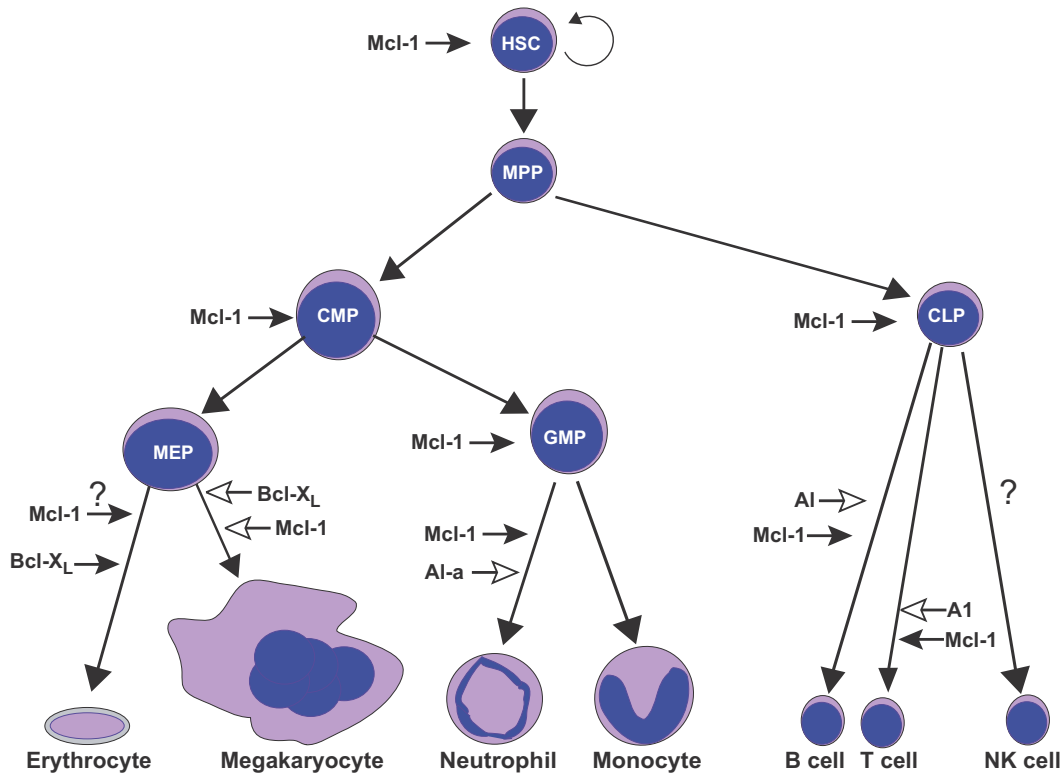
Figure 1.3.   Apoptotic Checkpoints during Hematopoiesis
All blood cell lineages arise from a hematopoietic stem cell (HSC) that is capable of self-renewal and has an indefinite life-span. HSCs give rise to multi-potent progenitors (MPPs) which still retain the ability to give rise to all blood cell lineages, but lack long-term self-renewal capacity. MPPs can produce two progenitors, common myeloid progenitors (CMPs) and common lymphoid progenitors (CLPs). CLPs can produce the lymphoid lineages (B, T, and perhaps NK cells). CMPs produce at least two other oligopotent progenitor populations, the megakaryocyte erythroid progenitor (MEP) that produce red blood cells (erythrocytes), megakaryocytes (generates platelets), and the granulocyte monocyte progenitor (GMP), which produces neutrophils and macrophages. Listed beside each differentiation step or progenitor population are the known anti-apoptotic regulators that promote the survival of the given population. Anti-apoptotic MCL-1 has multiple checkpoints as has been illustrated to be critical for the survival of several multipotent and oligopotent progenitor populations (HSC, CMP, CLP, and GMP) and has been shown to be critical for the differentiation of granulocytes, but interestingly not the monocyte lineage. A1-A, a murine ortholog of BFL-1, has also been shown to play an important role in promoting neutrophil survival in response to stress, but is not absolutely required for survival (indicated by open arrowhead). In the erythroid lineage, BCL-X_L is the essential survival molecule, but unpublished data indicates that MCL-1 may also play an essential role during early differentiation. In the megakaryocytic lineage it appears that while neither MCL-1 nor BCL-X_L is solely responsible for survival, the two pro-survival molecules appear to have overlapping functions (indicated by open arrowheads) in promoting megakaryocyte survival. The critical anti-apoptotic regulators of some lineages including NK cells are still uncertain.

MCL-1 Regulation

Mcl-1 is regulated at the transcriptional, translational, and post-translational levels. Growth factors and cytokines including interleukin-2 (IL-2), interleukin-7 (IL-7), and granulocyte-macrophage colony-stimulating factor (GM-CSF) induce *Mcl-1* transcription (Opferman et al., 2005; Opferman et al., 2003; Wang et al., 1999). Likewise, a variety of signaling pathways including MAP kinases, PI3K/Akt, and JAK/STAT modulate elements in *Mcl-1*'s promoter to increase transcription (Huang et al., 2000; Wang et al., 1999). In addition, *Mcl-1* mRNA translation is regulated by mTORC1 (Mills PNAS 2008).

MCL-1 protein expression is tightly regulated at the post-translational level. MCL-1 phosphorylation in response to cellular signaling is a critical control point for regulating its anti-apoptotic function. However, there is evidence of phosphorylation both promoting and inhibiting MCL-1 anti-apoptotic activity depending on the type of death stimuli. For example, oxidative stress promotes JNK-mediated phosphorylation of human MCL-1 at two residues (Ser-121 and Thr-163) resulting in a loss of anti-apoptotic function (Inoshita et al., 2002). In contrast, phosphorylation at the same residue (Thr-163) blocks ubiquitinylation, thus, extending the protein half-life and cellular survival (Domina et al., 2000; Li et al., 2007). MCL-1 phosphorylation is also potently regulated by growth factor availability. For example, cytokine withdrawal results in phosphorylation of *MCL-1* on Ser-159 by GSK-3 thereby facilitating its degradation (Maurer et al., 2006).

The short half-life (~2 hours) of MCL-1 distinguishes it from other anti-apoptotic BCL-2 family members; the amino-terminus possess several proline-glutamic acid-serine-threonine (PEST) regions, a common feature of rapidly degraded proteins. Nevertheless, the PEST regions are dispensable for MCL-1 protein turnover (Akgul et al., 2000). MCL-1 undergoes both ubiquitin-dependent and ubiquitin-independent degradation (Stewart et al., 2010a; Zhong et al., 2005). Three E3 ligases have been implicated in MCL-1 ubiquitinylation. The HECT-domain containing MULE targets MCL-1 for degradation by the proteosome (Zhong et al., 2005). Whether MULE-dependent ubiquitinylation of MCL-1 occurs in healthy cells or apoptotic cells remains controversial (Hao et al., 2012; Zhong et al., 2005). Both ß-TRCP and FBW7 are SKP1-cullin-1-F-box (SCF) complex E3 ligases that ubiquitinylate MCL-1 in a phosphorylation-dependent manner (Ding et al., 2007; Inuzuka et al., 2011). Furthermore, the deubiquitinase, USP9X, binds to MCL-1 and removes polyubiquitin chains, thus, stabilizing MCL-1 protein levels (Schwickart et al., 2010).

MCL-1 and Cancer

Dysregulated MCL-1 expression can inappropriately promote cell survival. For example, transgenic expression of *MCL-1* in mice can lead to tumorigenesis and hyperplasia (Matsushita et al., 2003; Zhou et al., 2001). MCL-1 is overexpressed and often associated with chemotherapeutic resistance in many different cancers including

acute lymphoblastic leukemia (ALL), acute myelogenous leukemia (AML), chronic myelogenous leukemia (CML), chronic lymphocytic leukemia (CLL), and multiple myeloma, (Kaufmann et al., 1998; Pepper et al., 2008; Wei et al., 2006). In addition, MCL-1 is upregulated in a variety of solid tumors including hepatocellular carcinoma, pancreatic cancer, testicular cancer, cervical cancer, lung cancer, and melanoma (Chung et al., 2002; Sano et al., 2005; Sieghart et al., 2006; Song et al., 2005; Zhuang et al., 2007). Furthermore, the *MCL-1* locus is frequently amplified in human cancers (Beroukhim et al., 2010). The expanding variety of malignancies that display high levels of MCL-1 expression illustrate the importance of understanding how MCL-1 expression and function are regulated.

Cancer cells often violate a number of cellular checkpoints including cell cycle arrest and the induction of apoptosis. For that reason, they often become dependent on anti-apoptotic molecules to bypass programmed cell death (Certo et al., 2006). As a result, small molecules that antagonize these pro-survival molecules have been developed as a therapeutic approach. ABT-737 is a small molecule that inhibits BCL-2 and BCL-X_L and promotes cell death. However, high levels of MCL-1 can contribute to resistance to ABT-737 (Certo et al., 2006). Consequently there has been much effort to find a small molecule that is capable of blocking the protective effects of MCL-1(Nguyen et al., 2007).

Dynamic Structure of Mitochondria

Mitochondria are dynamic organelles constantly undergoing fission and fusion to maintain a cellular network important for their function (Detmer and Chan, 2007) (**Fig. 1.4**). Under normal conditions, fission and fusion are balanced to support normal mitochondrial morphology; however, the disturbance of this equilibrium leads to dramatic alterations in their shape. For example, increases in fusion result in elongated mitochondria that are extremely interconnected (Smirnova et al., 2001) (**Fig. 1.5**). Conversely, cells with a high fission rate produce many small, fragmented mitochondria (Chen et al., 2003) (**Fig. 1.5**).

Internal Structure of Mitochondria

Mitochondria possess a selectively-permeable outer membrane and an inner membrane consisting of a larger surface area that folds and forms invaginations called cristae (Frey and Mannella, 2000). The two membranes surround two aqueous spaces, the matrix, where the TCA cycle enzymes and mitochondrial genome are located, and the intermembrane space, where cytochrome *c*, resides. Recent advances in electron microscopy techniques have revealed that the mitochondrial inner membrane can be subdivided into distinct domains: the inner boundary membrane, the cristae membrane, and the cristae junctions (Frey and Mannella, 2000) (**Fig. 1.6**). The inner boundary membrane consists of the areas where the inner membrane juxtaposes to the outer membrane; whereas the cristae membrane entwines and extends, increasing the surface area of the inner membrane (Mannella, 2006). The cristae junctions are constricted
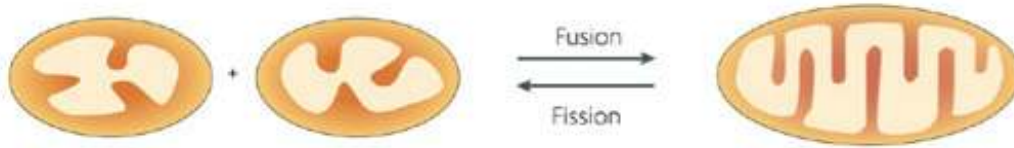
Figure 1.4.   Mitochondrial Dynamics

Mitochondrial fusion and fission control mitochondrial number and size. With fusion, two mitochondria become a single larger mitochondrion with continuous outer and inner membranes. Conversely, a single mitochondrion can divide into two distinct mitochondria by fission. Reprinted by permission from Macmillan Publishers Ltd: Detmer, S.A., and Chan, D.C. (2007). Functions and dysfunctions of mitochondrial dynamics. Nat Rev Mol Cell Biol *8*, 870-879.
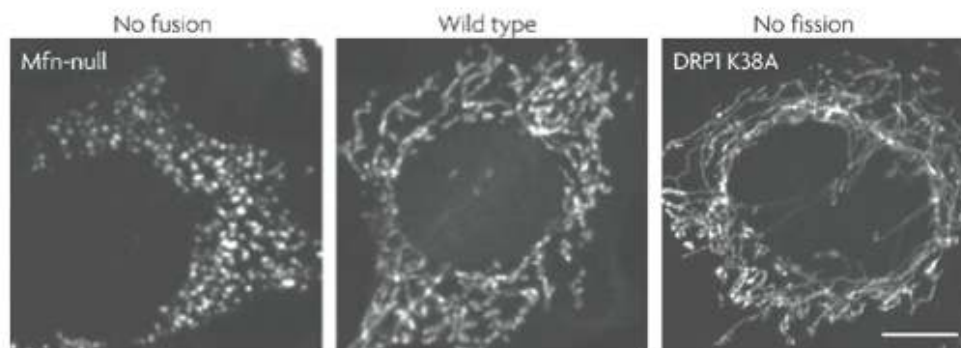
Figure 1.5.   Mitochondrial Morphology

Mitochondrial length, size and connectivity are determined by the relative rates of mitochondrial fusion and fission. In wild-type cells (shown in the central panel), mitochondria form tubules of variable length. In the absence of mitochondrial fusion (for example, in mitofusin (*Mfn*)-null cells (shown in the left panel), which lack MFN1 and MFN2), unopposed fission results in a population of mitochondria that are all fragmented. Conversely, decreased fission relative to fusion, for example, in DRP1 K38A cells (shown in the right panel), which have a dominant-negative form of dynamin-related protein-1 (DRP1), results in elongated and highly interconnected mitochondria. Scale bar represents 10 μm. Reprinted by permission from Macmillan Publishers Ltd: Detmer, S.A., and Chan, D.C. (2007). Functions and dysfunctions of mitochondrial dynamics. Nat Rev Mol Cell Biol *8*, 870-879.
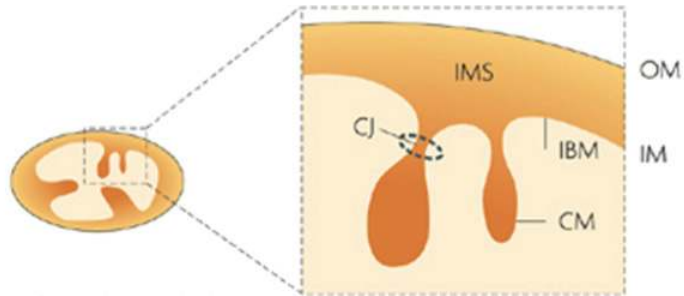
Figure 1.6.   Mitochondrial Ultrastructure
The diagram indicates the different regions of the inner membrane. CJ, cristae junction; CM, cristae membrane; IBM, inner boundary membrane; IM, inner membrane; IMS, intermembrane space; OM, outer membrane. Reprinted by permission from Macmillan Publishers Ltd: Detmer, S.A., and Chan, D.C. (2007). Functions and dysfunctions of mitochondrial dynamics. Nat Rev Mol Cell Biol 8, 870-879.

constricted regions that separate the inner membrane boundary from the cristae membrane (Mannella, 2006) (**Fig. 1.6**). Furthermore, immunoelectron microscopy has determined that proteins are differentially distributed among the different domains. For example, translocase of inner membrane proteins are localized to the inner boundary membrane whereas proteins of the respiratory complexes are localized to the cristae membranes (Vogel et al., 2006).

Regulators of Fusion and Fission

The major mediators of mitochondrial fission and fusion are evolutionarily conserved and consist of proteins from the dynamin family of GTPases (Okamoto and Shaw, 2005). Mitochondrial fusion incorporates fusion of both the outer and inner mitochondrial membranes. In mammalian cells, the early steps of mitochondrial fusion are regulated by Mitofusins, which are GTPases that reside on the outer mitochondrial membrane (Chen et al., 2003). There are two mitofusin homologues, Mitofusin 1 (*Mfn1*) and Mitofusin 2 (*Mfn2*), which have similar roles in mitochondrial fusion. Both Mfn1 and Mfn2 engage in homotypic interactions on adjacent mitochondria and through GTP hydrolysis bring the two mitochondria together (Koshiba et al., 2004). Cells that are deficient in both Mfn1 and Mfn2 have dramatically reduced levels of mitochondrial fusion (Chen et al., 2005a; Chen et al., 2003). Together with the mitofusins, OPA1 is another dynamin family GTPase that is critical for mitochondrial fusion. OPA1 localizes to the inner mitochondrial membrane and intermembrane space and is crucial for fusion of the inner mitochondrial membrane (Griparic et al., 2004). The *OPA1* gene undergoes alternative splicing to produce eight mRNA isoforms (Delettre et al., 2001). Additionally, OPA1 is proteolytically cleaved into additional isoforms that are necessary for mitochondrial fusion (Ishihara et al., 2006).

Drp1 is the member of the dynamin family of GTPases that regulates the opposing process of mitochondrial fission in mammalian cells. Drp1 localizes both to the cytosol and to the mitochondrial outer membrane (Smirnova et al., 2001). Drp1 forms oligomers around the mitochondrion, constricts it and utilizes GTP hydrolysis to drive mitochondrial division (Praefcke and McMahon, 2004). Expression of a dominant-negative *Drp1* in cells results in inhibition of endogenous Drp1 and excessive mitochondrial elongation (Lee et al., 2004; Smirnova et al., 2001). Based on these results, mitochondrial morphology is a highly dynamic process that is regulated by the opposing processes of fission and fusion.

Biological Functions

Perhaps the most important biological consequence of fission and fusion is maintenance of a healthy mitochondrial population. Mitochondria produce a substantial amount of reactive oxygen species (ROS); therefore, their genome is remarkably susceptible to DNA damage. Mitochondria protect themselves from accumulating excessive damage through fusion, which facilitates the exchange of lipid membranes and

the mitochondrial genome between organelles thereby allowing damaged mitochondria to be restored to normal. Whereas, fission is necessary to increase mitochondrial number and allow distribution to daughter cells during cell division (Chen and Chan, 2005; Mitra et al., 2009). Imbalances in fission and fusion lead to a variety of cellular and mitochondrial defects (Bleazard et al., 1999; Chen et al., 2003). For example, normal mitochondrial fusion is required for cell growth, efficient oxidative phosphorylation and ATP production (Chen et al., 2005a). Thus, the integrity of the mitochondrial network is intimately associated with cellular fate and bioenergetics.

The BCL-2 Family and Dynamics

In addition to their role in apoptosis, BCL-2 family proteins have also been shown to regulate mitochondrial dynamics (Autret and Martin, 2009). However, the mechanisms and functional impact through which individual BCL-2 proteins influence mitochondrial dynamics remains elusive, as in some cases the same molecules can promote both fission and fusion of the mitochondrial network. For example, the expression of anti-apoptotic BCL-X_L in various cell types promoted mitochondrial fusion and interacted with Mfn2 (Delivani et al., 2006). In cortical neurons, BCL-X_L expression increased both fission and fusion (Berman et al., 2009). Additionally, when over-expressed, the pro-apoptotic effectors BAX and BAK induced mitochondrial fission (Sheridan et al., 2008); however, *Bax* and *Bak* doubly-deficient cells also exhibited a fragmented mitochondrial network and had decreased rates of mitochondrial fusion (Karbowski et al., 2006). In a cell free system used to study mitochondrial fusion, the addition of recombinant BAX promoted fusion in an Mfn2-dependent manner (Hoppins et al., 2011b). The fusogenic function of BAX was limited to its monomeric form as oligomeric BAX abrogated its ability to promote fusion (Hoppins et al., 2011a). Direct interaction between Mfn2 and some of the BCL-2 family members, such as BCL-X_L and BAX, mechanistically demonstrates how BCL-2 proteins regulate mitochondrial dynamics. To better clarify their role, it is important to separate the apoptotic functions of the BCL-2 family members from their ability to regulate mitochondrial morphogenesis.

It is significant to note that the process of mitochondrial fission and fusion has also been shown to play a role in apoptosis. Studies have demonstrated that mitochondrial fragmentation can occur early during apoptosis (Frank et al., 2001). To what extent the fission machinery directly regulates apoptosis is still unclear. For example, the amount of mitochondrial fragmentation during apoptosis was shown to depend on Drp1, while reduced Drp1 expression reduced cytochrome *c* release (Breckenridge et al., 2003; Frank et al., 2001). However, other studies found that Drp1 inhibition did not affect cell death (Estaquier and Arnoult, 2007; Sheridan et al., 2008). The role mitochondrial fusion may play in apoptosis is also not well understood. Some evidence has suggested that inhibition of Mfn1- and Mfn2-induced mitochondrial fragmentation and sensitized cells to death-inducing agents (Jahani-Asl et al., 2007; Sugioka et al., 2004). Overexpression of Mfn2 delayed BAX activation and the release of cytochrome *c* (Neuspiel et al., 2005). Likewise, increased Mfn2 expression protected

neurons from apoptotic stimuli (Jahani-Asl et al., 2007). The link between regulators of inner mitochondrial membrane fusion and apoptosis has also been investigated. OPA1 expression was able to protect cells from cell death induced through the mitochondrial pathway (Frezza et al., 2006). In contrast another study found that expression of Mfn1, Mfn2, or OPA1 had no protective effect on cell death and that cytochrome *c* release occurs in mitochondria with a reticular network (Sheridan et al., 2008).

Supermolecular Protein Complexes in the Inner Mitochondrial Membrane

In addition to being the critical organelle at which the commitment to intrinsic apoptosis is made, mitochondria are also important for the production of energy by oxidative phosphorylation. This process includes electron transport chain complexes that pass electrons generated from the Krebs cycle in a stepwise method to reduce molecular oxygen and produce water. Protons are simultaneously pumped out of the mitochondrial matrix and into the cytosol generating an electrochemical gradient across the mitochondrial inner membrane (Mitchell, 1961) (**Fig. 1.7**). The protons then diffuse back into the mitochondria through the F_1F_0-ATP synthase to generate ATP from ADP (Wallace, 1999) (**Fig. 1.7**). The complexes of the electron transport chain are massive, multi-subunit complexes and consist of NADH dehydrogenase (complex I), succinate dehydrogenase (complex II), ubiquinone oxidoreductase (complex III), and cytochrome c oxidase (complex IV) (**Fig. 1.7**). To increase the efficiency of oxidative phosphorylation, the inner membrane is folded to generate cristae, which amplifies the enzymes participating in this metabolic process.

Respiratory Supercomplexes

The structural organization of the respiratory chain complexes I-IV have historically included the lateral diffusion of the individual complexes in the inner membrane, where electron transfer depends on the transient collision of these complexes (Lenaz and Genova, 2007) (**Fig. 1.7**). However, more recently blue-native gel electrophoresis (BN-PAGE) has revealed that these complexes are organized into megadalton supramolecular complexes, called supercomplexes. These supercomplexes are assemblies of the different respiratory components and are capable of respiration (Acin-Perez et al., 2008) (**Fig. 1.8**). Additionally, genetic mutations encoding one subunit of a complex result in the de-stabilization of other complexes (Acin-Perez et al., 2008). Likewise, the stability of the supercomplexes also depends on cardiolipin, an abundant phospholipid in the IMM (Pfeiffer et al., 2003). It is hypothesized that the formation of respiratory supercomplexes increases the efficiency of electron transfer between the complexes; therefore, reducing the generation of unstable reactive oxygen radicals.
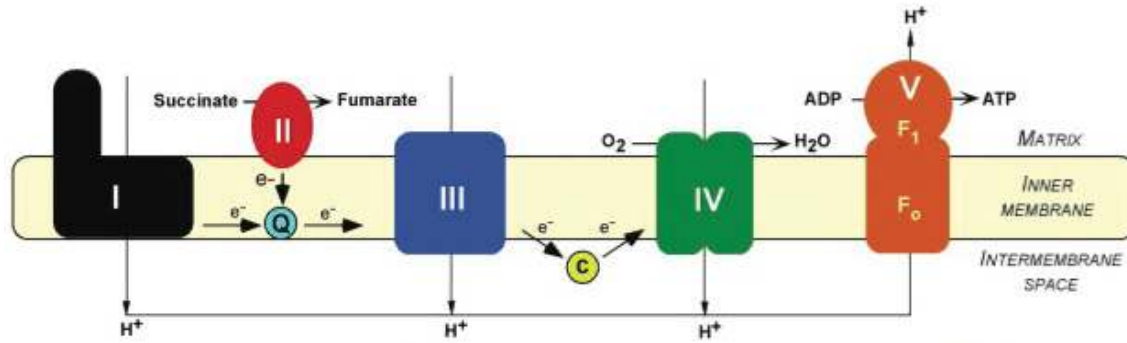
Figure 1.7. **Oxidative Phosphorylation**
Electrons derived from the Krebs cycle are passed through the electron transport
complexes to reduce oxygen to water. Simultaneously, protons are pumped out of the
mitochondrial matrix, generating an electrochemical gradient. Protons then diffuse back
into the matrix through the F1F0-ATP synthase, producing the energy required to make
ATP from ADP. Reprinted by permission from Macmillan Publishers Ltd: Acin-Perez,
R., Fernandez-Silva, P., Peleato, M.L., Perez-Martos, A., and Enriquez, J.A. (2008).
Respiratory active mitochondrial supercomplexes. Mol Cell *32*, 529-539.
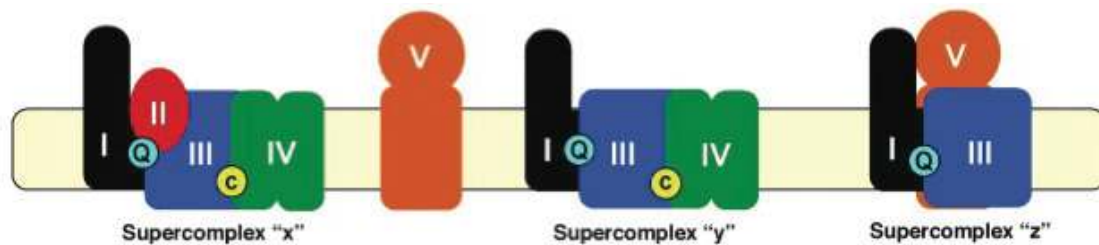
Figure 1.8. **Respiratory Supercomplexes**
Model for the organization of different subtypes of respiratory supercomplexes. The
respiratory complexes are assembled into supercomplexes of various types. Reprinted by
permission from Macmillan Publishers Ltd: Acin-Perez, R., Fernandez-Silva, P., Peleato,
M.L., Perez-Martos, A., and Enriquez, J.A. (2008). Respiratory active mitochondrial
supercomplexes. Mol Cell 32, 529-539.

F_1F_0-ATP Synthase Dimers and Oligomers

The F_1-F_0-ATP synthase (ATP synthase) is composed of a soluble catalytic unit, F_1, located inside the mitochondrial matrix, and a membrane-bound unit, F_0, which anchors the enzyme in the inner membrane and mediates the flow of protons through the membrane. ATP synthase exists in monomers but also forms supercomplexes containing homo-dimers and homo-oligomers (Schagger and Pfeiffer, 2000). The ATP synthase dimers and oligomers are necessary for generation of mitochondrial cristae and increase the efficiency of ATP production (Paumard et al., 2002; Strauss et al., 2008). The dimerization of ATP synthase predominantly involves the F_0 domains but also includes the F_1 domains. The F_0 domains are closely assembled, whereas the F_1 have a distant association. This arrangement produces a 40º angle between the monomers, curving the lipid membrane, which is thought to be responsible for the structure of the cristae (Minauro-Sanmiguel et al., 2005). In yeast, deletion of F_0 subunits e and g abolish dimerization and lead to cristae morphology abnormalities (Paumard et al., 2002). The F_1 regions of each monomer are indirectly associated by inhibitory factor 1 (IF_1), which connects the two monomers (Cabezon et al., 2003).

CHAPTER 2. MATERIALS AND EXPERIMENTAL PROCEDURES*

Cells and Cell Culture

SV40-transformed wild-type (wt) and *Mcl-1*-deficient mouse embryonic fibroblasts (MEFs) have been previously described (Opferman et al., 2003). *Mcl-1*[f/f] Rosa-ERCreT2 and wt Rosa-ERCreT2 MEFs were generated from E12.5 embryos and SV40-transformed. To induce *Mcl-1*-deletion, the MEFs were treated for 48 hours with 100 nM (4-hydroxy)-tamoxifen (Sigma) in culture media to induce Cre expression. HEK293T cells and human non-small cell lung cancer (NSCLC) cells were obtained from American Type Culture Collection. All cells were grown in Dulbecco's modified Eagle's medium (DMEM, Invitrogen) supplemented with 5% fetal bovine serum, 20mM L-glutamine (Gibco) and 10mM HEPES (Gibco). Cells grown in galactose were grown in glucose-free Dulbecco's modified Eagle's medium (DMEM, Invitrogen) supplemented with 10% fetal bovine serum, 2mM glutamine, and 10mM galactose.

Plasmids, Expression Constructs, and Generation of Mutants

All *Mcl-1* constructs were developed using mouse *Mcl-1* cDNA. The mutant *Mcl-1*[OM], in which arginines 5 and 6 were replaced by alanines, was generated by site-directed mutagenesis (Stratagene). The N-terminal 67 amino acids of MCL-1 (MCL-1$^{\Delta N}$) and the C-terminal 22 amino acids (MCL-1$^{\Delta C}$) were deleted by polymerase chain reaction (PCR). The MCL-1-hBCL-2 chimera was made by fusing the N-terminal 50 amino acids of MCL-1 to full-length human BCL-2 by PCR. The mutant *Mcl-1*[Matrix] was generated by fusing amino acids 1-58 of *N. crassa* ATP-synthase to *Mcl-1*$^{\Delta N}$. Mitochondrial morphology and fusion were measured using matrix-localized photoactivatable-GFP (Karbowski et al., 2004) and Mito-DsRed (Clontech). MCL-1$^{\Delta ATG1}$ was generated by PCR amplification using 5' -cgagctcgaattctagtttggcctgcggagaaac -3' (sense) and 5'-gcatatctaataagataggcgggcggatccgca - 3' (antisense). The non-canonical mRNA splicing mutant Mcl-1[SD;SAmut] was generated by mutating nucleotide 52 from G to A changing the amino acid sequence from glycine to serine and mutating nucleotide 189 from G to T creating a silent mutation and maintaining the amino acid valine (Kojima et al., 2010). The PCR primers for nucleotide 52 are forward primer (5'-aacctgtactgcggcagcgccagcctcggcgcg-3') and reverse primer (5'-cgcgccgaggctggcgctgccgcagtacaggtt-3); and for nucleotide 189 are forward primer (5'-cccggccgccgcccgttggcgccgaggacccccg-3') and reverse primer (5'-cggggtcctcggcgccaacgggcggcggccggg-3').

Ecotropic Retroviral Production and Cell Transduction

Ecotropic retroviruses were produced by co-transfection of retroviral expression plasmids in 293T cells with packaging plasmids (pMD-old-Gag-Pol and pCAG4-Eco) using FuGene6 (Roche Applied Bioscience).

Western Blotting, Co-immunoprecipitation, and Antibodies

For immunoblot analysis, cells were lysed in Flag Lysis Buffer (50mM Tris-HCl pH 7.4, 150mM NaCl, 1% TritonX-100, 1mM EDTA) containing complete protease inhibitors (Roche) on ice for 30 minutes. Whole cell lysates (WCL) were cleared by centrifugation and protein concentrations were determined by BCA assay. For co-immunoprecipitation studies, whole cell lysates (WCLs) were pre-cleared and then coupled with both anti-BIM short and anti-BIM long rat monoclonal antibodies (Millipore) or rat IgG (Santa Cruz Biotechnology) for 1 hour then precipitated with protein A/G-plus agarose (Santa Cruz Biotechnology). Immunocomplexes were recovered, washed, and resuspended in sample buffer. Immunocomplexes and post-immunoprecipitated supernatants were subjected to electrophoresis using Bis-Tris gels (Invitrogen), transferred to PVDF (Millipore) and developed using Western Lightning (Perkin Elmer). The following antibodies were used: anti-MCL-1 (Rockland Immunochemical), anti-BIM (BD Biosciences), anti-Tim50 (Abcam), anti-Tom40 (Santa Cruz), anti-Prohibitin1 (Abcam), anti-Opa1 (BD Biosciences), anti-MnSOD (BD Biosciences), anti-PDI (BD Biosciences), anti-hBCL-2 (Clone 6C8, gift of S. Korsmeyer), anti-mBCL-2 (Clone 3F11, gift of S. Korsmeyer), anti-Complex II subunit 70 (MitoSciences), anti-Complex IV subunit II (Mitosciences), anti-Complex I subunit NDUFA9 (MitoSciences), anti-Pyruvate dehydrogenase (Cell Signaling) and anti-Actin mouse monoclonal (Millipore), Complex I, anti-NDUFA9 (Molecular Probes); Complex II, anti-Fp70 (Molecular Probes); Complex III, anti-Core 2 (Molecular Probes); Complex IV, anti-Cox I (Molecular Probes); ATP Synthase, anti-5A1 (Proteintech Group); ATP Synthase, anti-5B (Santa Cruz Biotechnology); ATP Synthase, anti-gamma (GeneTex); ATP Synthase, anti-OSCP (Santa Cruz Biotechnology).

Cell Death Experiments

Both wt *Mcl-1* Rosa-ERCreT2 MEFs and *Mcl-1*$^{f/f}$ Rosa-ERCreT2 MEFs stably expressing murine stem cell virus (MSCV)-puro vector, wt MCL-1, MCL-1^{OM}, MCL-1^{Matrix}, or hBCL-2 were treated with tamoxifen for 48 hours and treated with etoposide or staurosporine (Calbiochem). Cell viability was determined by staining with Annexin-V-FITC and propidium iodide (PI) (BD Biosciences) and flow cytometry (FACSCalibur, BD Biosciences).

RNAi Experiments

For RNA-mediated interference (RNAi), MEFs were plated in Opti-MEM media (Invitrogen) and transfected with respective 70 nM Stealth siRNAs (Invitrogen) specific for mouse Tom40 and Tim50 using Lipofectamine RNAi-Max (Invitrogen). Six hours after transfection media was replaced with complete DMEM media. Seventy-two hours after transfection cells were collected, lysed and immunoblotted. Stealth siRNA sequences were: TOM40: ACUGAACAACUGGUUGGCUACAGUA, CCCUCUGUAUGAAAUAGUCAUCUUC, GAAGAUGACUAUUUCAUACAGAGGG; TIM50: GCCCUACUACCAGCCACCUUAUACA, UGUAUAAGGUGGCUGGUAGUAGGGC, UCAAGACCAUUGCACUGAACCAAGU

Measurement of Superoxide Anion

MitoSOX-red (Invitrogen) was used to measure reactive oxygen species (ROS) in SV40-transformed wt *Mcl-1* Rosa-ERCreT2 MEFs and *Mcl-1*$^{f/f}$ Rosa-ERCreT2 MEFs expressing MSCV-puro vector, wt MCL-1, MCL-1^{OM}, MCL-1^{Matrix}, and hBCL-2. Cells were treated with 5μM MitoSOX for 30 minutes. at 37°C and fluorescence measured by flow cytometry. Antimycin A (Sigma) (10 nM), which induces superoxide through the inhibition of complex III, was used as a positive control.

Isolation and Purification of Mouse Liver Mitochondria

Mouse livers were homogenized in Mito Isolation Buffer (MIB) buffer (200mM Manitol, 68mM Sucrose, 10mM Hepes-KOH pH 7.4, 10mM KCl, 1mM EDTA, 1mM EGTA. 0.1% BSA). Mitochondria were isolated using differential centrifugation and were purified using a Percoll-gradient consisting of 70% percoll, overlayed by 30% Percoll (Pierce) in 5mM MOPS and 0.3M mannitol. Protein content was determined by Bradford assay (BioRad).

Subcellular Fractionation and Isolation of Heavy Membrane from Cells

Cells were swollen in 220mM Mannitol, 70mM Sucrose, 10mM Hepes-KOH (pH 7.4) for 30 minutes on ice. Cells were homogenized 30 times with a 30 gauge needle. The non-lysed cells and nuclei were sedimented by centrifugation at 600xg for 10 minutes and disposed. The supernatant was centrifuged at 5,500xg for 15 minutes and the pellet was the heavy membrane fraction. The supernatant was centrifuged at 100,000xg for 30 minutes and the soluble fraction contains the purified cytosolic fraction.

Proteolysis of Heavy Membrane Fraction

The heavy membrane (HM) fraction was isolated from cells or mouse liver and protein concentration determined by Bradford assay. HM (40ug) were treated with the following treatments: proteinase K (0.2mg/ml), 20mM KCl (osmotic shock), 1% SDS (membrane solubilization) for 30 minutes on ice. Proteins were precipitated with tricholoroacetic acid (Sigma).

Oxygen Consumption

Respiration was measured in intact cells (64,000/well) seeded in poly-L-lysine-coated plates using the XF24 analyzer (Seahorse Bioscience) (Ferrick et al., 2008). After 5 hours, the cells were loaded into the machine to determine the oxygen consumption rate (OCR). Respiration was measured sequentially after addition of 0.5μM oligomycin, 0.5μM FCCP, and 0.5μM rotenone. After each injection, OCR was measured (3 minutes), the medium mixed (2 minutes), and measured (3 minutes).

Alkali Wash

Purified mouse liver mitochondria were sonicated (40W for 15 seconds, twice) on ice and then centrifuged at 10,000xg for 10 minutes to remove intact mitochondria. The supernatant was centrifuged at 100,000xg for 30 minutes and the supernatant is the soluble fraction. The pellet was treated with 0.1M sodium carbonate (pH 11.5) in MIB buffer for 30 minutes on ice and then centrifuged at 100,000xg for 30 minutes and supernatant and pellet collected.

Mitochondria Subfractionation

Mitochondria were swollen on ice for 30 minutes in 14 ml of 10mM KH_2PO_4 (pH 7.4). One-third volume of 1.8M sucrose, 10mM $MgCl_2$ was added on ice for 30 minutes to shrink the mitochondria. Mitochondria were sonicated (4 Amps for 5 seconds) in 2.5 ml aliquots then centrifuged at 12,000xg for 10 minutes to get supernatant 1 and pellet 1. Supernatant 1 was then spun at 100,000xg for 1 hour and the pellet 2 is the OM. Pellet 1 was resuspended in 7ml of 1.8M sucrose, 10mM $MgCl_2$ on ice for 5 minutes and centrifuged at 5,500xg for 15 minutes and pellet 3 is the mitoplast.

Cellular ATP

ATP assays were performed using the ATP Bioluminescence Assay Kit HSII (Roche) following the manufacturer's instructions. Briefly, cells were counted in triplicate and washed in PBS. Cells (0.5×10^6/ml) were resuspended in lysis buffer (5 minutes at 22°C). Lysed cells were incubated at 100°C for 2 minutes, centrifuged at

10,000xg for 5 minutes. Cell lysates (50 μl) were diluted in 50μl of dilution buffer, and 100μl of luciferase reagent was added. The luminescence was measured using a Luminometer (Biotek Synergy) and ATP concentration was determined by comparing values to a standard curve.

Mitochondrial Fusion Assay and Image Analysis

Cells were grown in 4-well chambers and were transiently-transfected using Fugene6 with a photoactivatable-GFP targeted to the mitochondrial matrix (Karbowski et al., 2004). Images were captured using a Marianas spinning disk confocal (SDC) imaging system consisting of a Zeiss Axio Observer (Carl Zeiss MicroImaging) inverted microscope with motorized XYZ stage, a CSU-X confocal head (Yokogawa Electric Corporation), LaserStack laser launch and Vector laser scanner head (Intelligent Imaging Innovations-3i). Images were collected using a Zeiss Plan-Apochromat 63x 1.4 NA oil objective and Evolve 512 EMCCD camera (Photometrics). 3-D time-lapse images of the cells were acquired from the top to the bottom of mitochondria with 0.4μm z-sections with varying time-intervals (10 initial frames at every 2 minutes, and at every 5 minutes after that for total of 2-3 hr). A small region of interest (~2μm) of the mitochondria was activated in the third time-frame using 405 nm laser at two middle planes of 3-D acquisition. The fluorescence intensity was measured using Slidebook (Intelligent Imaging Innovations-3i). The maximum intensity projections (MIP) of the z-stacks for each time point were created. The activated mitochondria were masked by thresholding the pixel intensities above the background. The total area of intensity (all pixels above threshold) was normalized to the post-activation time point and plotted over time.

Analysis of Mitochondrial Morphology and Shape

Cells were grown in 4-well chambers and were transiently transfected using Fugene6 with mito-DsRed (Clontech). Images were captured using a Marianas spinning disk confocal (SDC) imaging system using a 63X 1.4 NA Apochromat objective (Zeiss). Images were acquired from the top to the bottom of the mitochondria in 0.4μm z-sections. For morphological analysis, the fluorescence intensity was measured using Slidebook. A Laplacian 2-D spatial filter was applied to the MIP to highlight mitochondrial structures and an intensity threshold was applied to the images to mask mitochondrial objects. A shape factor consisting of $p^2/4\pi A$ (p=perimeter and A=area) was applied to all the mitochondrial objects in each cell type (Koopman et al., 2005).

Mitochondrial DNA Isolation and Quantification

Total cellular DNA was extracted using the DNeasy kit (Qiagen). The amount of mtDNA present per nuclear genome was determined by quantitative real-time PCR using the following primer pairs: mtDNA forward primer, cctatcacccttgccatcat; mtDNA reverse

primer, gaggctgttgcttgtgtgac. To quantify nuclear DNA we used primers for the *Pecam* gene on chromosome 6 Nuclear DNA forward primer, atggaaagcctgccatcatg; Nuclear DNA reverse primer, tccttgttgttcagcatcac. Quantification of relative copy number differences was carried out by analyzing the difference in threshold amplification between mtDNA and nuclear DNA (delta delta C(t) method).

Mitochondrial Membrane Potential and Image Analysis

Cells were stained in dark with 10 nM tetramethylrhodamine (TMRM) (Invitrogen) in Hank's balanced salt solution (HBSS, Gibco) at 37°C for 20 minutes. Images were captured on a Marianas spinning disk confocal (SDC) imaging system using a 63X 1.4 NA Apochromat objective (Zeiss). Imaging conditions (laser excitation power at 561 nm, exposure time and camera gain) were identical for all samples. Mean pixel intensity values of all mitochondria in the image (representative of mitochondrial potential) were obtained by masking the signal with Ridler-Calvard automatic thresholding algorithm implemented in Slidebook 5.0 (3i).

Transmission Electron Microscopy

Wild-type and *Mcl-1*-deficient MEFs and *Mcl-1*-deleted livers were fixed in 2.5% gluteraldehyde in 0.1M sodium cacodylate buffer and post fixed in 2% osmium tetroxide in 0.1M sodium cacodylate buffer with 0.3% potassium ferrocyanide for 2 hours. Tissue was enblocked stained with 4% aqueous uranyl acetate for 1 hour then dehydrated through a series of graded ethanol to propylene oxide, infiltrated and embedded in epoxy resin and polymerized at 70˚C overnight. Semi-thin sections (0.5 μm) were stained with toluidine blue for light microscope examination. Ultra-thin sections (80 nm) were cut and imaged using a JEOL 1200 electron microscope with an AMT XR 111 camera.

Immuno-electron Microscopy

Mitochondria were isolated from pI-pC-treated wt or *Mcl-1*[f/f] plus Mx1-Cre liver. Mitochondrial fractions were fixed for 2 hours using a 4% Paraformaldehyde in 0.1M Phosphate Buffer. The fractions were then embedding in a 12% gelatin and then immersed in 2.3M sucrose overnight. They were frozen using liquid nitrogen and were then cryo-sectioned at a thickness of 85 nm and a temperature of -110°C using a Leica UCT ultramicrotome. The cryo-sections were placed on formvar coated nickel grids and labeled with anti-MCL-1 primary antibody (Abcam) and protein A gold secondary (Cell Microscopy Center) as described previously (Peters et al., 2006). Briefly, Data Acquisition was carried out utilizing a JEOL 1200 EX II electron microscope equipped with an 11 megapixel AMT camera.

Immunofluorescence

Mcl-1-deficient MEFs were grown in 4-well chamber slides and transfected using Fugene6 with *Mcl-1* constructs. Cells were treated with Mitotracker red (Invitrogen) for 45 minutes at 37˚C. Cells were fixed in 4% paraformaldehyde and immunostained with anti-MCL-1 (Rockland) and Alexa488 anti-rabbit IgG (Invitrogen). Images were collected using Leica DM IRBE microscope equipped with a Leica TCS Confocal System using a 63X magnification.

Enzymatic Activity of Electron Transport Chain Components

For all the enzymatic assays mitochondria were isolated from pI-pC-treated wt or *Mcl-1*$^{f/f}$ plus Mx1-Cre liver (Opferman et al., 2005). The activity of NADH-ubiquinone oxidoreductase (complex I) was assayed as previously described (Frost et al., 2005). Briefly, mitochondria were lysed with dodecyl maltoside in a phosphate buffer (pH 7.4) containing $MgCl_2$ and NADH. The reaction was started by the addition of CoQ_1, upon which NADH oxidation was followed at 340 nm for several minutes. Changes in absorbance prior to the addition CoQ_1 were recorded as a blank. Activity was calculated using the extinction coefficient 6.22 $mM^{-1}cm^{-1}$ for NADH. Succinate-ubiquinone oxidoreductase (complex II) activity was assayed by measuring the succinate dependent reduction in DCIP, mediated by CoQ_1. The reaction was followed by recording absorbance at 600 nm following the addition of succinate (Miyadera et al., 2003). Succinate-independent absorbance changes were measured as a blank. Activity was calculated using the extinction coefficient of 21 $mM^{-1}cm^{-1}$ for DCIP. Cytochrome *c* oxidase activity (complex IV) was assayed by measuring the oxidation of cytochrome *c* at 550 nm and calculated using the extinction coefficient of 19.6 $mM^{-1}cm^{-1}$ as previously described (Miro et al., 1998). Pyruvate dehydrogenase (PDH) activity was assayed by measuring the pyruvate-dependent reduction of INT, mediated by PMS, as previously described (Hinman and Blass, 1981). Briefly, mitochondria lysed with dodecyl maltoside were incubated in a Tris (pH 7.4) buffer containing NAD+, TPP, CoA, $MgCl_2$, BSA, PMS, and pyruvate. Absorbance changes at 500 nm were recorded and activity was calculated using the absorption coefficient 12.4 $mM^{-1}cm^{-1}$. Identical samples lacking either mitochondria or pyruvate were prepared as blanks.

Isolation of Respiratory Complexes and Supercomplexes

Mitochondria were isolated from pI-pC-treated wt or *Mcl-1*$^{f/f}$ plus Mx1-Cre liver. Mitochondrial isolation was carried out as described previously (Fernandez-Vizarra et al., 2002). Isolation of the complexes and supercomplexes was completed as previously described (Acin-Perez et al., 2008).

Blue Native Polyacrylamide Gel Electrophoresis (BN-PAGE)

Mitochondrial membrane proteins (20 μg) were loaded and run on 3-12% first-dimension (1D) gradient BN-PAGE gel was as described earlier (Acin-Perez et al., 2008). The 1D gel was transferred onto PVDF and immunoblotted with indicated antibodies.

λ-Phosphatase Treatment

Wild-type MEFs were treated with DMSO or 10μM MG-132 for 4 hours after which the cells were lysed in 10mM Tris-HCl, pH 7.5, 150mM NaCl, 1mM EDTA, 1% NP-40, 1mM DTT, 1mM PMSF containing protease inhibitors on ice for 30 minutes. Lysates were incubated with or without λ-protein phosphatase (New England Biolabs) for 30 minutes at 30°C. Samples were resolved and immunoblotted with anti-MCL-1 (Rockland), anti-Phospho-AKT(Ser473) (Cell Signaling), anti-AKT (Cell Signaling) and anti-Actin (Millipore).

Edman Sequencing of MCL-1

MCL-1 protein was immunoprecipitated from transiently-transfected 293T cells using FLAG Lysis Buffer (30 mg of input), resolved by SDS-PAGE, and transferred to PVDF membrane. Coomassie-stained membrane was excised and submitted to the W.M. Keck Foundation Biotechnology Resource Laboratory at Yale University and subjected to 8 rounds of N-terminal sequencing.

CHAPTER 3.   RESULTS*

Mcl-1-deletion Results in Mitochondrial Morphology Defects

SV40-transformed wild-type (wt) or *Mcl-1*$^{f/f}$ Rosa-ERCreT2 murine embryonic fibroblasts (MEFs) in which endogenous *Mcl-1* can be deleted by tamoxifen-mediated induction of the Cre-recombinase were generated (hereafter referred to as *Mcl-1*-deletion) **(Fig. 3.1a)**. Inducible *Mcl-1*-deletion in MEFs did not trigger spontaneous apoptosis **(Fig. 3.1b)**, but resulted in defective proliferation **(Fig. 3.1c)**. Notably, *Mcl-1*-deletion induced the appearance of punctate mitochondria and the loss of the normal tubular mitochondrial network that was present in control cells **(Fig. 3.2a, b)**. Furthermore, ultrastructural defects including defective cristae harboring balloon-like, vesicular structures were readily apparent within the majority of mitochondria in *Mcl-1*-deficient MEFs **(Fig. 3.2c, d)**. These abnormal cristae morphologies were not limited to transformed MEFs as similar defects were observed in primary *Mcl-1*-deleted liver mitochondria **(Fig. 3.3a)**. Proteins involved in oxidative phosphorylation are enriched in the inner mitochondrial membranes (IMM) that make up the cristae (Gilkerson et al., 2003; Vogel et al., 2006); therefore, we assessed whether *Mcl-1*-deletion altered the enzymatic activity of the respiratory chain complexes. *Mcl-1*-deletion in mouse liver mitochondria significantly decreased the ability of NADH dehydrogenase (complex I), succinate dehydrogenase (complex II), and cytochrome *c* oxidase (complex IV) to transfer electrons; whereas pyruvate dehydrogenase (PDH) activity was unchanged **(Fig. 3.3b)**. Deletion of *Mcl-1* in transformed MEFs did not result in massive apoptosis, probably because MEFs do not express high levels of BH3 proteins; thus, are not "primed" for death. However, the small amount of apoptosis observed may be enough to cause a change in proliferation since cell growth is logarithmic and cell death is not. Loss of MCL-1 expression in MEFs and hepatocytes did result in dysregulation of the normal reticular mitochondrial network, cristae morphological abnormalities, and defects in electron transport chain enzymatic function.

MCL-1 Localizes to Two Distinct Mitochondrial Sub-compartments

To understand the mechanisms underlying the dependence on MCL-1 for normal cristae morphology, we investigated the localization of MCL-1 within mitochondria. By immunoblot analysis MCL-1 appeared as a doublet or triplet in percoll-purified liver mitochondria devoid of contaminating endoplasmic reticulum (ER) **(Fig. 3.4a)**. MCL-1 is a phosphorylated protein (Domina et al., 2004; Maurer et al., 2006; Morel et al., 2009); however, phosphatase-treatment of cell lysates did not abolish the 40 kD species
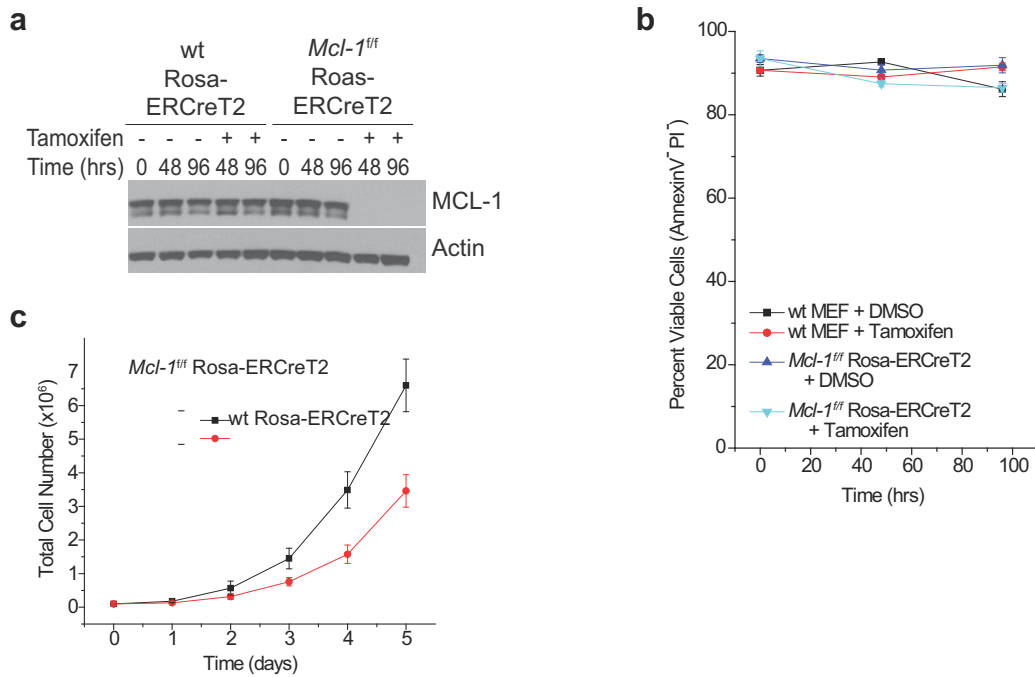
Figure 3.1.   Inducible *Mcl-1*-deletion in MEFs Does Not Affect the Cell Viability.
(a) *Mcl-1*$^{f/f}$ Rosa-ERCreT2 or wild-type (wt) Rosa-ERCreT2 MEFs (control MEFs) were treated with tamoxifen or DMSO for indicated times to induce deletion of endogenous *Mcl-1* then immunoblotted for MCL-1 or Actin (loading control). (b) *Mcl-1*$^{f/f}$ Rosa-ERCreT2 or wt control MEFs were treated with tamoxifen or DMSO (vehicle control) for indicated times, to induce deletion of endogenous *Mcl-1*, and assessed for cell death. Annexin-V and PI double-negative cells were scored as viable. Bars represent the average of 3 independent experiments and the error bars denote the SEM. (c) *Mcl-1*$^{f/f}$ Rosa-ERCreT2 or wt Rosa-ERCreT2 MEFS were treated with tamoxifen (48 hours), seeded, and counted by hemocytometer at the indicated times. The data represent averages and SEM of 3 independent experiments.

Figure 3.2.   Inducible *Mcl-1*-deletion in MEFS Results in Mitochondrial Morphology Defects.

(a) *Mcl-1*$^{f/f}$ Rosa-ERCreT2 or wt Rosa-ERCreT2 MEFs expressing matrix-targeted DsRed fluorescent protein were treated with DMSO or tamoxifen for 96 hours to induce deletion of endogenous *Mcl-1*, then imaged to detect mitochondrial morphology. Scale bars represent 10µm. (b) Average shape factor of mitochondrial matrix for *Mcl-1*$^{f/f}$ Rosa-ERCreT2 or control MEFs 96 hours after deletion. A shape factor of 1.0 indicates circular mitochondria and the higher the number, the more reticular the network. A shape factor consisting of $p^2/4\pi A$ (p=perimeter and A=area) was applied to all the mitochondrial objects in each cell type (Koopman et al., 2005). Error bars represent the standard error of the mean (SEM) from 10 imaged cells (~3000 mitochondria) and statistical significance was determined by unpaired t-test (*$p<0.01$). (c) Transmission electron micrographs of wt or *Mcl-1*-deficient MEFs. Scale bars represent 500 nm. (d) Quantification of mitochondrial cristae morphology from wt or *Mcl-1*-deficient MEFs. Mitochondria were counted from ~100 individual cells and scored for normal (lamellar) or ballooned and swollen cristae (disorganized). Error bars indicated the SEM from 3 independent experiments.

a

| | wt Rosa-ERCreT2 | *Mcl-1*^{f/f} Rosa-ERCreT2 |

DMSO

Tamoxifen

b

Time (days)

Shape Factor (Arbitrary Units)

DMSO
Tamoxifen

wt Rosa-ERCreT2   *Mcl-1*^{f/f} Rosa-ERCreT2

c

wt   *Mcl-1*-deficient

12,000X

wt   *Mcl-1*-deficient

20,000X

d

Lamellar
Disorganized

Cristae Morphology (% of mitochondria)

wt   *Mcl-1* Deficient

27

Mcl-1-deleted
hepatocyte

2,500 X   10,000 X
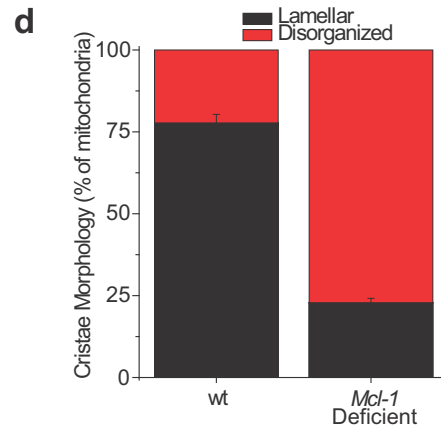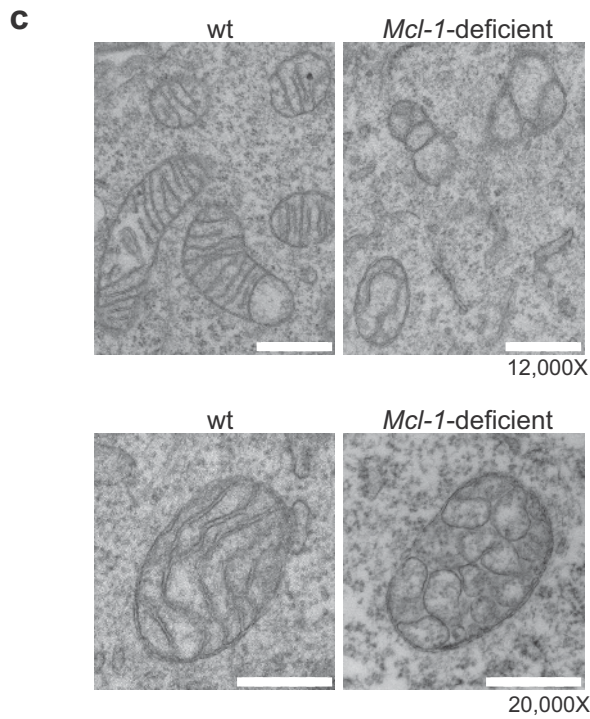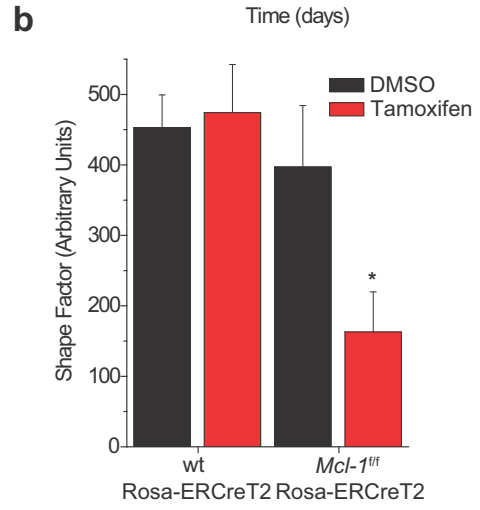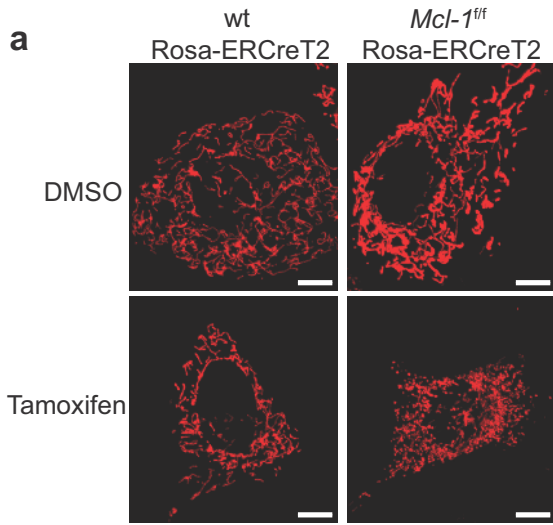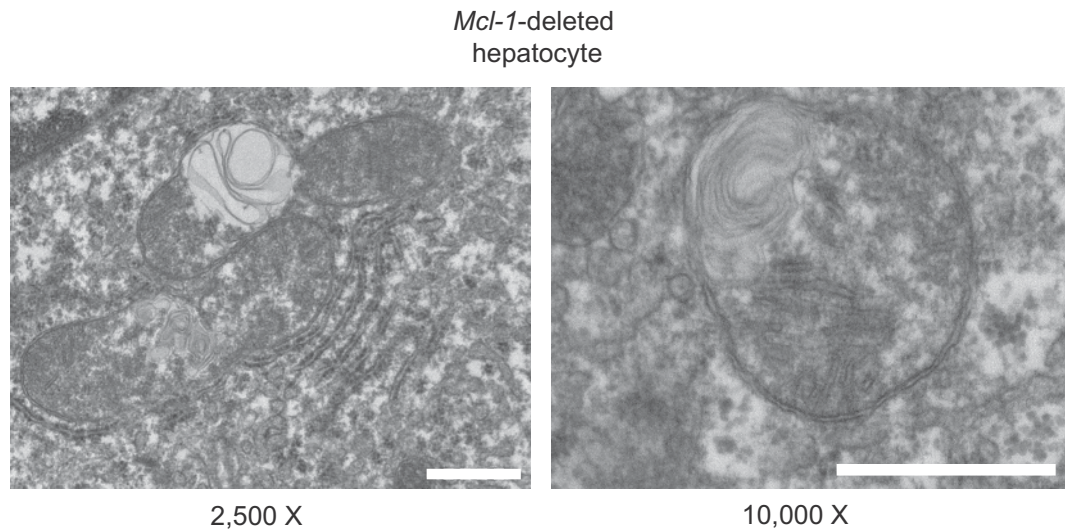
b
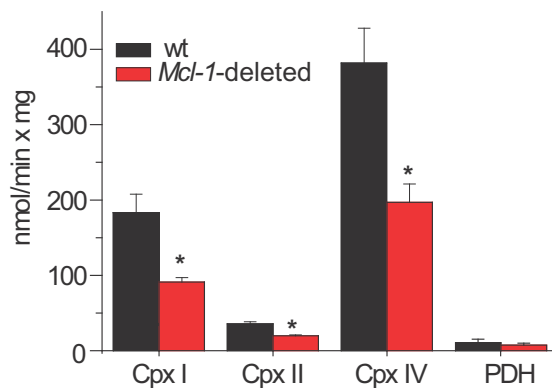
Figure 3.3.   *Mcl-1*-deletion Induces Mitochondrial Abnormalities.
(a) Transmission electron micrographs of pI-pC-treated *Mcl-1*$^{f/f}$ Mx1-Cre mouse liver 14
days after pI-pC treatment. Size bars represent 500 nm. (b) Enzymatic assays for
indicated electron transport chain components and pyruvate dehydrogenase (PDH) from
mouse liver mitochondria prepared from *Mcl-1*$^{f/f}$ Mx1-Cre or wt Mx1-Cre (wt) mice 14
days after treatment with pI-pC. Three independent animals were assayed in triplicate
(n=9) and error bars indicated the SEM. Statistical significance was determined by
unpaired t-test (*p<0.01).
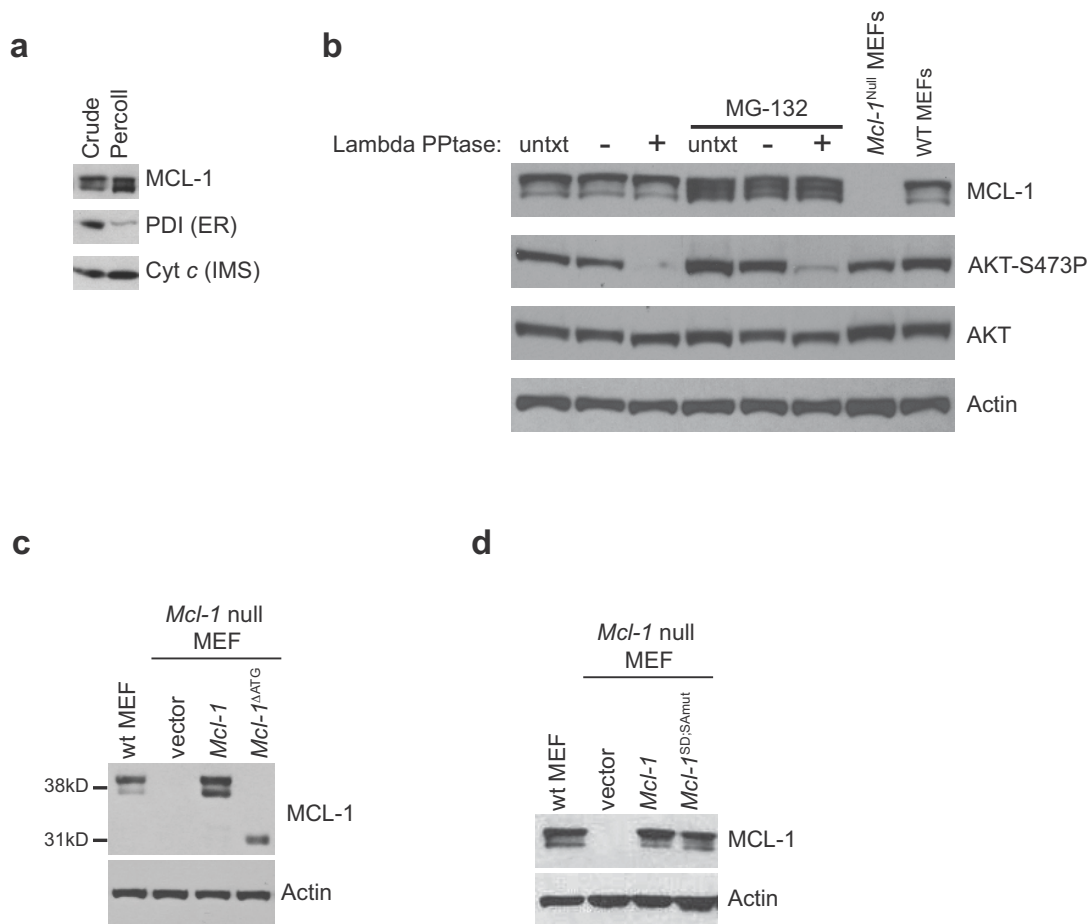
Figure 3.4.   Origin of MCL-1 Protein Species.
(a) Crude or Percoll-purified mouse liver mitochondria were western blotted for
expression of MCL-1, Protein Disulphide Isomerase (PDI, endoplasmic reticulum, ER),
or cytochrome c (inner membrane space, IMS). (b) Wild-type (wt) MEFs were either
treated with or without proteasome inhibitor (MG-132), then cell lysates were incubated
in the absence or presence of λ-protein phosphatase. Lysates were immunoblotted with
anti-MCL-1, anti-Phospho-AKT (Ser473), anti-AKT, and Actin for loading control. (c)
Lysates from wt MEFs or Mcl-1-deleted stably-expressing vector, wild-type Mcl-1, or
Mcl-1 in which its ATG start codon was mutated to TAG (Mcl-1$^{\Delta ATG}$) were
immunoblotted using anti-MCL-1 and anti-Actin for loading control. (d) Lysates from
Mcl-1-deleted or wt MEFs stably-expressing vector, wild-type Mcl-1, or Mcl-1 in which
the putative cryptic splice donor/acceptor pair (nucleotide: 52 G to A and 189 G to T)
was mutated (Mcl-1$^{1SD;SAmut}$) were immunoblotted using anti-MCL-1 and anti-Actin
(loading control).

indicating its slower migration is not due to differential phosphorylation **(Fig. 3.4b)**. It has been proposed that non-canonical translational initiation at a non-ATG leads to the production a faster-migrating 36 kD truncated protein (Warr and Shore, 2008); however, removal of MCL-1's start codon did not produce a 36 kD protein, instead it produced a 31 kD truncated-protein from a downstream ATG codon **(Fig. 3.4c)**. It has also been proposed that non-canonical mRNA splicing generates the 36 kD species (Kojima et al., 2010); however, ablation of the putative splice donor and acceptor pairs still produced the doublet in cells **(Fig. 3.4d)**. Thus, proteolytic cleavage appears to be the most likely contributor to generate the faster migrating 36 kD species (De Biasio et al., 2007; Huang and Yang-Yen, 2010). Indeed, amino-terminal Edman sequencing of immunoprecipitated MCL-1 detected two amino-terminal cleavage sites: the first between MCL-1's isoleucine-10 and glycine-11 and another between leucine-33 and valine-34. Consequently, proteolysis of MCL-1's amino-terminus gives rise to three different molecular weight MCL-1 species: full-length (40 kD), cleaved at isoleucine-10 (38 kD), and cleaved at leucine-33 (36 kD).

Unexpectedly, the variant forms of MCL-1 exhibited different mitochondrial sub-localization; the slowly migrating bands of MCL-1 (40 kD and 38 kD) were enriched in the OMM, while the faster migrating form (36 kD) was only detected in the mitoplast fraction, consisting mainly of IMM and matrix **(Fig. 3.5a)**. Indeed, while both the 40 kD and 36 kD forms of MCL-1 were tightly associated with disrupted and alkali-washed mitochondrial membranes, only the 38 kD species exhibited a looser association with membranes **(Fig. 3.5b)**. Furthermore, when mitochondria isolated from MEFs were treated with proteinase K, the 40 kD and 38 kD forms of MCL-1 were sensitive to protease digestion, but the 36 kD species remained resistant to degradation even after osmotic shock-mediated permeabilization of the OMM **(Fig. 3.5c)**. Moreover, mitochondria from mouse liver and human non-small cell lung cancer cell lines exhibited the same protease sensitivity, suggesting that the sub-mitochondrial localization of MCL-1 is conserved in both primary murine tissues and human cell lines **(Fig. 3.5d, e)**. Immunoelectron microscopy of isolated liver mitochondria also indicated that endogenous MCL-1 localized to both the OMM and IMM **(Fig. 3.6)**. Together, these results indicate that the 40 kD and 38 kD forms of MCL-1 reside on the outer leaflet of the OMM, whereas the 36 kD form is associated with the inner membrane and is confined within the mitochondrial matrix.

During mitochondrial protein import, nuclear encoded proteins are processed by importation machinery consisting of the translocases of outer membrane (TOM) and inner membrane (TIM) proteins (Schmidt et al., 2010). RNAi-mediated gene silencing of either TOM40 or TIM50 prevented MCL-1's mitochondrial import rendering it completely protease sensitive **(Fig. 3.7)**. Accordingly, MCL-1 undergoes TOM- and TIM-dependent mitochondrial import.
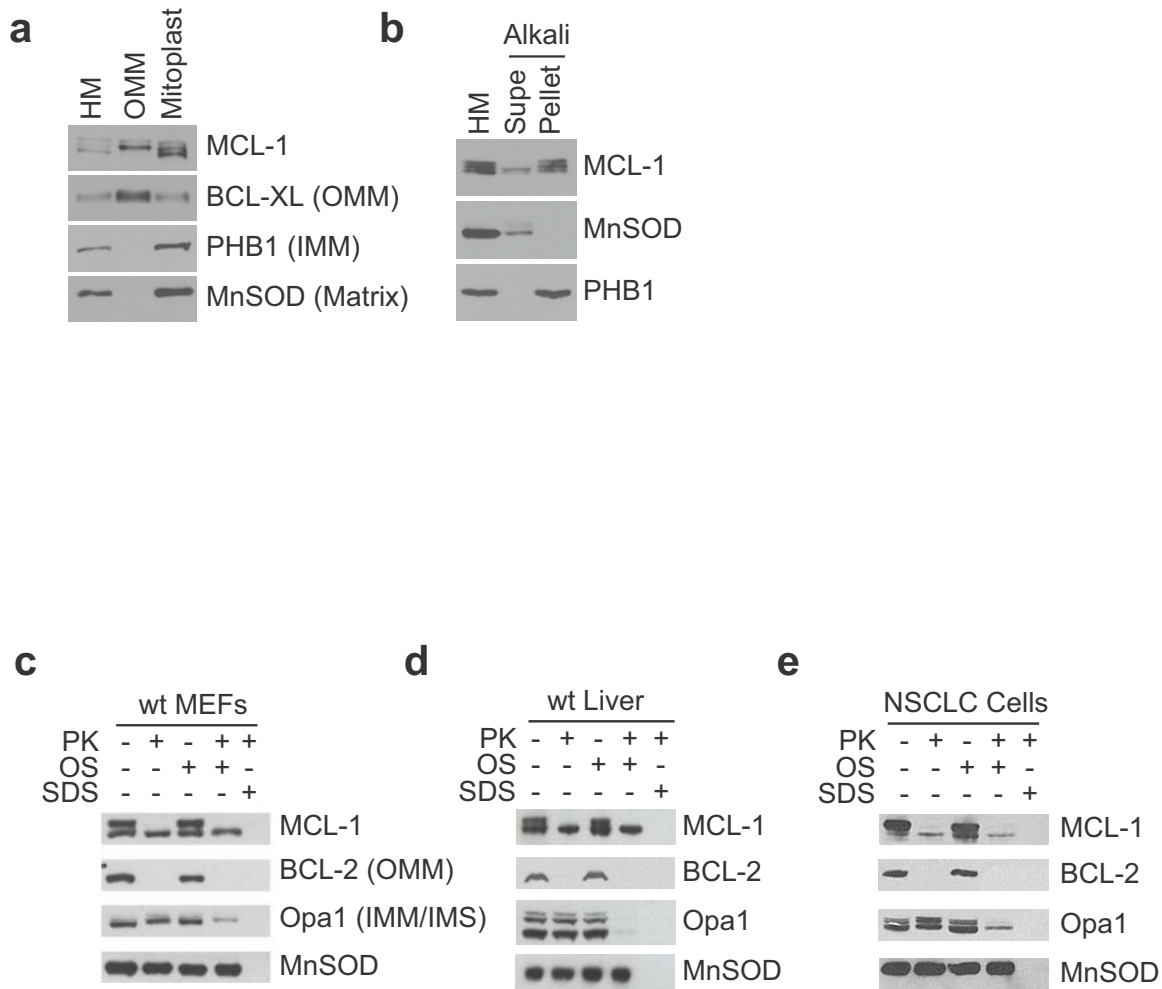
Figure 3.5. **MCL-1 Resides in Different Sub-mitochondrial Localizations.**
(a) Mouse liver mitochondria (HM) were sub-fractionated into outer mitochondrial membrane or mitoplast and western blotted for MCL-1, BCL-X$_L$ (outer mitochondrial membrane, OMM), Prohibitin1 (inner mitochondrial membrane, IMM), or MnSOD (matrix). (b) Mouse liver mitochondria (HM) were swollen and sonicated to disrupt membranes, washed with alkali buffer (pH 11.5) to detach loosely-associated proteins from membranes, and then re-isolated by ultra-centrifugation. Supernatant (Supe) and membrane fractions (Pellet) were western blotted for MCL-1, Prohibitin1, or MnSOD. (c, d, & e) Mitochondria isolated from (c) wt MEFs, (d) wt mouse liver, or (e) human Non-Cell Lung Cancer (NSCLC) cells were subjected to proteinase K (PK) proteolysis to digest exposed proteins, osmotic shock (OS) was used to disrupt the outer mitochondrial membrane, and detergent (SDS) was used to disrupt both inner and outer mitochondrial membranes. Lysates were resolved and subjected to immunoblot analyses.

31
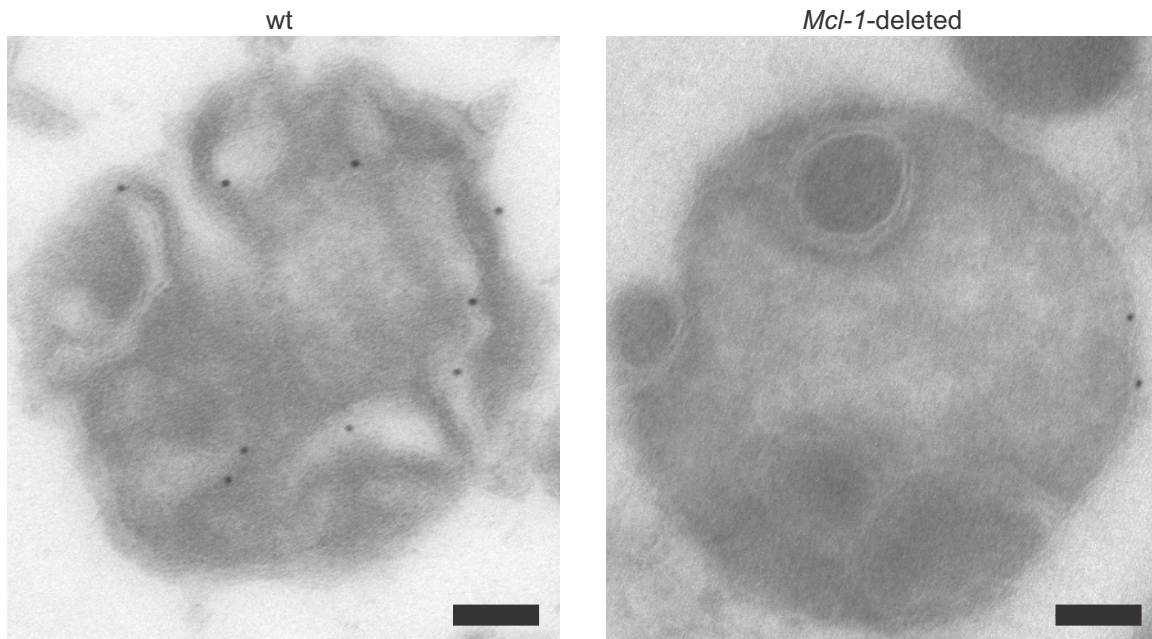
Figure 3.6.   MCL-1 Is Localized to Both the Outer and Inner Mitochondrial Membranes.
Mouse liver mitochondria from *Mcl-1*[f/f] Mx1-Cre (*Mcl-1*-deleted) or wt Mx1-Cre (wt) mice 14 days after treatment with pI-pC were fixed 4% paraformaldehyde in 0.1 M Phosphate Buffer and subjected to immuno-electron microscopy. Magnification is 20,000X and scale bar represents 100 nm.
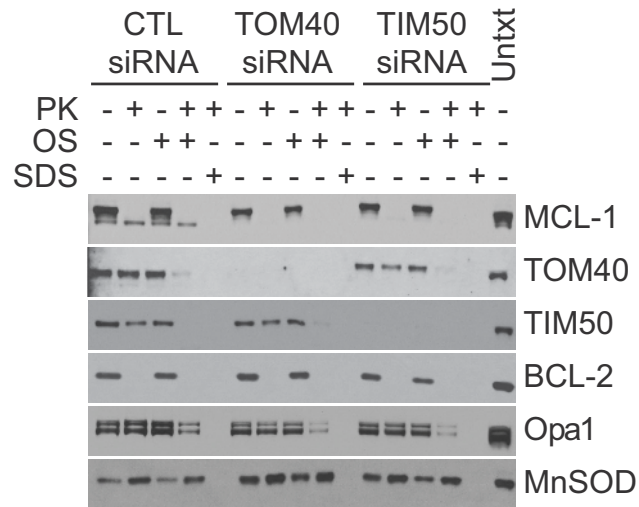
Figure 3.7.   MCL-1 Undergoes TIM/TOM Mitochondrial Import.
Mitochondria isolated from wt MEFs transfected with control or siRNA-oligos specific to
TOM40 or TIM50 were subjected to protease treatment as described in **Fig. 3.5**.

MCL-1 Possesses a Mitochondrial Targeting Sequence

MCL-1 shares sequence homology to BCL-2 in its carboxy-terminal region; however, its amino-terminus is poorly conserved (Kozopas et al., 1993). To define the domains necessary for appropriate localization to mitochondria, MCL-1 mutants were generated **(Fig. 3.8a)**. Both MCL-1's amino- and carboxy-terminal domains were necessary for its proper mitochondrial localization and generation of a doublet by immunoblot analysis **(Fig. 3.8b, c)**. Proteins imported into the mitochondrial matrix often contain mitochondrial targeting sequences (MTS) (Schmidt et al., 2010). To determine if the amino-terminus on MCL-1 contains a MTS, the first 50 amino-terminal amino acids of MCL-1 were fused to the amino-terminus of human BCL-2 (hBCL-2). Human BCL-2 is normally restricted to the OMM; however, the chimeric protein formed a doublet of which the faster migrating species appeared in the matrix, thus validating that MCL-1's amino-terminus possesses an MTS **(Fig. 3.8d)**. Imported mitochondrial proteins often possess MTS's containing charged residues (Schmidt et al., 2010). Mutagenesis of the arginine residues at MCL-1's positions 5 and 6 to alanine (hereafter called MCL-1^{OM}) maintained its localization to mitochondria, but abrogated the formation of MCL-1's 36 kD form **(Fig. 3.9a, b, c)**. Notably, MCL-1^{OM} was completely sensitive to proteolysis indicating that the mutagenesis blocks mitochondrial import **(Fig. 3.9d)**. To generate a MCL-1 mutant that resides solely within the mitochondrial matrix, we used the mitochondrial targeting sequence of matrix-localized ATP-synthase (Pfanner et al., 1987) and fused it to amino-truncated MCL-1 (hereafter called MCL-1^{Matrix}) **(Fig. 3.9a)**. MCL-1^{Matrix} localized to mitochondria, and only produced a single protein species **(Fig. 3.9b, c)**. Moreover, MCL-1^{Matrix} was completely resistant to protease attack even under conditions of osmotic shock illustrating that it localizes to the matrix **(Fig. 3.9d)**.

Inhibition of Cell Death Requires Outer Membrane-localized MCL-1

Given that MCL-1 antagonizes cell death, we assessed the anti-apoptotic activities of the different mitochondrial localized mutants of MCL-1. Similar levels of wt MCL-1, MCL-1^{OM}, or MCL-1^{Matrix} were stably expressed in *Mcl-1*$^{f/f}$ Rosa-ERCreT2 MEFs **(Fig. 3.10a)**. *Mcl-1*-deletion in MEFs did not induce spontaneous apoptosis **(Fig. 3.1 b)**, but rendered them highly susceptible to cell death stimuli **(Fig. 3.10b, c)**. Expression of either wt MCL-1 or MCL-1^{OM} protected the MEFs from apoptosis; however, MCL-1^{Matrix} expressing MEFs were completely sensitive to cell death **(Fig. 3.10b, c)**. Furthermore, the expression of hBCL-2 in the *Mcl-1*-deleted MEFs rendered cells substantially more resistant to death stimuli **(Fig. 3.10b, c)**. MCL-1 binds and sequesters pro-apoptotic BH3-only molecules, such as BIM, preventing OMM permeabilization and activation of the downstream apoptotic cascade (Opferman et al., 2003). Both the 40 kD species of wt MCL-1 and MCL-1^{OM} co-immunoprecipitated with pro-apoptotic BIM; however, no interaction was detectable between BIM and the 36 kD species of wt MCL-1 or between BIM and MCL-1^{Matrix} **(Fig. 3.10d)**. Thus, MCL-1^{OM} can bind pro-apoptotic modulators and prevent cell death similarly to wt MCL-1, but MCL-1^{Matrix} cannot sequester pro-apoptotic modulators or prevent apoptosis.

Figure 3.8.   Both the Amino (N)- and Carboxy (C)-termini Are Required for Proper Mitochondrial Localization of MCL-1.

(a) Schematic illustration of MCL-1 deletion mutants. Yellow boxes indicate BCL-2 homology (BH) domains and the red box indicates the C-terminal hydrophobic domain. (b) Confocal immunofluorescence of *Mcl-1*-deficient MEFs transiently-expressing indicated *Mcl-1* constructs were fixed and stained for MCL-1 (green), mitochondria (Mitotracker, in red), and nucleus (DAPI, in blue). Co-localization of green and red channels is shown in yellow overlay. Size bars represent 10µm. (c) Whole cell lysates (WCL), isolated heavy membranes (HM) enriched for mitochondria or cytosolic (cyto) sub-cellular fractions were isolated from *Mcl-1*-deleted MEFs stably-expressing indicated MCL-1 constructs. Fractions were western blotted for MCL-1, BAX (cytosolic marker) or MnSOD (mitochondrial marker). (d) Mitochondria from *Mcl-1*-deficient MEFs stably-expressing human BCL-2 (hBCL-2) or a chimeric fusion of the first 50 amino acids of MCL-1 to hBCL-2 (mMCL-1^{50}-hBCL-2) were subjected to protease treatment as described in **Fig. 3.5**. Both the fusion protein and hBCL-2 were detected with anti-hBCL-2 antibody.

a

									331
wt	BH4	MCL-1	BH3	BH1	BH2	C			

ΔN — 67 — MCL-1ΔN — BH3 — BH1 — BH2 — C

ΔC — BH4 — MCL-1ΔC — BH3 — BH1 — BH2

b

MCL-1 Mitotracker DAPI Overlay

Mcl-1

*Mcl-1*ΔN

*Mcl-1*ΔC

c

Mcl-1   *Mcl-1*ΔN   *Mcl-1*ΔC

WCL Cyto HM   WCL Cyto HM   WCL Cyto HM

MCL-1

BAX (Cytosol)

MnSOD

d

         mMCL-1^50-

hBCL-2   hBCL-2

PK   - + - + +   - + - + +
OS   - - + + -   - - + + -
SDS - - - - +   - - - - +

hBCL-2

mBCL-2

Opa1

MnSOD

36
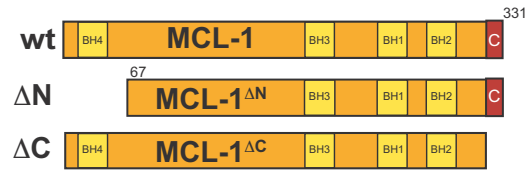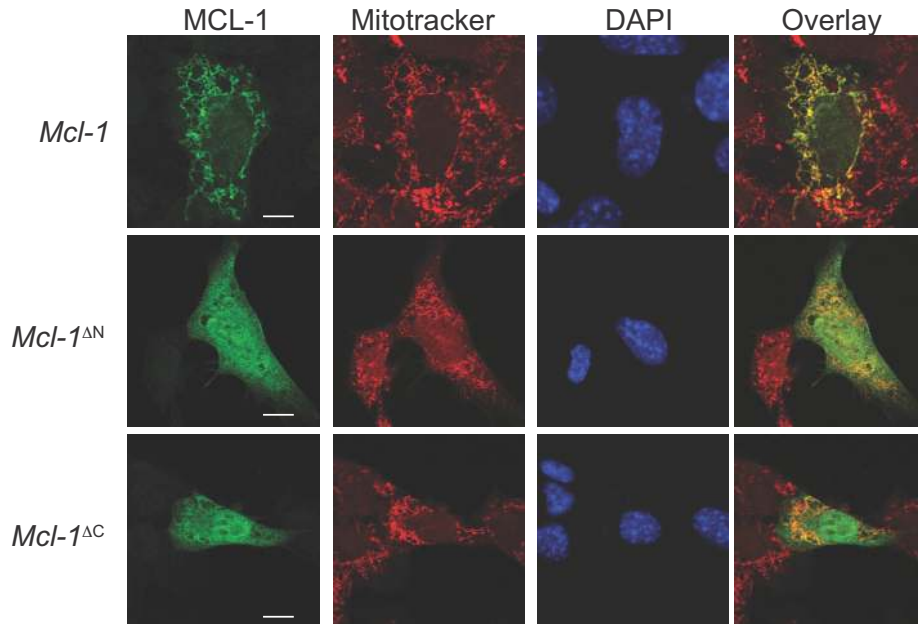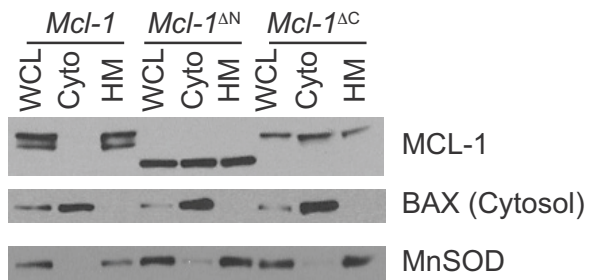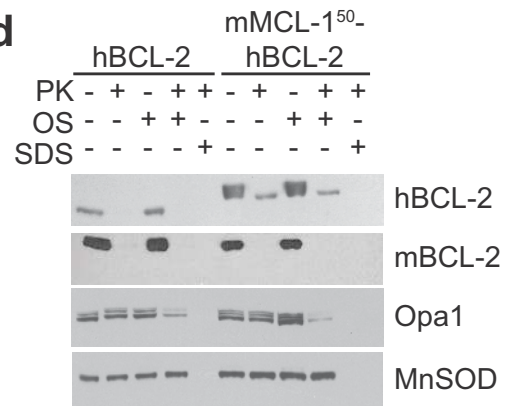
Figure 3.9.   MCL-1 Mutants Restrict Mitochondrial Localization.
(a) Schematic illustration of MCL-1 mutants. Yellow boxes indicate BCL-2 homology (BH) domains and the red box indicates the carboxy (C)-terminal hydrophobic domain. Point mutations are indicated with the original amino acid, site-position and mutated residue. N. crassa ATP-synthase MTS is indicated in green. (b) Confocal immunofluorescence of *Mcl-1*-deficient MEFs transiently expressing indicated *Mcl-1* constructs were fixed and stained for MCL-1 (green), mitochondria (Mitotracker, in red), and nucleus (DAPI, in blue). Co-localization of green and red channels is shown in yellow overlay. Scale bars represent 10µm. (c) Mitochondria enriched, heavy membrane (HM) or cytosol (cyto) sub-cellular fractions were isolated from *Mcl-1*-deficient MEFs stably-expressing indicated constructs. Whole cell lysates (WCL) were run as a control. Fractions were resolved and western blotted for MCL-1, BAX (cytosol) or MnSOD (matrix). (d) Mitochondria from *Mcl-1*-deficient MEFs stably-expressing indicated constructs were subjected to protease treatment as described in **Fig. 3.5**.

a

b

c

d

38
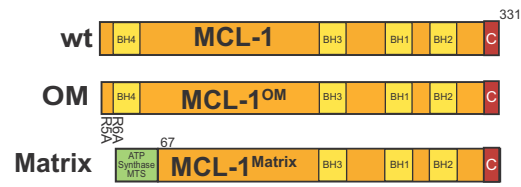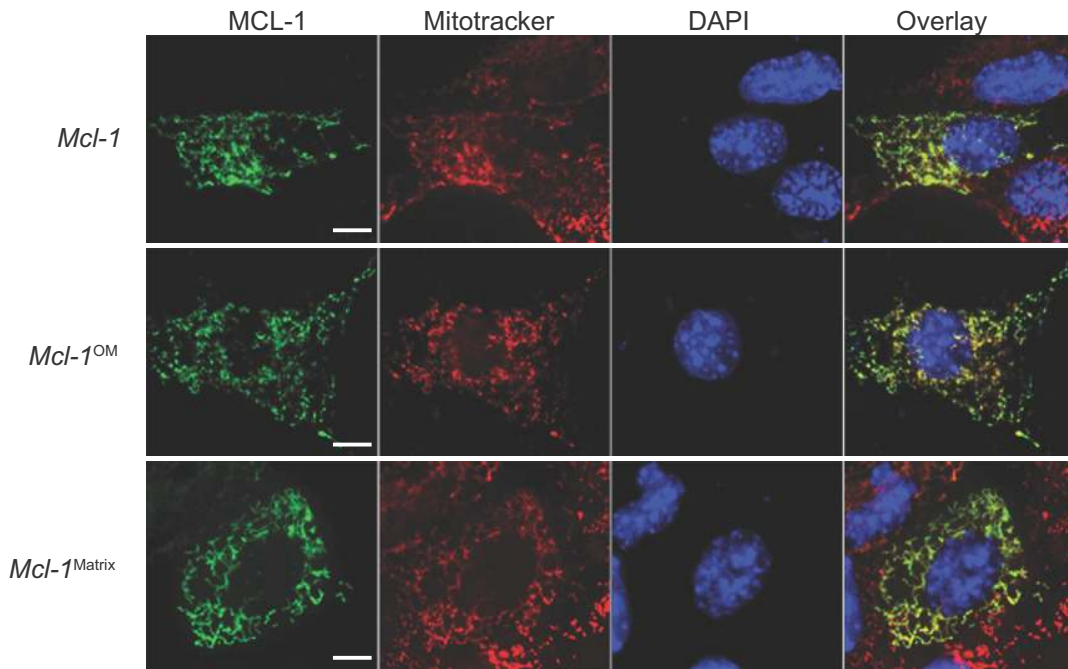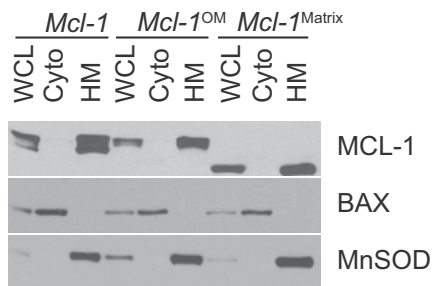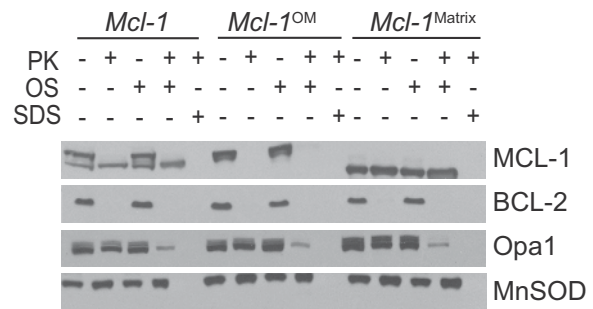
Figure 3.10. Anti-apoptotic Activity of MCL-1 Requires Localization to the Outer Mitochondrial Membrane.

(a) *Mcl-1*$^{f/f}$ Rosa-ERCreT2 MEFs stably-expressing indicated constructs were treated for 48 hours with tamoxifen to induce deletion of endogenous *Mcl-1* then western blotted for MCL-1, hBCL-2, or Actin (loading control). Vector-expressing, tamoxifen-treated wt Rosa-ERCreT2 MEFs (lane 1) serve as control. (b & c) Rosa-ERCreT2 MEFs stably-expressing indicated constructs were treated for 96 hours with tamoxifen to induce deletion of endogenous *Mcl-1* and were administered indicated doses of (b) staurosporine for 16 hours or (c) etoposide for 24 hours after which cell death was determined. Annexin-V and PI double-negative cells were scored as viable. Bars represent the average of 3 independent experiments and the error bars denote the SEM. Vector-expressing, tamoxifen-treated wt Rosa-ERCreT2 MEFs serve as control. (d) Lysates were immunoprecipitated with anti-BIM or anti-rat IgG antibody and immune complexes were resolved and immunoblotted for MCL-1 and hBCL-2. Endogenous murine BCL-2 (mBCL-2) serves as a control for equal BIM immunoprecipitation. 1/10th input of immunoprecipitation is depicted. Post-immunoprecipitated supernatants (Unbound Flow Through) indicate non-precipitated proteins remaining in lysate.
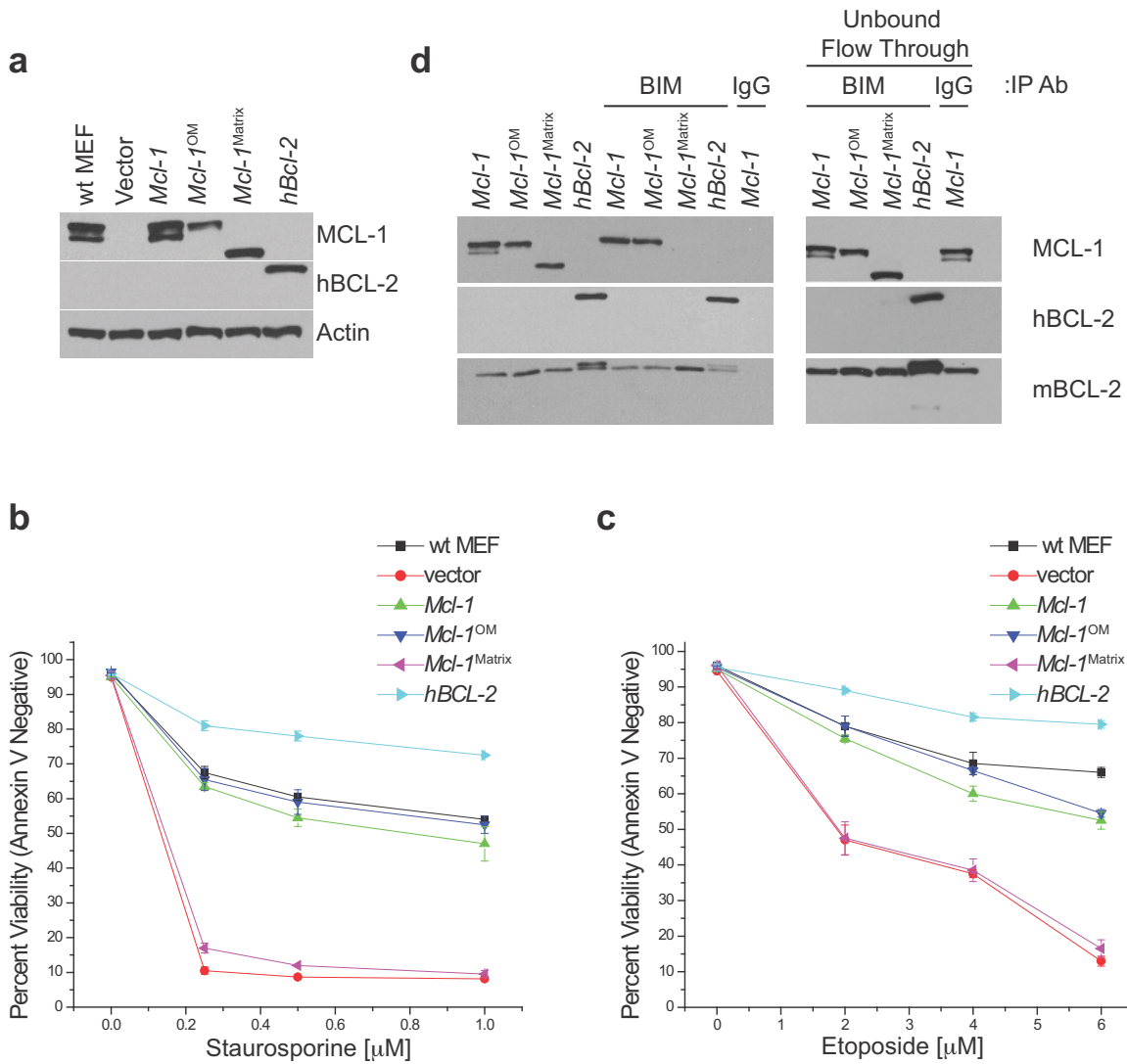
MCL-1 Matrix-localized MCL-1 Is Required for Normal IMM Structure and Efficient Mitochondrial Fusion

Since *Mcl-1*-deletion resulted in ultrastructural abnormalities in both primary and transformed cells **(Fig. 3.2c, d & Fig. 3.3a)** we investigated whether reintroduction of MCL-1^{Matrix} can rescue the abnormal IMM structure. Expression of either wt MCL-1 or MCL-1^{Matrix} largely restored normal IMM structure whereas MCL-1^{OM} did not **(Fig. 3.11a, b)**. Because mitochondrial structure is regulated by the opposing processes of fission and fusion (Chen et al., 2010) and *Mcl-1*-deleted cells had fragmented mitochondria **(Fig. 3.2a, b)**, we asked which form of MCL-1 is required for normal matrix fusion. Accordingly, we used photo-activatable-GFP targeted to the mitochondrial matrix (Karbowski et al., 2004). Upon *Mcl-1*-deletion, there was a significant delay in mitochondrial fusion that could be corrected by expression of either wt MCL-1 or MCL-1^{Matrix} but not by MCL-1^{OM} or hBCL-2 **(Fig. 3.11c, d)**. Furthermore, expression of human MCL-1 could ameliorate the delay in fusion and functionally compensated for loss of mouse MCL-1 implying this function is evolutionarily conserved **(Fig. 3.12)**. Therefore, matrix-localized MCL-1 is necessary to promote normal IMM structure, efficient mitochondrial fusion and maintenance of the mitochondrial reticular network.

Normal Mitochondrial Bioenergetics Requires Matrix-localized MCL-1

Whereas the structure of the IMM is intricately linked to the metabolic status of the mitochondria (Vogel et al., 2006) and defects in mitochondrial morphology are associated with respiratory dysfunction (Chen et al., 2010), we examined the role of MCL-1^{Matrix} in promoting efficient ATP generation and oxidative phosphorylation. Transformed MEFs generate energy predominantly by glycolysis rather than by oxidative phosphorylation, therefore to stimulate mitochondrial respiration they were cultured in glucose-free media supplemented with galactose (Reitzer et al., 1979; Rossignol et al., 2004). Under these conditions, *Mcl-1*-deletion significantly reduced ATP levels, but expression of either wt MCL-1 or MCL-1^{Matrix} restored normal ATP levels **(Fig. 3.13a)**. In contrast, expression of either MCL-1^{OM} or hBCL-2 in the *Mcl-1*-deleted MEFs did not rescue ATP levels, suggesting that merely restoring anti-apoptotic function is insufficient to promote normal energy production **(Fig. 3.13a)**. Since the proton gradient across the IMM drives ATP synthesis, we assessed whether the mitochondrial membrane potential was altered in cells lacking MCL-1. Indeed, *Mcl-1*-deletion decreased mitochondrial membrane potential, which was improved by stable expression of either wt MCL-1 or MCL-1^{Matrix}, but not MCL-1^{OM} **(Fig. 3.13b, c)**. When grown in galactose-media, *Mcl-1*-deleted MEFs also exhibited slower proliferation compared to control cells **(Fig. 3.13d)**. Expression of either wt MCL-1 or MCL-1^{Matrix} corrected the proliferative defect, whereas MCL-1^{OM} or hBCL-2 expression was unable to compensate for endogenous *Mcl-1*-deletion **(Fig. 3.13d)**. This suggests that the proliferative defect is not due to a small amount of apoptosis since MCL-1^{Matrix} does not reatain anti-apoptotic activity but proliferates faster than MCL-1^{OM}. Consequently, MEFs lacking matrix-localized MCL-1

Figure 3.11.   Lacking Matrix-localized MCL-1 Results in Mitochondrial IMM Structure and Fusion Defects.
(a) Transmission electron micrographs (12,000X) of *Mcl-1*$^{f/f}$ Rosa-ERCreT2 MEFs stably-expressing indicated constructs were treated with tamoxifen to induce deletion of endogenous *Mcl-l*. Scale bars represent 500 nm. (b) Quantification of mitochondrial cristae morphology from *Mcl-1*$^{f/f}$ Rosa-ERCreT2 MEFs stably-expressing indicated constructs that were treated with tamoxifen to induce deletion of endogenous *Mcl-1*. Mitochondria were cunted from ~100 individual cells and scored for normal (lamellar) or ballooned and swollen cristae (disorganized). Error bars indicated the SEM from 3 independent experiments. (c) Mitochondrial fusion was measured 96 hours after *Mcl-1*-deletion in *Mcl-1*$^{f/f}$ Rosa-ERCreT2 MEFs stably-expressing indicated constructs. Cells were transiently-transfected with photoactivatable-GFP (PA-GFP) targeted to the mitochondrial matrix. Depicted are representative images from 2, 30, and 60 minutes after PA-GFP activation. Scale bars represent 10µm. (d) Quantitation of the rate of mitochondrial fusion measured 96 hours after *Mcl-1*-deletion as the ratio of remaining activated mitochondrial area. Data represent average and SEM of fluorescence area over time of 3 independent experiments (n=16 cells). As mitochondria fuse, the PA-GFP signal dilutes decreasing intensity of signal in the area of activation.

a

Mcl-1

Mcl-1^{OM}

Mcl-1^{Matrix}

b

Cristae Morphology (% of mitochondria)

- Lamellar
- Disorganized

Vector   *Mcl-1*   *Mcl-1*^{OM}   *Mcl-1*^{Matrix}

c

Time After Photoactivation (min)

2   30   60

Vector

Mcl-1

Mcl-1^{OM}

Mcl-1^{Matrix}

d

Remaining Ratio of Activated Mitochondria

- Vector
- *Mcl-1*
- *Mcl-1*^{OM}
- *Mcl-1*^{Matrix}
- hBCL-2

Time (Minutes)

43
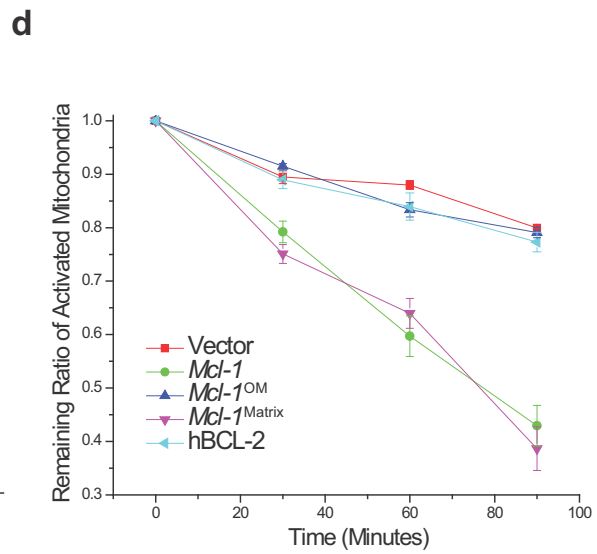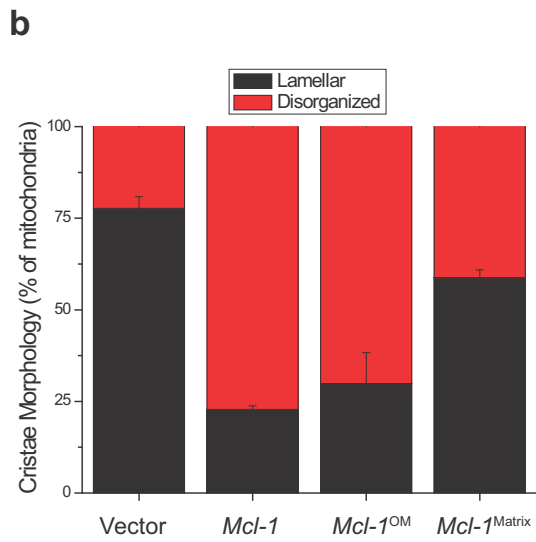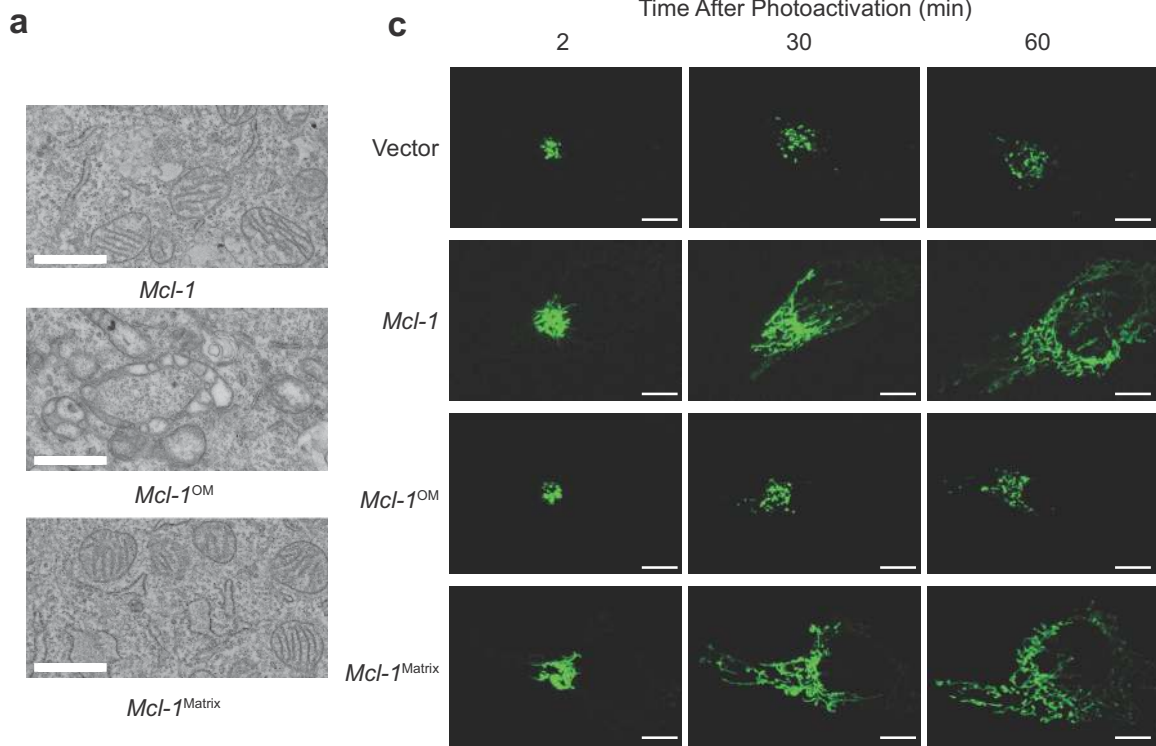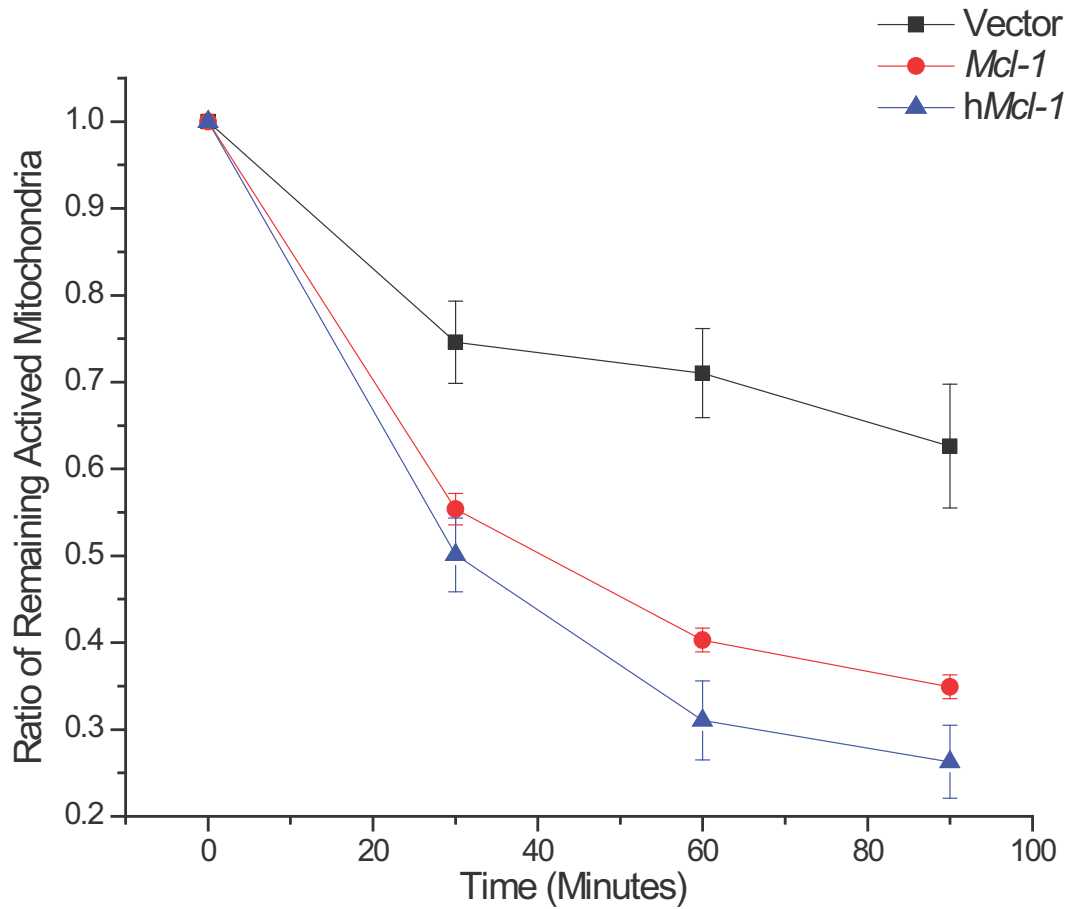
Figure 3.12. **Human MCL-1 Rescues Mitochondrial Fusion Defect.**
Mitochondrial fusion was measured 96 hours after *Mcl-1*-deletion in *Mcl-1*[f/f] Rosa-ERCreT2 MEFs stably-expressing indicated constructs. Cells were transiently-transfected with photoactivatable-GFP (PA-GFP) targeted to the mitochondrial matrix. Quantification rate of mitochondrial fusion is indicated as a ratio of remaining activated mitochondrial area. Data represent average and SEM of fluorescence area over time of 3 independent experiments (n=16 cells).

Figure 3.13.   Matrix-localized MCL-1 Is Required for Efficient Bioenergetics and Proliferation.

(a) *Mcl-1*$^{f/f}$ Rosa-ERCreT2 MEFs stably-expressing indicated constructs were grown in glucose-free media containing galactose and treated for 96 hours with tamoxifen to induce deletion of endogenous *Mcl-1* and total cellular ATP was evaluated in galactose media. Vector-expressing, tamoxifen-treated wt Rosa-ERCreT2 MEFs serve as positive control. Data represent the averages of 3 independent experiments and the error bars denote the SEM. Statistical significance was determined by unpaired t-test (*p<0.01).
(b) Quantification of mitochondrial membrane potential from *Mcl-1*$^{f/f}$ Rosa-ERCreT2 MEFs, stably-expressing indicated constructs, were treated for 96 hours with tamoxifen to induce deletion of endogenous *Mcl-1* and stained with 10 nM TMRM and imaged. Data represent average mean fluorescence intensities and SEM from 20 cells. (c) *Mcl-1*$^{f/f}$ Rosa-ERCreT2 MEFs stably-expressing indicated constructs that were treated for 96 hours with tamoxifen to induce deletion of endogenous *Mcl-1* and were stained with 20 nM TMRM and imaged for mitochondrial membrane potential.   (d) *Mcl-1*$^{f/f}$ Rosa-ERCreT2 MEFS stably-expressing indicated constructs were grown in glucose-free media containing galactose and were treated with tamoxifen (48 hours), seeded in glucose-free media containing galactose, and counted by hemocytometer at the indicated times. Vector-expressing, tamoxifen-treated wt Rosa-ERCreT2 MEFs serve as a control. The data represent averages and SEM of 3 independent experiments. Statistical significance of control versus *Mcl-1*-deleted and MCL-1^{OM} versus MCL-1^{Matrix} were determined by unpaired t-test (p<0.001).

a

Total Cellular ATP (mM)

wt MEF | Vector | *Mcl-1* | *Mcl-1*^{OM} | *Mcl-1*^{Matrix}

b

TMRM (Mean Fluorescence Intensity)

Vector | *Mcl-1* | *Mcl-1*^{OM} | *Mcl-1*^{Matrix}

c

Deleted | *Mcl-1*

Mcl-1^{OM} | *Mcl-1*^{Matrix}

d

Total Cell Number(X10^6)

Time (Days)

- ■ wt *Mcl-1*
- ● *Mcl-1*^{Deleted}
- ▲ *Mcl-1*^{Deleted}+*Mcl-1*
- ▼ *Mcl-1*^{Deleted}+*Mcl-1*^{OM}
- ◄ *Mcl-1*^{Deleted}+*Mcl-1*^{Matrix}
- ► *Mcl-1*^{Deleted}+hBCL-2
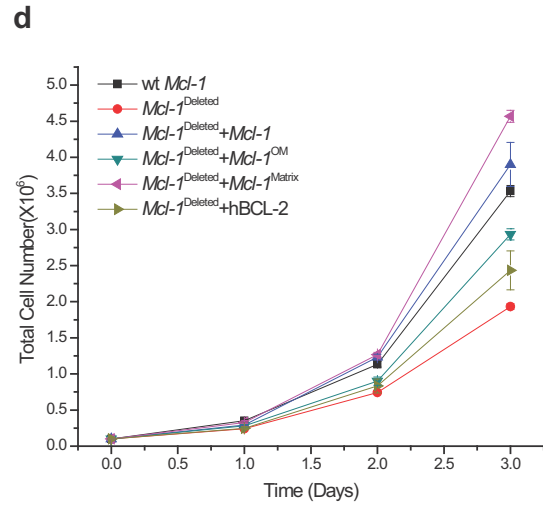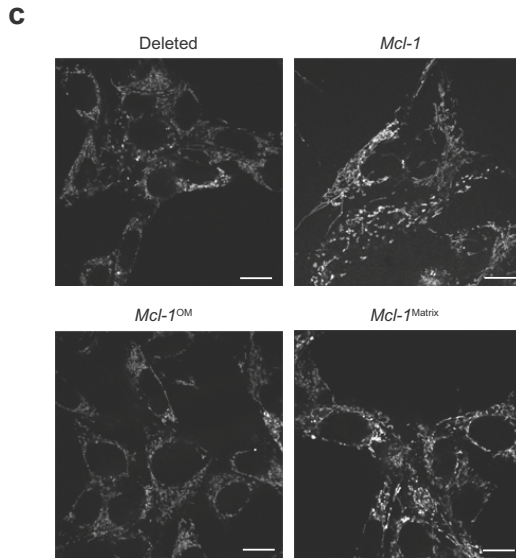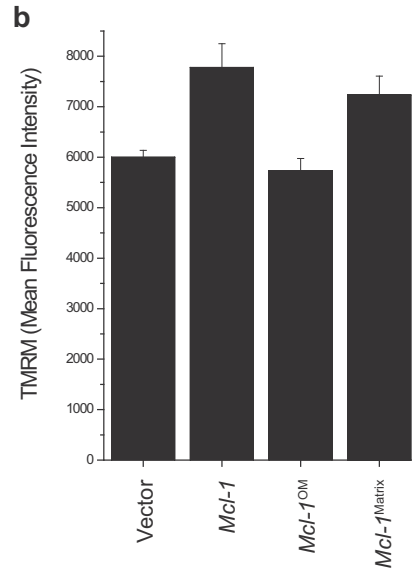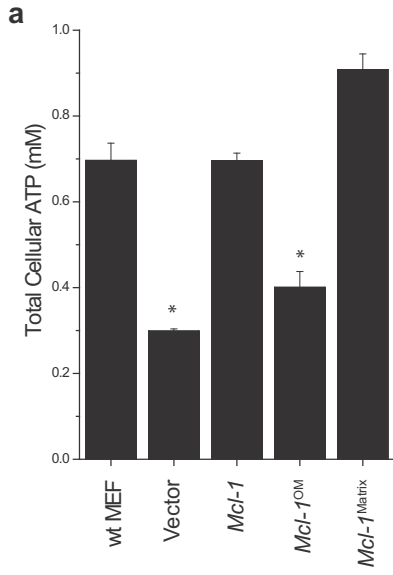
generate less energy, have decreased mitochondrial membrane potential, and grow poorly in galactose-media even in the presence of anti-apoptotic MCL-1 on the OMM.

Respiratory complexes pass electrons through the electron transport chain components to reduce molecular oxygen, thus generating a proton gradient that drives ATP production by the F_1F_0-ATP synthase (Wallace, 1999). Since both mitochondrial membrane potential and ATP production were decreased in *Mcl-1*-deleted MEFs **(Fig. 3.13a, b, c)** we determined if respiration was altered by measuring oxygen consumption rates (OCR) using the Seahorse XF24 analyzer (Ferrick et al., 2008). *Mcl-1*-deletion decreased basal OCR by ~50% compared to non-deleted MEFs **(Fig. 3.14a)**. Expression of either wt MCL-1 or MCL-1^{Matrix} fully restored basal OCR; whereas neither MCL-1^{OM} nor hBCL-2 expression could restore normal basal OCR **(Fig. 3.14a)**. To induce maximal OCR, a proton ionophore, FCCP, was added in order to dissipate the proton gradient, thereby activating maximum respiration (Nicholls, 1974). Strikingly, *Mcl-1*-deleted MEFs were incapable of increasing their OCR above basal rates when treated with FCCP **(Fig. 3.14b)**; however, maximal OCR was completely restored by expression of either wt MCL-1 or MCL-1^{Matrix}, but not by MCL-1^{OM} or hBCL-2 **(Fig. 3.14b)**. Collectively, matrix-localized MCL-1 is required for optimal oxidative phosphorylation in cells, a function that is acutely separate from its anti-apoptotic role at the OMM.

Elevations in mitochondrial reactive oxygen species (ROS) are common in cells with mitochondrial dysfunction (Wallace, 1999). Upon *Mcl-1*-deletion, mitochondrial superoxide levels were elevated, but expression of either wt MCL-1 or MCL-1^{Matrix} prevented the increase in mitochondrial superoxide production, consistent with their ability to rescue normal mitochondrial function **(Fig. 3.14c)**. In contrast, neither hBCL-2 nor MCL-1^{OM} could prevent increased superoxide generation, indicating that merely restoring anti-apoptotic function is inadequate to prevent superoxide induction **(Fig. 3.14c)**. Hence, expression of the mitochondrial matrix form of MCL-1 is sufficient to both maintain mitochondrial respiration and prevent potentially dangerous ROS production in cells.

MCL-1 Is Required for Assembly of F1F0-ATP Synthase Oligomers

The movement of electrons through the respiratory complexes depends on the structure and assembly of the electron transport chain complexes (Acin-Perez et al., 2008). Structural and functional evidence has revealed that the individual electron transport chain complexes (I, II, III, and IV) organize into inter-complex assemblies known as supercomplexes, which are disrupted in the absence of one of their component complexes (Acin-Perez et al., 2008). The supramolecular organization of respiratory complexes is hypothesized to increase the efficiency of electron transport and minimize ROS production (Acin-Perez et al., 2008; Genova et al., 2008). *Mcl-1*-deletion did not affect the total protein expression of nuclear-encoded respiratory chain subunits; however, the mitochondrial DNA-encoded subunits of complex IV (Cox 1 and Cox 2) protein levels were decreased **(Fig. 3.15a)**. Therefore, we investigated whether the decreased Cox 1 and Cox 2 expression may be due to alterations in mitochondrial DNA

Figure 3.14. Cells Deficient in Matrix-localized MCL-1 Have Defects in Oxygen Consumption.

(a & b) Oxygen consumption measured 96 hours after *Mcl-1*-deletion in *Mcl-1*$^{f/f}$ Rosa-ERCreT2 MEFs stably-expressing indicated constructs under (a) basal and (b) FCCP-uncoupled (maximal) respiration. Vector-expressing, tamoxifen-treated wt Rosa-ERCreT2 MEFs serve as positive control. Experiments were performed in triplicate and the bars represent averages (n=9) and the error bars denote the standard of deviation. Statistical significance was determined by unpaired t-test (*p<0.01, **p<0.05). (c) Superoxide was detected by mitoSOX fluorescence 96 hours after *Mcl-1*-deletion in *Mcl-1*$^{f/f}$ Rosa-ERCreT2 MEFs stably-expressing indicated constructs. Vector-expressing, tamoxifen-treated wt MEFs serve as a negative control. Average mean fluorescence intensity (MFI) of 3 independent experiments and error bars indicate the SEM. Statistical significance was determined by unpaired t-test (*p<0.01).
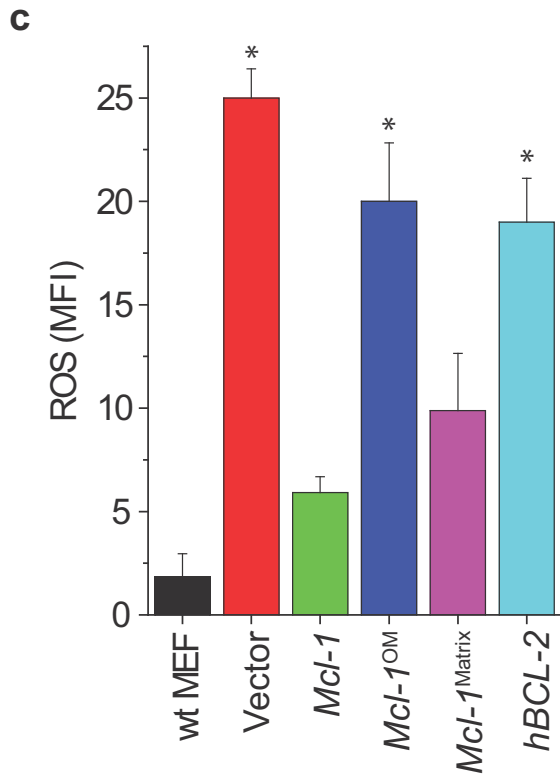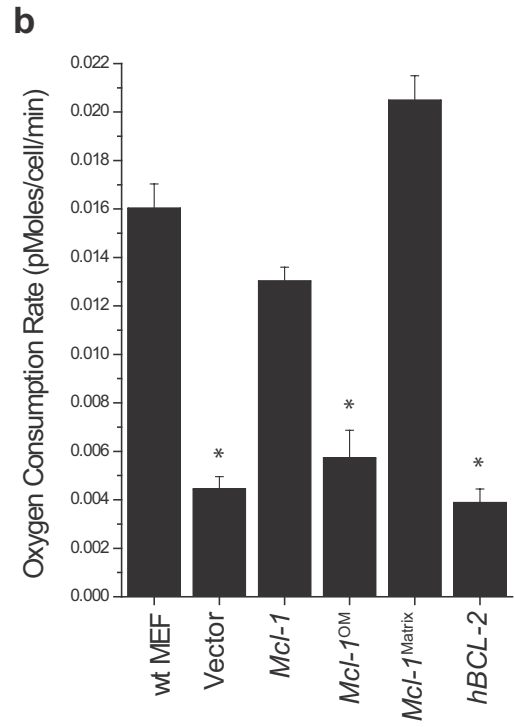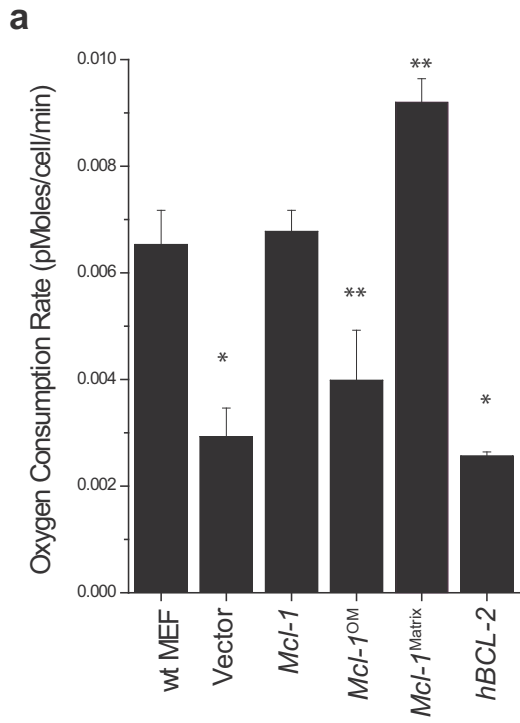
Figure 3.15.   MCL-1 Is Required for Assembly of Supercomplexes.
(a) Total mouse liver lysates from *Mcl-1*[f/f] Mx1-Cre (*Mcl-1*-deleted) or wt Mx1-Cre (wt) mice 14 days after treatment with pI-pC were lysed in RIPA and resolved by SDS-PAGE. Immunoblot were probed to determine expression of Complex I (NDUFA9), Complex II (Fp70), Complex III (Core 2), Complex IV (Cox I and Cox 2), ATP Synthase subunit F0 B (5F1), ATP Synthase F1 subunit beta (5B), Succinate dehydrogenase, MnSOD, and MCL-1. Asterix (*) denotes mtDNA-encoded protein (b) Assessment of mtDNA and nDNA by quantitative real-time PCR. (c & d) Mouse liver mitochondria from *Mcl-1*[f/f] Mx1-Cre (*Mcl-1*-deleted) or wt Mx1-Cre (wt) mice 14 days after treatment with pI-pC were lysed in digitonin and resolved by blue native gel polyacrylamide electrophoresis (BN-PAGE) and blotted to determine native complexes and supercomplexes (SC). (c) complex I (CI, detected by NDUFA9), complex II (CII, detected by Fp70), complex III (CIII, detected by Core 2) and complex IV (CIV, detected by Cox I) and (d) ATP Synthase subunit F0 B (5F1), F1 subunit beta (5B). The native migration of monomers, dimers, and oligomers are denoted.

a

MCL-1

Cox 2 (Complex IV) *

Cox 1 (Complex IV) *

NDUFA9 (Complex I)

Fp 70 (Complex II)

Core 2 (Complex III)

ATP5F1
(F0 Subunit B)

ATP5B
(F1 Subunit beta)

Succinate Dehydrogenase

MnSOD

b

c

NDUFA9
(Complex I)

Fp 70
(Complex II)

Core 2
(Complex III)

Cox 1
(Complex IV)

d

ATP5F1
(F0 Subunit B)

ATP5B
(F1 Subunit beta)

51
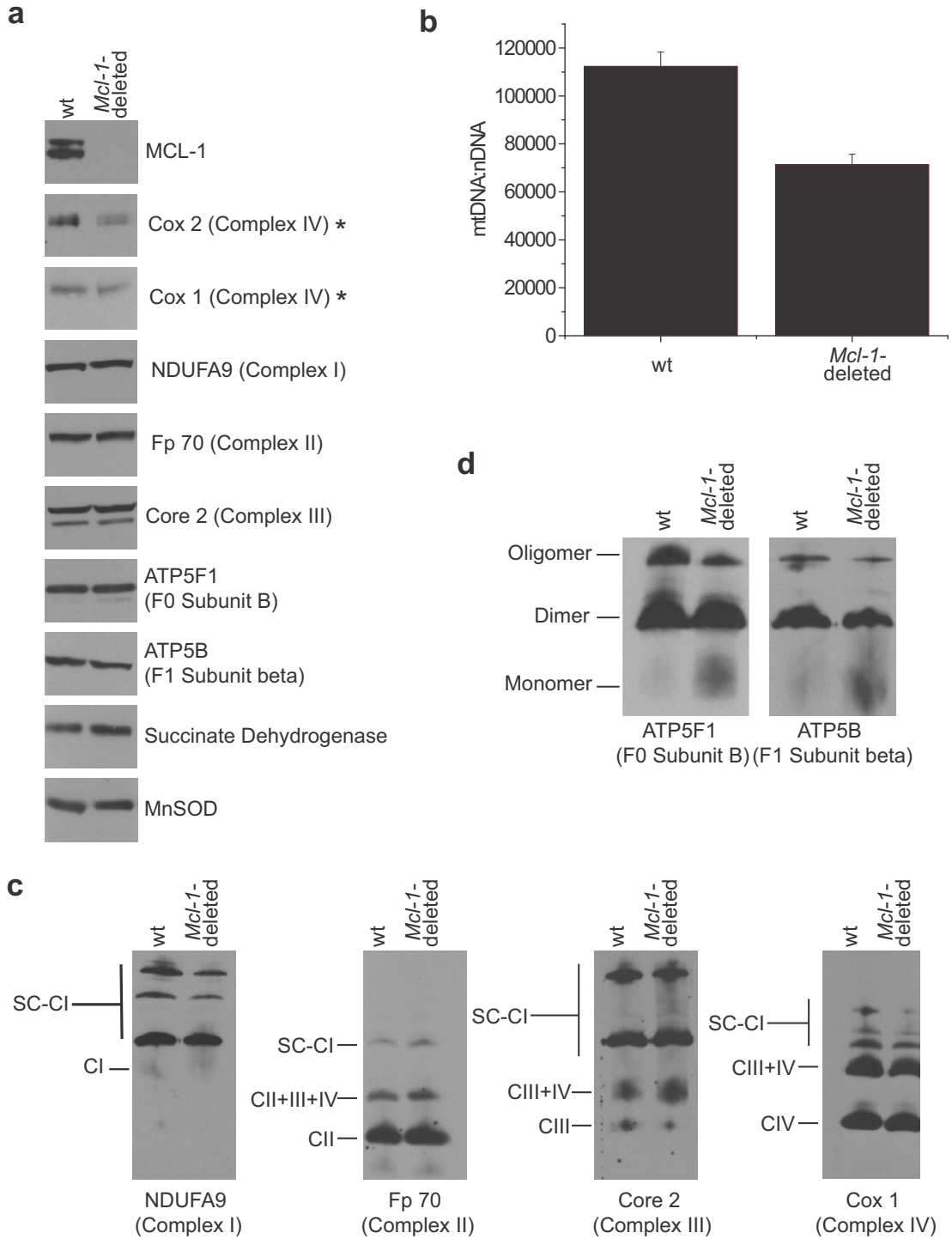
(mtDNA). Indeed, *Mcl-1*-deletion decreased mtDNA content **(Fig. 3.15b)**. To investigate the structure of the respiratory complexes and supercomplexes, we used blue native-polyacrylamide gel electrophoresis (BN-PAGE). Consistent with the loss of the Cox 1 and Cox 2 subunits of complex IV, *Mcl-1*-deleted liver mitochondria also exhibited aberrant assembly of large supercomplexes (composed of complexes I, III, and IV) as detected by Cox 1 immunoblot **(Fig. 3.15c)**. This is in agreement with the effects of deletion of complex IV preventing the assembly of large supercomplexes (Acin-Perez et al., 2008; Diaz et al., 2006). In contrast, the smaller respiratory supercomplexes appeared relatively unaffected by *Mcl-1*-deletion **(Fig. 3.15c)**. Therefore, *Mcl-1*-deletion results in diminished mtDNA, reduced protein expression of Cox 1 and Cox 2 subunits, and alterations in the large supercomplexes containing complexes I, III, and IV.

The F_1F_0-ATP synthase also adopts supramolecular structures including the constitutive assembly of ATP synthase homo-dimers and higher-order homo-oligomers (Krause et al., 2005). Furthermore, the assemblage into dimers and oligomers proffered as a determinant of the mitochondrial cristae structure and suggested to enhance efficiency of function (Giraud et al., 2002; Gomes et al., 2011; Thomas et al., 2008). As such, mutations that prevent the oligomerization of ATP synthase result in disorganized cristae membranes that form concentric circles and onion-like structures (Bornhovd et al., 2006; Paumard et al., 2002). By BN-PAGE, *Mcl-1*-deficient liver mitochondria possessed less oligomeric ATP synthase and exhibited a corresponding increase in the monomer **(Fig. 3.15d)**. The lack of F_1F_0-ATP synthase oligomers was not due to loss of the individual subunits, implying that the defect is in the oligomerization of ATP synthase **(Fig. 3.15a, d)**. Accordingly, *Mcl-1* is required for efficient assembly of F_1F_0-ATP synthase oligomers and in the absence of *Mcl-1* there is an increase in the monomeric form.

CHAPTER 4. DISCUSSION

MCL-1 in Normal Cells

MCL-1 is a unique anti-apoptotic BCL-2 family member in that its genetic ablation results in cell autonomous deficiencies in a myriad of cellular lineages (Arbour et al., 2008; Dzhagalov et al., 2008; Dzhagalov et al., 2007; Opferman et al., 2005; Opferman et al., 2003; Rinkenberger et al., 2000; Steimer et al., 2009). However, *Mcl-1* gene ablation disables both its anti-apoptotic activity at the OMM as well as its ability to facilitate mitochondrial function within the matrix. For that reason, it will be important to determine the relative contributions of MCL-1's different functional roles for promoting the survival and development of hematopoietic and neuronal lineages. It is conceivable that both roles of MCL-1 may be critical for normal cell viability. For example, differentiating cells are subjected to expansion, selection, and homeostatic regulation often regulated by the access to growth factors in the cellular microenvironments. As such, MCL-1's critical function during these stages may be to support cell survival by antagonizing apoptosis. However, it is also possible that during cellular proliferation and differentiation, metabolic demands on the mitochondria are modulated. Thus, MCL-1's critical function during such stages may be to facilitate mitochondrial fitness thereby opposing increased demands for oxidative phosphorylation. We anticipate that genetic studies separating MCL-1's functional role at the OMM and matrix will be necessary to delineate the contribution of these roles to normal cellular development and survival.

MCL-1 in Embryonic Development

Germline ablation of *Mcl-l* in mice results in an early preimplantation embryonic lethality at embryonic day 3.5 and, specifically, the embryos have a defective trophoectoderm (Rinkenberger et al., 2000). Other anti-apoptotic BCL-2 family members do not display such a severe developmental phenotype, suggesting that MCL-1 plays a unique role during early embryonic development. While apoptosis is extremely important during development, none of the other apoptotic regulators are required at such an early embryonic developmental stage (Ranger et al., 2001). Mitochondria have been shown to play an important role during the preimplantation stage embryo as aerobic metabolism is the primary source of ATP in the mouse blastocyst (Benos and Balaban, 1983). Furthermore, mitochondria in the trophoectoderm of the blastocyst have a high inner membrane potential, indicating that these mitochondria are actively respiring, which is important for early embryonic development (Van Blerkom et al., 2006). Precisely why *Mcl-1* is required for implantation has remained elusive. One possibility is that MCL-1 facilitates mitochondrial energy production that is required for differentiation of cytotrophoblasts into the intermediate trophoblast and the syncytiotrophoblast. Failure of the cytotrophoblasts to differentiate could result in a defective trophoectoderm that is unable to implant. Another possibility is that MCL-1 is requisite for the mitochondria in the trophoectoderm to produce enough energy to allow invasion of the placenta. For these

reasons, it is plausible that MCL-1's role during embryonic development is not only to antagonize cell death but is also to promote normal mitochondrial function, assisting in differentiation and placental invasion of the trophoblast cells that compose the blastoyst. To determine if the anti-apoptotic or the mitochondrial functions of MCL-1 are important for early embryonic development, a knock-in gene targeting strategy using MCL-1 ^{OM} or MCL-1^{Matrix} could be used. If neither MCL-1 ^{OM} nor MCL-1^{Matrix} is sufficient for embryonic development then both functions of MCL-1 may be required. In that case, a polycistronic viral vector can be utilized to co-express both MCL-1 ^{OM} and MCL-1^{Matrix}.

MCL-1 in Hematopoiesis

The BCL-2 family members are important regulators of hematopoiesis. While transgenic expression of *BCL-2* in hematopoietic stem cells (HSCs) can increase their numbers in vivo (Domen et al., 2000), mice that are deficient for *Bcl-2* or *Bcl-x* deficient ES cells can both still produce hematopoietic cells; however, they exhibit effects later during specific lineage development (Motoyama et al., 1995; Veis et al., 1993). Instead, MCL-1 is the key pro-survival molecule during hematopoiesis as inducible deletion of *Mcl-1* results in rapid multi-lineage hematopoietic failure (Opferman et al., 2005). Along these lines, MCL-1 is unique because it is the essential survival factor for all early hematopoietic lineages.

The hematopoietic system gives rise to a variety of mature cells including myeloid and lymphoid lineages. HSCs maintain their populations through a balance of self-renewal and differentiation and it is unclear how much of a direct role apoptosis has in the regulation of this balance. In contrast, the more committed lineages, such as lymphocytes are potently regulated by apoptosis particularly through regulation by cytokines and growth factors (Opferman, 2007; Opferman and Korsmeyer, 2003). Evidence has shown that HSCs have a low mitochondrial membrane potential and are predominantly glycolytic (Simsek et al., 2010). This metabolic phenotype is a consequence of the hypoxic niche in the bone marrow (Simsek et al., 2010). Furthermore, long-term hematopoietic stem cells (LT-HSCs), which retain the capacity to self-renew, are in a quiescent state with a reduced metabolic rate (Wilson et al., 2008). In contrast, differentiation into the more committed progenitor cells is a high-energy demand process that requires mitochondrial function (Inoue et al., 2010).

Accordingly, the profound requirement for *Mcl-1* in hematopoietic stem cells may result from a synergy of both the anti-apoptotic and mitochondrial functions. It is possible that the signals for differentiation and proliferation are coupled such that matrix-localized and outer membrane-localized MCL-1 cooperate to provide increased energy upon differentiation into progenitor and antagonize apoptosis to sustain maintenance of the stem cell pool **(Fig. 4.1)**. Nevertheless, *Mcl-1* may have separate roles in distinct hematopoietic lineages. For example, matrix-localized MCL-1 may be important for early progenitors where proper mitochondrial function is required for differentiation whereas anti-apoptotic MCL-1 may be important for survival of the mature cells **(Fig. 4.1)**.
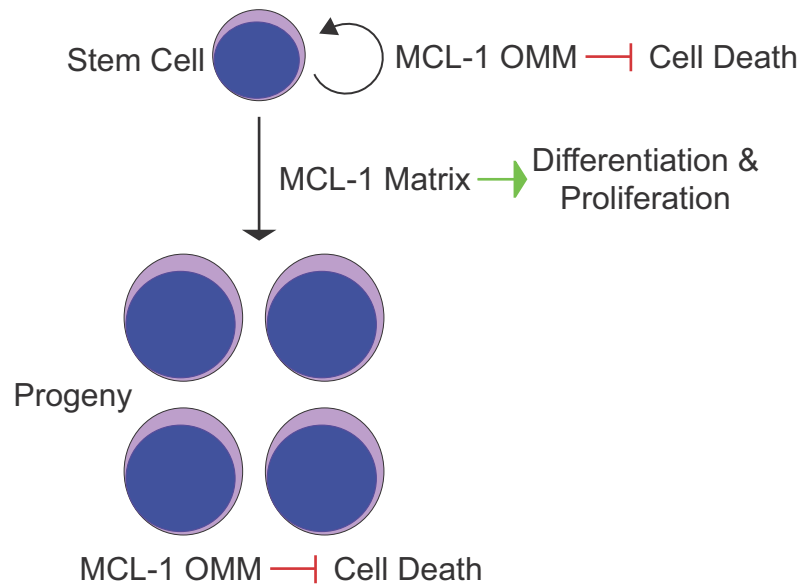
Figure 4.1.   Possible MCL-1 Functions in Normal Homeostasis
In normal stem cells, it is possible that the homeostatic control on self-renewal is regulated primarily by MCL-1's OMM anti-apoptotic activity. In contrast, the proliferation and differentiation of stem cells into progenitors and terminally differentiated lineages may require efficient energy production promoted by the truncated MCL-1 targeted to the matrix. Lastly, proper homeostasis of terminally differentiated cells is likely controlled primarily by MCL-1's OMM anti-apoptotic activity.

MCL-1 in the Brain

  The requirement of *Mcl-1* in the developing nervous system further illustrates the significance of this pro-survival molecule. In the absence of *Mcl-1* widespread apoptosis occurs in the embryo resulting in embryonic lethality at embryonic day 16 (Arbour et al., 2008). The development of the cerebral cortex is heavily dependent on apoptosis in order to select for appropriate cortical neurons before differentiation (Blaschke et al., 1996) Therefore, MCL-1 may help maintain the balance between proliferation and cell death during embryonic development of the cerebral cortex. However, in addition to apoptosis, neurons are extensively dependent on mitochondrial dynamics. The imbalance between healthy and dysfunctional mitochondria can be a determinant for neurodegenerative diseases such as Alzheimer's and Parkinson's (Chen et al., 2007). Mitochondria are abundant in synaptic regions since synaptic transmission requires a high ATP demand (Chan, 2006). It is possible that the different functional roles of MCL-1 at the OMM and the matrix may have different spatial and temporal requirements for maintaining neuronal survival and health. For example, during development of the nervous system, while neurons are being established and eliminated, the anti-apoptotic role of MCL-1 on the OMM may be the principal function.   Anti-apoptotic MCL-1 may be necessary to maintain the balance between life and death in developing neurons that are controlled by homeostatic selection processes. In comparison, MCL-1 may have an additional functional role in adult neurons. Mitochondrial fusion is necessary for mitochondria to travel long distances from the neuronal cell body to the axonal termini where they generate ATP, particularly in the motor and sensory neurons that enervate the hands and feet. In addition to antagonizing cell death, MCL-1 may also promote mitochondrial fusion in post-mitotic neurons.

Role of MCL-1 in Cancer and Cancer Therapy

  MCL-1 is one of the most highly amplified genes in a variety of human cancers (Beroukhim et al., 2010); therefore, it is imperative to understand the contribution of MCL-1's functions to oncogenesis. Furthermore, its expression is often associated with chemotherapeutic resistance and relapse (Wei et al., 2006; Wuilleme-Toumi et al., 2005). In many malignancies, MCL-1 appears to be a critical survival molecule. For instance, MCL-1 is critical for the development and maintenance of acute myeloid leukemia (Glaser et al., 2012; Xiang et al., 2010). Moreover, MCL-1 overexpression dramatically accelerates Myc-induced lymphomagenesis (Campbell et al., 2010). Similar to studies in normal cells, the majority of investigations into the role of *Mcl-1* in mouse models of cancer have genetically ablated both the anti-apoptotic and the mitochondrial functions of MCL-1 making it difficult to separate the functional contributions of MCL-1's anti-apoptotic and mitochondrial functions.

  Oncogenesis can activate tumor suppressor pathways that frequently initiate cell death pathways. Cancer cells often violate these key cellular checkpoints that would normally drive the cells to die by programmed cell death. As a result, they often overcome the apoptotic stress either by reducing the expression of pro-apoptotic factors

or, more frequently by up regulating anti-apoptotic molecules (Hanahan and Weinberg, 2011). For example, the amplification of *Myc* is one of the most frequent oncogenic occurrences observed in human cancers and drives carcinogenesis (Beroukhim et al., 2010). Oncogenic levels of Myc induce apoptosis that must be overcome in part by over-expression of anti-apoptotic molecules (Bissonnette et al., 1992; Eischen et al., 2001; Evan et al., 1992; Shi et al., 1992; Zindy et al., 1998). Accordingly, the anti-apoptotic function of MCL-1 and other anti-apoptotic family members may be obligate in their promotion of survival as a result of oncogenic stress.

Nevertheless, cancer cells are often rapidly dividing and require increases in biomass to support abnormal proliferation. Although cancer cells often metabolize extremely high levels of glucose by glycolysis, glutamine is another essential metabolite that is excessively consumed through glutaminolysis (Eagle, 1955; Reitzer et al., 1979). Glutamine is a mitochondrial-oxidizable substrate that is essential for macromolecular synthesis of nucleic acids, proteins, and lipids required for assembling new cells (DeBerardinis et al., 2007). In particular, oncogenic Myc has been linked to increased glutaminolysis through activation of a transcriptional program that renders cancer cells glutamine dependent (Wise et al., 2008; Yuneva et al., 2007).

Since *Mcl-1* is requisite for oncogenesis of Myc leukemia (Xiang et al., 2010) it is conceivable that both the anti-apoptotic and mitochondrial functions of MCL-1 play an important role in promoting the survival of Myc-induced cancer. Myc transformation causes cells to become dependent on anti-apoptotic molecules in order to overcome apoptotic stress; therefore, the anti-apoptotic activity of MCL-1 may be indispensable. Nevertheless, it is possible that the non-apoptotic function of MCL-1 may help fulfill the requirements for rapid cell proliferation in Myc-cancer cells by facilitating the generation of byproducts from mitochondrial metabolism (DeBerardinis et al., 2007; Deberardinis et al., 2008).

Cancer Stem Cells and Differentiation Therapy

Normal stem cells undergo self-renewing cell division, which means they generate daughter cells that have the ability to self-replicate and produce more differentiated cell lineages (Rossi et al., 2008). Cancer stem cells are defined as cancer cells that are capable of self-renewal and can give rise to a heterogeneous population of cancer cells (Vermeulen et al., 2008). For this reason, cancer stem cells can only be defined experimentally by their ability to generate the same clonal tumor when serially transplanted into immuno-compromised mice (Vermeulen et al., 2008). If cancer stem cells are ultimately responsible for tumor maintainance then a theurapeutic strategy capable of depleting the cancer stem cell pool may control malignancy. One potential way to deplete a cancer stem cell population is to induce the differentiation of the stem cells. As previously mentioned, differentiation is a process that requires increased mitochondrial function and, for this reason, the role of MCL-1 inside the matrix may be to facilitate differentiation. If matrix-localized MCL-1 promotes differentiation, then

utilizing the MCL-1^{Matrix} mutant as a strategy to induce differentiation and deplete the cancer stem cell pool may be an alternative strategy to treat cancer.

BCL-2 Family Inhibitors

There has been an increasing interest in developing BCL-2 family inhibitors as a cancer therapeutic strategy, focusing on antagonizing anti-apoptotic activity to foster cell death (Oltersdorf et al., 2005). One such inhibitor, obatoclax, is a BH3-mimetic that binds to BCL-2, BCL-X$_L$, and MCL-1 to disrupt their interaction with the pro-apoptotic molecules (Nguyen et al., 2007). Although obatoclax exhibits single-agent activity and can kill certain types of cancer cells *in-vitro*, it also has non-specific effects in which non-apoptotic cell death occurs (Li et al., 2008; McCoy et al., 2010; Tse et al., 2008). Additionally, ligands and modified peptides that are also BH3-mimetics modeled specifically for MCL-1's BH3-binding groove have been developed but to date appear to be only effective when combined with chemotherapeutic agents (Lee et al., 2008; Stewart et al., 2010b). One possibility for the lack of single-agent activity is that these BH3-mimetics only antagonize MCL-1's anti-apoptotic activity leaving its mitochondrial function unaffected; thus, they may be insufficient to promote cell death unless combined with another death-inducing agent. Paradoxically, genetic deletion of *Mcl-1* induces cell death in cancer cells regardless of complementary expression of other endogenous anti-apoptotic family members (Glaser et al., 2012; Xiang et al., 2010). Only when other anti-apoptotic BCL-2 family members are ectopically expressed can loss of MCL-1 be tolerated in these cancer cells (Glaser et al., 2012; Xiang et al., 2010). Thus, it is possible that the non-apoptotic, mitochondrial function of MCL-1 is important to promoting cancer cell survival and proliferation, but that overexpression of pro-survival molecules can overcome this stress. In light of the potential for MCL-1 to promote both cancer cell apoptotic resistance and to support the high rate of proliferation often observed in cancer cells, it is possible that inhibition of both the anti-apoptotic and mitochondrial functions of MCL-1 may synergize by restricting cancer cell expansion and activating cell death, thereby leading to more effective therapies.

Post-translational Regulation of MCL-1

Although MCL-1 has been shown to be ubiquitinated by several E3 ligases including, MULE, ßTRCP and FBW7, it is difficult to observe both the 40 kD and 36 kD isoforms of MCL-1 in these studies (Ding et al., 2007; Inuzuka et al., 2011; Zhong et al., 2005). However, the different MCL-1 isoforms were shown to possess different protein half-lives (De Biasio et al., 2007; Stewart et al., 2010a). For example, full length (40 kD) MCL-1 has an extremely short half-life, approximately 2 hours, while the N-terminally cleaved isoform (36 kD) is greater than 6 hours (Stewart et al., 2010a). This may be due to the differential localization of these MCL-1 isoforms, since the turnover of outer membrane and inner membrane proteins of the mitochondrion are quite different (Brunner and Neupert, 1968). The average half-life of outer mitochondrial membrane proteins was found to be ~4 days, which differs considerably from the half-life of inner

membrane proteins, ~12 days (Brunner and Neupert, 1968). In addition to observing that the MCL-1 isoforms have differential protein turnover rates, Stewart et al. also generated a lysine-less MCL-1 mutant where 14 lysine residues were mutated to arginine (MCL-1^{KR})(Stewart et al., 2010a). This mutant was unable to be ubiquitinated but, surprisingly did not change the turnover rate of the 40 kD MCL-1 isoform, however, dramatically changed the half-life of the 36 kD isoform from greater than 6 hours to ~2 hours (Stewart et al., 2010a). These observations are unexpected because MCL-1^{KR} was predicted to increase MCL-1 half-life since it could not be marked for degradation by the proteasome. A simple explanation for the rapid turnover of the 36 kD isoform of MCL-1^{KR} is that this mutant protein is not properly folding inside the mitochondria due to the 14 point mutations which may cause aberrations in the protein secondary structure. Consequently, the 36 kD isoform of MCL-1^{KR} may be misfolded and degraded inside the mitochondrial matrix by the AAA$^+$ family of ATPases, such as Lon and ClpXP (Tatsuta and Langer, 2008). This hypothesis could simply be tested by RNA interference against Lon or ClpXP proteases then monitoring MCL-1^{KR} half-life. An alternative explanation is that MCL-1 undergoes protein acetylation, which may facilitate the binding of another adaptor protein that is important for MCL-1 protein stability inside the mitochondria. MCL-1^{KR} cannot be acetylated, due to the lack of lysine residues, and therefore dissociates with its binding partner, destabilizing the 36 kD isoform. In order to test if MCL-1 is acetylated, tandem mass spectroscopy can be used to identify potential MCL-1 acetylation sites. Validation of acetylation could be carried out by labeling cells with [H3]acetate, immunoprecipitating MCL-1 then analyzing via fluorography.

Despite observations that MCL-1 protein is rapidly degraded by the proteasome, inhibition of the proteasome did not result in increased expression of the 40 kD isoform, rather, it led to accumulation of the 38 kD isoform (De Biasio et al., 2007; Stewart et al., 2010a). Indeed, findings from De Biaso et al. revealed that full length MCL-1 was continually processed to the 36 kD isoform (De Biasio et al., 2007). Furthermore, the processing of MCL-1 to the 36 kD form was shown to depend on a functional mitochondrial membrane potential, suggesting that the cleavage occurs inside the mitochondria (Warr et al., 2011). Along these lines, RNAi-mediated silencing of the mitochondrial processing peptidase (MPP) ablated the formation of the 36 kD isoform of MCL-1, indicating that MCL-1 processing takes place in the matrix (Huang and Yang-Yen, 2010). In addition to proteasome-dependent degradation, proteolytic cleavage of full-length MCL-1 may represent another mechanism for regulating its protein turnover. It is possible that both inhibiting the proteasome and dissipating the mitochondrial membrane potential may dramatically increase the half-life of full length MCL-1. To that end, the MCL-1^{OM} mutant could be predicted to have a longer half-life because it is unable to be proteolytically cleaved, and therefore accumulates on the OMM. Alternatively, MCL-1 ^{OM} could have a shorter half-life due to easier access by the proteasome.

Differential regulation of MCL-1 isoforms resulting from a variety of cellular stresses has also been documented. For example, DNA-damaging agents such as etoposide and UV irradiation both increased the turnover rate of the 40 kD isoform with no effect on the 36 kD form of MCL-1 (De Biasio et al., 2007; Stewart et al., 2010a).

However, this may just be a reflection of the differential half lives of the two isoforms. In contrast, nutrient-induced stress, such as cytokine or glucose withdrawal, appears to reduce the levels of both isoforms of MCL-1 (Coloff et al., 2011; Maurer et al., 2006). However, the nutrient deprivation appears to be regulating MCL-1 translation via mTOR and could explain why there is less of both isoforms (Coloff et al., 2011; Pradelli et al., 2010).

Regulation of Mitochondrial Function by MCL-1

My data suggests a new role of MCL-1 in regulating mitochondrial metabolism and dynamics; a function separate from its ability to antagonize cell death that requires its import into the mitochondrial matrix. During import, the MCL-1 protein undergoes amino-terminal proteolytic cleavage resulting in the production of multiple proteins from the same polypeptide. The generation of the matrix-localized MCL-1 requires two proteolysis events and importation into the mitochondria by the translocases of the outer and inner membrane (TOM and TIM complexes). It has also been shown that full-length MCL-1 continually undergoes processing to the matrix-localized isoform that depends on a functional mitochondrial membrane potential and may be processed by the MPP inside the mitochondrial matrix (De Biasio et al., 2007; Huang and Yang-Yen, 2010; Warr et al., 2011). Further studies will be required to identify whether cleavage at both sites occurs within the mitochondria and/or whether other cellular proteases are involved.

Functionally, the OMM-localized MCL-1 possesses anti-apoptotic activity, inhibiting cell death and binding pro-apoptotic molecules **(Fig. 4.2)**. In contrast, the matrix-localized MCL-1 does not possess anti-apoptotic function, but instead facilitates normal mitochondrial physiology and energy metabolism. The matrix-localized MCL-1 promotes normal mitochondrial ultrastructure by maintaining cristae morphology as well as the dynamics of mitochondrial fusion. Additionally, the MCL-1 matrix isoform supports oxidative phosphorylation, ATP production and maintenance of mitochondrial membrane potential. Thus, MCL-1 functions both to directly oppose apoptosis and to promote mitochondrial physiology.

MCL-1 Modulates Inner Membrane Structure, Dynamics, and Function

While my data suggests that MCL-1 is required inside the mitochondrial matrix for normal mitochondrial cristae structure, fusion, and bioenergetics, including oxidative phosphorylation (OXPHOS), precisely how MCL-1 can promote this function is still uncertain. Mitochondrial morphology, dynamics, and function are closely linked. Particularly, the structure of the inner membrane is highly organized and dynamic. The mitochondrial cristae are pleomorphic and adapt different structures according to the metabolic status of the cell. For example, when ADP is low and ATP is abundant the cristae are short and flat with fewer cristae junctions and an expanded matrix, called "orthodox" (Hackenbrock, 1968). Whereas, under conditions of high ADP and low ATP, the cristae have multiple tubular connections and a compact matrix, called "condensed"
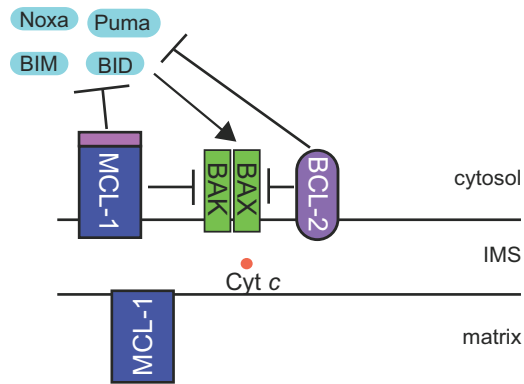
Figure 4.2.   Classical Anti-apoptotic MCL-1
On the outer mitochondrial membrane (OMM), MCL-1 functions like other antiapoptotic BCL-2 family members where it antagonizes the activation of BAX and BAK and prevents cell death. MCL-1 can directly bind BH3-only family members, such as BIM, sequestering them away from the pro-apoptotic effectors BAX or BAK. Alternatively, MCL-1 may directly bind BAX and BAK and maintain them in an inactive conformation.

(Hackenbrock, 1968). Since cells lacking MCL-1 inside the mitochondrial matrix have profound deficits in bioenergetics, it is possible that MCL-1 may directly modulate the function of one or more of the ETC components. In the absence of matrix-localized MCL-1, the capacity for OXPHOS is diminished and ATP production plummets, thereby indirectly affecting the cristae morphology and dynamics.

However, it is also possible that the dynamic transition between "orthodox" and "condensed" requires an active fission and fusion process and MCL-1 could directly modify this process. For example, MCL-1 could influence the function of OPA1, a well-characterized regulator of inner membrane fusion. In the absence of MCL-1 inside the mitochondrial matrix, OPA1 activity may be perturbed resulting in fusion defects. Furthermore, defects in mitochondrial fusion cause dysfunctional mitochondria. Cells that are fusion incompetent generate less energy by OXPHOS and have increased ROS production in addition to fragmented mitochondria (Chen et al., 2005a; Chen et al., 2007). This is because fusion maintains a healthy mitochondrial population through the exchange of contents between mitochondria including mtDNA. The mtDNA genome is organized into nucleoids and encodes for essential components of the respiratory chain. Fusion enables the exchange of mtDNA nucleoids between mitochondria, however, in cells incapable of fusion there is a loss of nucleoids (Chen et al., 2007; Legros et al., 2004). Consequently, a possible explanation for the decreased mtDNA content observed in *Mcl-1*-deleted cells may be an effect of incompetent mitochondrial fusion; subsequently, resulting in bioenergetic abnormalities such as inefficient respiration and decreased membrane potential. Moreover, mitochondrial membrane potential influences fusion efficiency (Song et al., 2007) and, therefore could cause a feed-forward inhibition of fusion rate.

Alternatively, MCL-1 may regulate inner membrane structure by directly facilitating the dimerization and oligomerizaton of F_1F_0-ATP synthase. ATP synthase dimers and oligomers constrain and curve the IMM and this is required for maintaining the proper organization of the IMM (Dudkina et al., 2005; Giraud et al., 2002; Thomas et al., 2008). The assembly of ATP synthase into dimers and oligomers is aberrant in mitochondria lacking MCL-1 **(Fig. 4.3)**. It is possible that MCL-1 is an accessory protein that bridges either the F_1 or F_0 domains, stabilizing the complex **(Fig. 4.3)**. On the other hand, MCL-1 could indirectly support dimerization through another accessory protein such as inhibitory factor 1 (IF$_1$). IF$_1$ is a protein that binds to ATP synthase and prevents the hydrolysis of ATP (Pullman and Monroy, 1963). IF$_1$ regulates mitochondrial ultrastructure by promoting dimerization of ATP synthase (Campanella et al., 2008).

Mcl-1-deleted mitochondria exhibit a loss of oligomeric ATP synthase and a corresponding increase in monomeric form, indicating that those oligomers are less stable in the absence of MCL-1. It is plausible that the loss of ATP synthase oligomers in *Mcl-1*-deleted mitochondria may be responsible for the ultrastructural defects including disorganized cristae. Similar defects were seen in the assembly of electron transport chain (ETC) complexes into "supercomplexes" in MCL-1 deficient mouse liver mitochondria **(Fig. 4.3)**. It has been demonstrated that the assembly of the ETC
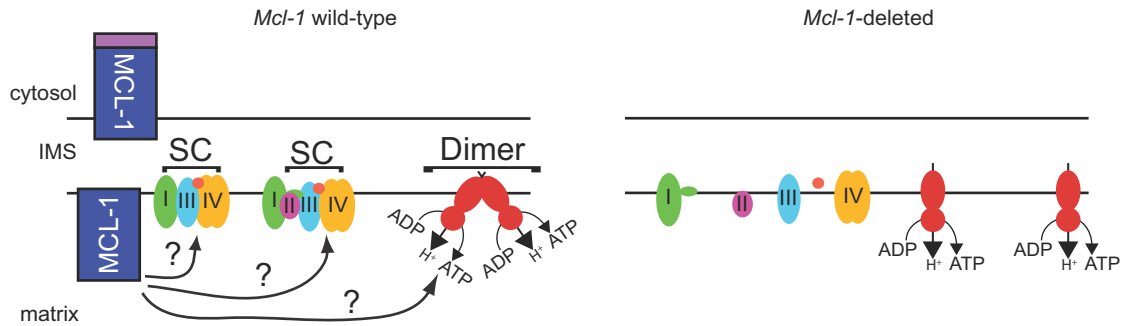
Figure 4.3.   MCL-1's Potential Functions Inside Mitochondria
During mitochondrial importation, the full-length MCL-1 is proteolytically truncated on its amino-terminus. The truncated, matrix localized MCL-1 resides within the inner mitochondrial membrane where it functions to maintain mitochondrial cristae ultrastructure and promotes the assembly of the electron transport chain complexes into higher-order assemblies known as supercomplexes (SC). The assembly into supercomplexes has been shown to facilitate electron transport efficiency and reduce the production of deleterious reactive oxygen species. Additionally, matrix-localized MCL-1 facilitates the assembly of the higher-order assembly of the ATP synthase complexes into dimers and oligomers. Proper assembly of oligomeric ATP synthase has been implicated in being an important determinate of inner membrane cristae structure. Whether MCL-1 acts directly or indirectly to facilitate these macromolecular assemblies of the electron transport supercomplexes or ATP synthase oligomers is still unclear.

complexes into supercomplexes promotes efficient energy production and decreases the production of harmful reactive oxygen species (Acin-Perez et al., 2008). Since abnormalities in mitochondrial cristae ultrastructure can promote the breakdown of the reticular mitochondrial network, this could explain the observed mitochondrial fusion defect and subsequent bioenergetic abnormalities in *Mcl-1*-deficient cells (Velours et al., 2009).

Another possible cause of the ultrastructural defects is an aberrant lipid inner mitochondrial membrane. MCL-1 may directly or indirectly regulate the lipid content of the inner mitochondrial membrane. For example, MCL-1 could facilitate the structure and/or function of cardiolipin. Cardiolipin is an abundant lipid in the inner mitochondrial membrane that affects mitochondrial ultrastructure and function (Houtkooper and Vaz, 2008). Furthermore, cardiolipin regulates supercomplex assembly of the repiratory complexes and ATP synthase oligomerization (Wittig and Schagger, 2009). It is possible that MCL-1 could indirectly affect cardiolipin structure. In the absence of MCL-1, cardiolipin structure may be disrupted and this could alter the fusion of the lipids in the inner mitochondrial membrane. Indeed, the lipid structure is very important for membrane fusion (Cullis et al., 1986). Alternatively, MCL-1 could directly interact with cardiolipin to facilitate its function, such that in the absence of this interaction a functional change occurs, possibly even disrupting other cardiolipin complexes.

Concluding Remarks

My findings regarding MCL-1-regulated mitochondrial physiology and its separable functions as an anti-apoptotic molecule at the OMM and regulator of mitochondrial bioenergetics inside the matrix, may have a major impact in our understanding of MCL-1 biology in normal cells, and represent a new clinical target. Recently, another anti-apoptotic BCL-2 family member, BCL-X_L, was found inside the mitochondrial matrix where it also played a role in mitochondrial metabolism (Alavian et al., 2011). While BCL-X_L was found to regulate mitochondrial metabolism, there was no indication that it played a role in mitochondrial morphology (Alavian et al., 2011). For this reason, BCL-X_L may be able to functionally compensate for the metabolic role of MCL-1 inside the mitochondrial matrix. Additionally, if BCL-X_L was also able to compensate for the morphology abnormalities observed in *Mcl-1*-deficient cells, this would suggest that the regulation of mitochondrial metabolism is MCL-1's primary role inside the mitochondria. Undoubtedly, defining the mechanism by which MCL-1 regulates mitochondrial physiology as well as identifying MCL-1-interacting partners inside the mitochondrial matrix will be important to understanding its function. Future studies delineating the relative contributions of MCL-1's anti-apoptotic and metabolic functions in both normal and diseased cells may help to develop more effective MCL-1 inhibitors with reduced toxicity to normal cells.

LIST OF REFERENCES

Acin-Perez, R., Fernandez-Silva, P., Peleato, M.L., Perez-Martos, A., and Enriquez, J.A. (2008). Respiratory active mitochondrial supercomplexes. Mol Cell 32, 529-539.

Akgul, C., Moulding, D.A., White, M.R., and Edwards, S.W. (2000). In vivo localisation and stability of human Mcl-1 using green fluorescent protein (GFP) fusion proteins. FEBS Lett 478, 72-76.

Alavian, K.N., Li, H., Collis, L., Bonanni, L., Zeng, L., Sacchetti, S., Lazrove, E., Nabili, P., Flaherty, B., Graham, M., et al. (2011). Bcl-xL regulates metabolic efficiency of neurons through interaction with the mitochondrial F1FO ATP synthase. Nature cell biology 13, 1224-1233.

Arbour, N., Vanderluit, J.L., Le Grand, J.N., Jahani-Asl, A., Ruzhynsky, V.A., Cheung, E.C., Kelly, M.A., MacKenzie, A.E., Park, D.S., Opferman, J.T., et al. (2008). Mcl-1 is a key regulator of apoptosis during CNS development and after DNA damage. J Neurosci 28, 6068-6078.

Autret, A., and Martin, S.J. (2009). Emerging role for members of the Bcl-2 family in mitochondrial morphogenesis. Mol Cell 36, 355-363.

Benos, D.J., and Balaban, R.S. (1983). Energy metabolism of preimplantation mammalian blastocysts. Am J Physiol 245, C40-45.

Berman, S.B., Chen, Y.B., Qi, B., McCaffery, J.M., Rucker, E.B., 3rd, Goebbels, S., Nave, K.A., Arnold, B.A., Jonas, E.A., Pineda, F.J., et al. (2009). Bcl-x L increases mitochondrial fission, fusion, and biomass in neurons. J Cell Biol 184, 707-719.

Beroukhim, R., Mermel, C.H., Porter, D., Wei, G., Raychaudhuri, S., Donovan, J., Barretina, J., Boehm, J.S., Dobson, J., Urashima, M., et al. (2010). The landscape of somatic copy-number alteration across human cancers. Nature 463, 899-905.

Bissonnette, R.P., Echeverri, F., Mahboubi, A., and Green, D.R. (1992). Apoptotic cell death induced by c-myc is inhibited by bcl-2. Nature 359, 552-554.

Blaschke, A.J., Staley, K., and Chun, J. (1996). Widespread programmed cell death in proliferative and postmitotic regions of the fetal cerebral cortex. Development 122, 1165-1174.

Bleazard, W., McCaffery, J.M., King, E.J., Bale, S., Mozdy, A., Tieu, Q., Nunnari, J., and Shaw, J.M. (1999). The dynamin-related GTPase Dnm1 regulates mitochondrial fission in yeast. Nat Cell Biol 1, 298-304.

Bornhovd, C., Vogel, F., Neupert, W., and Reichert, A.S. (2006). Mitochondrial membrane potential is dependent on the oligomeric state of F1F0-ATP synthase supracomplexes. J Biol Chem 281, 13990-13998.

Breckenridge, D.G., Stojanovic, M., Marcellus, R.C., and Shore, G.C. (2003). Caspase cleavage product of BAP31 induces mitochondrial fission through endoplasmic reticulum calcium signals, enhancing cytochrome c release to the cytosol. The Journal of cell biology 160, 1115-1127.

Brunner, G., and Neupert, W. (1968). Turnover of outer and inner membrane proteins of rat liver mitochondria. FEBS letters 1, 153-155.

Cabezon, E., Montgomery, M.G., Leslie, A.G., and Walker, J.E. (2003). The structure of bovine F1-ATPase in complex with its regulatory protein IF1. Nat Struct Biol 10, 744-750.

Campanella, M., Casswell, E., Chong, S., Farah, Z., Wieckowski, M.R., Abramov, A.Y., Tinker, A., and Duchen, M.R. (2008). Regulation of mitochondrial structure and function by the F1Fo-ATPase inhibitor protein, IF1. Cell Metab 8, 13-25.

Campbell, K.J., Bath, M.L., Turner, M.L., Vandenberg, C.J., Bouillet, P., Metcalf, D., Scott, C.L., and Cory, S. (2010). Elevated Mcl-1 perturbs lymphopoiesis, promotes transformation of hematopoietic stem/progenitor cells, and enhances drug resistance. Blood 116, 3197-3207.

Certo, M., Del Gaizo Moore, V., Nishino, M., Wei, G., Korsmeyer, S., Armstrong, S.A., and Letai, A. (2006). Mitochondria primed by death signals determine cellular addiction to antiapoptotic BCL-2 family members. Cancer Cell 9, 351-365.

Chan, D.C. (2006). Mitochondria: dynamic organelles in disease, aging, and development. Cell 125, 1241-1252.

Chen, H., and Chan, D.C. (2005). Emerging functions of mammalian mitochondrial fusion and fission. Hum Mol Genet 14 Spec No. 2, R283-289.

Chen, H., Chomyn, A., and Chan, D.C. (2005a). Disruption of fusion results in mitochondrial heterogeneity and dysfunction. J Biol Chem 280, 26185-26192.

Chen, H., Detmer, S.A., Ewald, A.J., Griffin, E.E., Fraser, S.E., and Chan, D.C. (2003). Mitofusins Mfn1 and Mfn2 coordinately regulate mitochondrial fusion and are essential for embryonic development. J Cell Biol 160, 189-200.

Chen, H., McCaffery, J.M., and Chan, D.C. (2007). Mitochondrial fusion protects against neurodegeneration in the cerebellum. Cell 130, 548-562.

Chen, H., Vermulst, M., Wang, Y.E., Chomyn, A., Prolla, T.A., McCaffery, J.M., and Chan, D.C. (2010). Mitochondrial fusion is required for mtDNA stability in skeletal muscle and tolerance of mtDNA mutations. Cell 141, 280-289.

Chen, L., Willis, S.N., Wei, A., Smith, B.J., Fletcher, J.I., Hinds, M.G., Colman, P.M., Day, C.L., Adams, J.M., and Huang, D.C. (2005b). Differential Targeting of Prosurvival Bcl-2 Proteins by Their BH3-Only Ligands Allows Complementary Apoptotic Function. Mol Cell 17, 393-403.

Cheng, E.H., Wei, M.C., Weiler, S., Flavell, R.A., Mak, T.W., Lindsten, T., and Korsmeyer, S.J. (2001). BCL-2, BCL-X(L) sequester BH3 domain-only molecules preventing BAX- and BAK-mediated mitochondrial apoptosis. Mol Cell 8, 705-711.

Chipuk, J.E., Moldoveanu, T., Llambi, F., Parsons, M.J., and Green, D.R. (2010). The BCL-2 family reunion. Mol Cell 37, 299-310.

Chung, T.K., Cheung, T.H., Lo, W.K., Yim, S.F., Yu, M.Y., Krajewski, S., Reed, J.C., and Wong, Y.F. (2002). Expression of apoptotic regulators and their significance in cervical cancer. Cancer Lett 180, 63-68.

Coloff, J.L., Mason, E.F., Altman, B.J., Gerriets, V.A., Liu, T., Nichols, A.N., Zhao, Y., Wofford, J.A., Jacobs, S.R., Ilkayeva, O., et al. (2011). Akt requires glucose metabolism to suppress puma expression and prevent apoptosis of leukemic T cells. The Journal of biological chemistry 286, 5921-5933.

Cory, S., and Adams, J.M. (2002). The Bcl2 family: regulators of the cellular life-or-death switch. Nat Rev Cancer 2, 647-656.

Cullis, P.R., Hope, M.J., and Tilcock, C.P. (1986). Lipid polymorphism and the roles of lipids in membranes. Chemistry and physics of lipids 40, 127-144.

Danial, N.N., and Korsmeyer, S.J. (2004). Cell death: critical control points. Cell 116, 205-219.

Day, C.L., Chen, L., Richardson, S.J., Harrison, P.J., Huang, D.C., and Hinds, M.G. (2005). Solution structure of prosurvival Mcl-1 and characterization of its binding by proapoptotic BH3-only ligands. J Biol Chem 280, 4738-4744.

De Biasio, A., Vrana, J.A., Zhou, P., Qian, L., Bieszczad, C.K., Braley, K.E., Domina, A.M., Weintraub, S.J., Neveu, J.M., Lane, W.S., et al. (2007). N-terminal truncation of antiapoptotic MCL1, but not G2/M-induced phosphorylation, is associated with stabilization and abundant expression in tumor cells. J Biol Chem 282, 23919-23936.

DeBerardinis, R.J., Mancuso, A., Daikhin, E., Nissim, I., Yudkoff, M., Wehrli, S., and Thompson, C.B. (2007). Beyond aerobic glycolysis: transformed cells can engage in glutamine metabolism that exceeds the requirement for protein and nucleotide synthesis. Proc Natl Acad Sci U S A 104, 19345-19350.

Deberardinis, R.J., Sayed, N., Ditsworth, D., and Thompson, C.B. (2008). Brick by brick: metabolism and tumor cell growth. Curr Opin Genet Dev 18, 54-61.

Delettre, C., Griffoin, J.M., Kaplan, J., Dollfus, H., Lorenz, B., Faivre, L., Lenaers, G., Belenguer, P., and Hamel, C.P. (2001). Mutation spectrum and splicing variants in the OPA1 gene. Hum Genet 109, 584-591.

Delivani, P., Adrain, C., Taylor, R.C., Duriez, P.J., and Martin, S.J. (2006). Role for CED-9 and Egl-1 as regulators of mitochondrial fission and fusion dynamics. Mol Cell 21, 761-773.

Detmer, S.A., and Chan, D.C. (2007). Functions and dysfunctions of mitochondrial dynamics. Nat Rev Mol Cell Biol 8, 870-879.

Diaz, F., Fukui, H., Garcia, S., and Moraes, C.T. (2006). Cytochrome c oxidase is required for the assembly/stability of respiratory complex I in mouse fibroblasts. Mol Cell Biol 26, 4872-4881.

Ding, Q., He, X., Hsu, J.M., Xia, W., Chen, C.T., Li, L.Y., Lee, D.F., Liu, J.C., Zhong, Q., Wang, X., et al. (2007). Degradation of Mcl-1 by beta-TrCP mediates glycogen synthase kinase 3-induced tumor suppression and chemosensitization. Mol Cell Biol 27, 4006-4017.

Domen, J., Cheshier, S.H., and Weissman, I.L. (2000). The role of apoptosis in the regulation of hematopoietic stem cells: Overexpression of Bcl-2 increases both their number and repopulation potential. J Exp Med 191, 253-264.

Domina, A.M., Smith, J.H., and Craig, R.W. (2000). Myeloid cell leukemia 1 is phosphorylated through two distinct pathways, one associated with extracellular signal-regulated kinase activation and the other with G2/M accumulation or protein phosphatase 1/2A inhibition. J Biol Chem 275, 21688-21694.

Domina, A.M., Vrana, J.A., Gregory, M.A., Hann, S.R., and Craig, R.W. (2004). MCL1 is phosphorylated in the PEST region and stabilized upon ERK activation in viable cells, and at additional sites with cytotoxic okadaic acid or taxol. Oncogene 23, 5301-5315.

Dudkina, N.V., Heinemeyer, J., Keegstra, W., Boekema, E.J., and Braun, H.P. (2005). Structure of dimeric ATP synthase from mitochondria: an angular association of monomers induces the strong curvature of the inner membrane. FEBS Lett 579, 5769-5772.

Dzhagalov, I., Dunkle, A., and He, Y.W. (2008). The anti-apoptotic Bcl-2 family member Mcl-1 promotes T lymphocyte survival at multiple stages. J Immunol 181, 521-528.

Dzhagalov, I., St John, A., and He, Y.W. (2007). The antiapoptotic protein Mcl-1 is essential for the survival of neutrophils but not macrophages. Blood 109, 1620-1626.

Eagle, H. (1955). Nutrition needs of mammalian cells in tissue culture. Science 122, 501-514.

Eischen, C.M., Woo, D., Roussel, M.F., and Cleveland, J.L. (2001). Apoptosis triggered by Myc-induced suppression of Bcl-X(L) or Bcl-2 is bypassed during lymphomagenesis. Mol Cell Biol 21, 5063-5070.

Estaquier, J., and Arnoult, D. (2007). Inhibiting Drp1-mediated mitochondrial fission selectively prevents the release of cytochrome c during apoptosis. Cell death and differentiation 14, 1086-1094.

Evan, G.I., Wyllie, A.H., Gilbert, C.S., Littlewood, T.D., Land, H., Brooks, M., Waters, C.M., Penn, L.Z., and Hancock, D.C. (1992). Induction of apoptosis in fibroblasts by c-myc protein. Cell 69, 119-128.

Fernandez-Vizarra, E., Lopez-Perez, M.J., and Enriquez, J.A. (2002). Isolation of biogenetically competent mitochondria from mammalian tissues and cultured cells. Methods 26, 292-297.

Ferrick, D.A., Neilson, A., and Beeson, C. (2008). Advances in measuring cellular bioenergetics using extracellular flux. Drug Discov Today 13, 268-274.

Frank, S., Gaume, B., Bergmann-Leitner, E.S., Leitner, W.W., Robert, E.G., Catez, F., Smith, C.L., and Youle, R.J. (2001). The role of dynamin-related protein 1, a mediator of mitochondrial fission, in apoptosis. Dev Cell 1, 515-525.

Frey, T.G., and Mannella, C.A. (2000). The internal structure of mitochondria. Trends Biochem Sci 25, 319-324.

Frezza, C., Cipolat, S., Martins de Brito, O., Micaroni, M., Beznoussenko, G.V., Rudka, T., Bartoli, D., Polishuck, R.S., Danial, N.N., De Strooper, B., et al. (2006). OPA1 controls apoptotic cristae remodeling independently from mitochondrial fusion. Cell 126, 177-189.

Frost, M.T., Wang, Q., Moncada, S., and Singer, M. (2005). Hypoxia accelerates nitric oxide-dependent inhibition of mitochondrial complex I in activated macrophages. Am J Physiol Regul Integr Comp Physiol 288, R394-400.

Fujise, K., Zhang, D., Liu, J., and Yeh, E.T. (2000). Regulation of apoptosis and cell cycle progression by MCL1. Differential role of proliferating cell nuclear antigen. J Biol Chem 275, 39458-39465.

Genova, M.L., Baracca, A., Biondi, A., Casalena, G., Faccioli, M., Falasca, A.I., Formiggini, G., Sgarbi, G., Solaini, G., and Lenaz, G. (2008). Is supercomplex organization of the respiratory chain required for optimal electron transfer activity? Biochim Biophys Acta 1777, 740-746.

Germain, M., and Duronio, V. (2007). The N terminus of the anti-apoptotic BCL-2 homologue MCL-1 regulates its localization and function. J Biol Chem 282, 32233-32242.

Gilkerson, R.W., Selker, J.M., and Capaldi, R.A. (2003). The cristal membrane of mitochondria is the principal site of oxidative phosphorylation. FEBS Lett 546, 355-358.

Giraud, M.F., Paumard, P., Soubannier, V., Vaillier, J., Arselin, G., Salin, B., Schaeffer, J., Brethes, D., di Rago, J.P., and Velours, J. (2002). Is there a relationship between the supramolecular organization of the mitochondrial ATP synthase and the formation of cristae? Biochim Biophys Acta 1555, 174-180.

Glaser, S.P., Lee, E.F., Trounson, E., Bouillet, P., Wei, A., Fairlie, W.D., Izon, D.J., Zuber, J., Rappaport, A.R., Herold, M.J., et al. (2012). Anti-apoptotic Mcl-1 is essential for the development and sustained growth of acute myeloid leukemia. Genes Dev 26, 120-125.

Goldstein, J.C., Waterhouse, N.J., Juin, P., Evan, G.I., and Green, D.R. (2000). The coordinate release of cytochrome c during apoptosis is rapid, complete and kinetically invariant. Nat Cell Biol 2, 156-162.

Gomes, L.C., Di Benedetto, G., and Scorrano, L. (2011). During autophagy mitochondria elongate, are spared from degradation and sustain cell viability. Nat Cell Biol 13, 589-598.

Griparic, L., van der Wel, N.N., Orozco, I.J., Peters, P.J., and van der Bliek, A.M. (2004). Loss of the intermembrane space protein Mgm1/OPA1 induces swelling and localized constrictions along the lengths of mitochondria. J Biol Chem 279, 18792-18798.

Hackenbrock, C.R. (1968). Ultrastructural bases for metabolically linked mechanical activity in mitochondria. II. Electron transport-linked ultrastructural transformations in mitochondria. J Cell Biol 37, 345-369.

Hanahan, D., and Weinberg, R.A. (2011). Hallmarks of cancer: the next generation. Cell 144, 646-674.

Hao, Z., Duncan, G.S., Su, Y.W., Li, W.Y., Silvester, J., Hong, C., You, H., Brenner, D., Gorrini, C., Haight, J., et al. (2012). The E3 ubiquitin ligase Mule acts through the ATM-p53 axis to maintain B lymphocyte homeostasis. J Exp Med 209, 173-186.

Hinman, L.M., and Blass, J.P. (1981). An NADH-linked spectrophotometric assay for pyruvate dehydrogenase complex in crude tissue homogenates. J Biol Chem 256, 6583-6586.

Hoppins, S., Collins, S.R., Cassidy-Stone, A., Hummel, E., Devay, R.M., Lackner, L.L., Westermann, B., Schuldiner, M., Weissman, J.S., and Nunnari, J. (2011a). A mitochondrial-focused genetic interaction map reveals a scaffold-like complex required for inner membrane organization in mitochondria. The Journal of cell biology 195, 323-340.

Hoppins, S., Edlich, F., Cleland, M.M., Banerjee, S., McCaffery, J.M., Youle, R.J., and Nunnari, J. (2011b). The soluble form of Bax regulates mitochondrial fusion via MFN2 homotypic complexes. Molecular cell 41, 150-160.

Houtkooper, R.H., and Vaz, F.M. (2008). Cardiolipin, the heart of mitochondrial metabolism. Cellular and molecular life sciences : CMLS 65, 2493-2506.

Huang, C.R., and Yang-Yen, H.F. (2010). The fast-mobility isoform of mouse Mcl-1 is a mitochondrial matrix-localized protein with attenuated anti-apoptotic activity. FEBS Lett 584, 3323-3330.

Huang, H.M., Huang, C.J., and Yen, J.J. (2000). Mcl-1 is a common target of stem cell factor and interleukin-5 for apoptosis prevention activity via MEK/MAPK and PI-3K/Akt pathways. Blood 96, 1764-1771.

Inoshita, S., Takeda, K., Hatai, T., Terada, Y., Sano, M., Hata, J., Umezawa, A., and Ichijo, H. (2002). Phosphorylation and inactivation of myeloid cell leukemia 1 by JNK in response to oxidative stress. J Biol Chem 277, 43730-43734.

Inoue, S., Noda, S., Kashima, K., Nakada, K., Hayashi, J., and Miyoshi, H. (2010). Mitochondrial respiration defects modulate differentiation but not proliferation of hematopoietic stem and progenitor cells. FEBS Lett 584, 3402-3409.

Inuzuka, H., Shaik, S., Onoyama, I., Gao, D., Tseng, A., Maser, R.S., Zhai, B., Wan, L., Gutierrez, A., Lau, A.W., et al. (2011). SCF(FBW7) regulates cellular apoptosis by targeting MCL1 for ubiquitylation and destruction. Nature 471, 104-109.

Ishihara, N., Fujita, Y., Oka, T., and Mihara, K. (2006). Regulation of mitochondrial morphology through proteolytic cleavage of OPA1. EMBO J 25, 2966-2977.

Jahani-Asl, A., Cheung, E.C., Neuspiel, M., MacLaurin, J.G., Fortin, A., Park, D.S., McBride, H.M., and Slack, R.S. (2007). Mitofusin 2 protects cerebellar granule neurons against injury-induced cell death. J Biol Chem 282, 23788-23798.

Karbowski, M., Arnoult, D., Chen, H., Chan, D.C., Smith, C.L., and Youle, R.J. (2004). Quantitation of mitochondrial dynamics by photolabeling of individual organelles shows that mitochondrial fusion is blocked during the Bax activation phase of apoptosis. J Cell Biol 164, 493-499.

Karbowski, M., Norris, K.L., Cleland, M.M., Jeong, S.Y., and Youle, R.J. (2006). Role of Bax and Bak in mitochondrial morphogenesis. Nature 443, 658-662.

Kaufmann, S.H., Karp, J.E., Svingen, P.A., Krajewski, S., Burke, P.J., Gore, S.D., and Reed, J.C. (1998). Elevated expression of the apoptotic regulator Mcl-1 at the time of leukemic relapse. Blood 91, 991-1000.

Kojima, S., Hyakutake, A., Koshikawa, N., Nakagawara, A., and Takenaga, K. (2010). MCL-1V, a novel mouse antiapoptotic MCL-1 variant, generated by RNA splicing at a non-canonical splicing pair. Biochem Biophys Res Commun 391, 492-497.

Koopman, W.J., Verkaart, S., Visch, H.J., van der Westhuizen, F.H., Murphy, M.P., van den Heuvel, L.W., Smeitink, J.A., and Willems, P.H. (2005). Inhibition of complex I of the electron transport chain causes O2-. -mediated mitochondrial outgrowth. Am J Physiol Cell Physiol 288, C1440-1450.

Koshiba, T., Detmer, S.A., Kaiser, J.T., Chen, H., McCaffery, J.M., and Chan, D.C. (2004). Structural basis of mitochondrial tethering by mitofusin complexes. Science 305, 858-862.

Kozopas, K.M., Yang, T., Buchan, H.L., Zhou, P., and Craig, R.W. (1993). MCL1, a gene expressed in programmed myeloid cell differentiation, has sequence similarity to BCL2. Proc Natl Acad Sci U S A 90, 3516-3520.

Krajewski, S., Bodrug, S., Krajewska, M., Shabaik, A., Gascoyne, R., Berean, K., and Reed, J.C. (1995). Immunohistochemical analysis of Mcl-1 protein in human tissues. Differential regulation of Mcl-1 and Bcl-2 protein production suggests a unique role for Mcl-1 in control of programmed cell death in vivo. Am J Pathol 146, 1309-1319.

Krause, F., Reifschneider, N.H., Goto, S., and Dencher, N.A. (2005). Active oligomeric ATP synthases in mammalian mitochondria. Biochem Biophys Res Commun 329, 583-590.

Lee, E.F., Czabotar, P.E., van Delft, M.F., Michalak, E.M., Boyle, M.J., Willis, S.N., Puthalakath, H., Bouillet, P., Colman, P.M., Huang, D.C., et al. (2008). A novel BH3 ligand that selectively targets Mcl-1 reveals that apoptosis can proceed without Mcl-1 degradation. J Cell Biol 180, 341-355.

Lee, Y.J., Jeong, S.Y., Karbowski, M., Smith, C.L., and Youle, R.J. (2004). Roles of the mammalian mitochondrial fission and fusion mediators Fis1, Drp1, and Opa1 in apoptosis. Mol Biol Cell 15, 5001-5011.

Legros, F., Malka, F., Frachon, P., Lombes, A., and Rojo, M. (2004). Organization and dynamics of human mitochondrial DNA. J Cell Sci 117, 2653-2662.

Lenaz, G., and Genova, M.L. (2007). Kinetics of integrated electron transfer in the mitochondrial respiratory chain: random collisions vs. solid state electron channeling. Am J Physiol Cell Physiol 292, C1221-1239.

Li, J., Viallet, J., and Haura, E.B. (2008). A small molecule pan-Bcl-2 family inhibitor, GX15-070, induces apoptosis and enhances cisplatin-induced apoptosis in non-small cell lung cancer cells. Cancer Chemother Pharmacol 61, 525-534.

Li, Q.M., Tep, C., Yune, T.Y., Zhou, X.Z., Uchida, T., Lu, K.P., and Yoon, S.O. (2007). Opposite regulation of oligodendrocyte apoptosis by JNK3 and Pin1 after spinal cord injury. J Neurosci 27, 8395-8404.

Mannella, C.A. (2006). Structure and dynamics of the mitochondrial inner membrane cristae. Biochim Biophys Acta 1763, 542-548.

Matsushita, K., Okita, H., Suzuki, A., Shimoda, K., Fukuma, M., Yamada, T., Urano, F., Honda, T., Sano, M., Iwanaga, S., et al. (2003). Islet cell hyperplasia in transgenic mice overexpressing EAT/mcl-1, a bcl-2 related gene. Mol Cell Endocrinol 203, 105-116.

Maurer, U., Charvet, C., Wagman, A.S., Dejardin, E., and Green, D.R. (2006). Glycogen synthase kinase-3 regulates mitochondrial outer membrane permeabilization and apoptosis by destabilization of MCL-1. Mol Cell 21, 749-760.

McCoy, F., Hurwitz, J., McTavish, N., Paul, I., Barnes, C., O'Hagan, B., Odrzywol, K., Murray, J., Longley, D., McKerr, G., et al. (2010). Obatoclax induces Atg7-dependent autophagy independent of beclin-1 and BAX/BAK. Cell Death Dis 1, e108.

Minauro-Sanmiguel, F., Wilkens, S., and Garcia, J.J. (2005). Structure of dimeric mitochondrial ATP synthase: novel F0 bridging features and the structural basis of mitochondrial cristae biogenesis. Proc Natl Acad Sci U S A 102, 12356-12358.

Miro, O., Cardellach, F., Barrientos, A., Casademont, J., Rotig, A., and Rustin, P. (1998). Cytochrome c oxidase assay in minute amounts of human skeletal muscle using single wavelength spectrophotometers. J Neurosci Methods 80, 107-111.

Mitchell, P. (1961). Coupling of phosphorylation to electron and hydrogen transfer by a chemi-osmotic type of mechanism. Nature 191, 144-148.

Mitra, K., Wunder, C., Roysam, B., Lin, G., and Lippincott-Schwartz, J. (2009). A hyperfused mitochondrial state achieved at G1-S regulates cyclin E buildup and entry into S phase. Proc Natl Acad Sci U S A 106, 11960-11965.

Miyadera, H., Shiomi, K., Ui, H., Yamaguchi, Y., Masuma, R., Tomoda, H., Miyoshi, H., Osanai, A., Kita, K., and Omura, S. (2003). Atpenins, potent and specific inhibitors of mitochondrial complex II (succinate-ubiquinone oxidoreductase). Proc Natl Acad Sci U S A 100, 473-477.

Morel, C., Carlson, S.M., White, F.M., and Davis, R.J. (2009). Mcl-1 integrates the opposing actions of signaling pathways that mediate survival and apoptosis. Mol Cell Biol 29, 3845-3852.

Motoyama, N., Wang, F., Roth, K.A., Sawa, H., Nakayama, K., Negishi, I., Senju, S., Zhang, Q., Fujii, S., and et al. (1995). Massive cell death of immature hematopoietic cells and neurons in Bcl-x-deficient mice. Science 267, 1506-1510.

Neuspiel, M., Zunino, R., Gangaraju, S., Rippstein, P., and McBride, H. (2005). Activated mitofusin 2 signals mitochondrial fusion, interferes with Bax activation, and reduces susceptibility to radical induced depolarization. The Journal of biological chemistry 280, 25060-25070.

Nguyen, M., Marcellus, R.C., Roulston, A., Watson, M., Serfass, L., Murthy Madiraju, S.R., Goulet, D., Viallet, J., Belec, L., Billot, X., et al. (2007). Small molecule obatoclax (GX15-070) antagonizes MCL-1 and overcomes MCL-1-mediated resistance to apoptosis. Proc Natl Acad Sci U S A 104, 19512-19517.

Nicholls, D.G. (1974). The influence of respiration and ATP hydrolysis on the proton-electrochemical gradient across the inner membrane of rat-liver mitochondria as determined by ion distribution. Eur J Biochem 50, 305-315.

Okamoto, K., and Shaw, J.M. (2005). Mitochondrial morphology and dynamics in yeast and multicellular eukaryotes. Annu Rev Genet 39, 503-536.

Oltersdorf, T., Elmore, S.W., Shoemaker, A.R., Armstrong, R.C., Augeri, D.J., Belli, B.A., Bruncko, M., Deckwerth, T.L., Dinges, J., Hajduk, P.J., et al. (2005). An inhibitor of Bcl-2 family proteins induces regression of solid tumours. Nature 435, 677-681.

Opferman, J.T. (2007). Life and death during hematopoietic differentiation. Curr Opin Immunol 19, 497-502.

Opferman, J.T. (2008). Apoptosis in the development of the immune system. Cell Death Differ 15, 234-242.

Opferman, J.T., Iwasaki, H., Ong, C.C., Suh, H., Mizuno, S., Akashi, K., and Korsmeyer, S.J. (2005). Obligate role of anti-apoptotic MCL-1 in the survival of hematopoietic stem cells. Science 307, 1101-1104.

Opferman, J.T., and Korsmeyer, S.J. (2003). Apoptosis in the development and maintenance of the immune system. Nat Immunol 4, 410-415.

Opferman, J.T., Letai, A., Beard, C., Sorcinelli, M.D., Ong, C.C., and Korsmeyer, S.J. (2003). Development and maintenance of B and T lymphocytes requires antiapoptotic MCL-1. Nature 426, 671-676.

Paumard, P., Vaillier, J., Coulary, B., Schaeffer, J., Soubannier, V., Mueller, D.M., Brethes, D., di Rago, J.P., and Velours, J. (2002). The ATP synthase is involved in generating mitochondrial cristae morphology. Embo J 21, 221-230.

Pepper, C., Lin, T.T., Pratt, G., Hewamana, S., Brennan, P., Hiller, L., Hills, R., Ward, R., Starczynski, J., Austen, B., et al. (2008). Mcl-1 expression has in vitro and in vivo significance in chronic lymphocytic leukemia and is associated with other poor prognostic markers. Blood 112, 3807-3817.

Perciavalle, R.M., Stewart, D.P., Koss, B., Lynch, J., Milasta, S., Bathina, M., Temirov, J., Cleland, M.M., Pelletier, S., Schuetz, J.D., et al. (2012). Anti-apoptotic MCL-1 localizes to the mitochondrial matrix and couples mitochondrial fusion to respiration. Nature Cell Biology 14, 575-583.

Peters, P.J., Bos, E., and Griekspoor, A. (2006). Cryo-immunogold electron microscopy. Curr Protoc Cell Biol Chapter 4, Unit 4 7.

Pfanner, N., Muller, H.K., Harmey, M.A., and Neupert, W. (1987). Mitochondrial protein import: involvement of the mature part of a cleavable precursor protein in the binding to receptor sites. Embo J 6, 3449-3454.

Pfeiffer, K., Gohil, V., Stuart, R.A., Hunte, C., Brandt, U., Greenberg, M.L., and Schagger, H. (2003). Cardiolipin stabilizes respiratory chain supercomplexes. J Biol Chem 278, 52873-52880.

Pradelli, L.A., Beneteau, M., Chauvin, C., Jacquin, M.A., Marchetti, S., Munoz-Pinedo, C., Auberger, P., Pende, M., and Ricci, J.E. (2010). Glycolysis inhibition sensitizes tumor cells to death receptors-induced apoptosis by AMP kinase activation leading to Mcl-1 block in translation. Oncogene 29, 1641-1652.

Praefcke, G.J., and McMahon, H.T. (2004). The dynamin superfamily: universal membrane tubulation and fission molecules? Nat Rev Mol Cell Biol 5, 133-147.

Pullman, M.E., and Monroy, G.C. (1963). A Naturally Occurring Inhibitor of Mitochondrial Adenosine Triphosphatase. J Biol Chem 238, 3762-3769.

Ranger, A.M., Malynn, B.A., and Korsmeyer, S.J. (2001). Mouse models of cell death. Nat Genet 28, 113-118.

Reitzer, L.J., Wice, B.M., and Kennell, D. (1979). Evidence that glutamine, not sugar, is the major energy source for cultured HeLa cells. J Biol Chem 254, 2669-2676.

Rinkenberger, J.L., Horning, S., Klocke, B., Roth, K., and Korsmeyer, S.J. (2000). Mcl-1 deficiency results in peri-implantation embryonic lethality. Genes Dev 14, 23-27.

Rossi, D.J., Jamieson, C.H., and Weissman, I.L. (2008). Stems cells and the pathways to aging and cancer. Cell *132*, 681-696.

Rossignol, R., Gilkerson, R., Aggeler, R., Yamagata, K., Remington, S.J., and Capaldi, R.A. (2004). Energy substrate modulates mitochondrial structure and oxidative capacity in cancer cells. Cancer Res 64, 985-993.

Sano, M., Nakanishi, Y., Yagasaki, H., Honma, T., Oinuma, T., Obana, Y., Suzuki, A., and Nemoto, N. (2005). Overexpression of anti-apoptotic Mcl-1 in testicular germ cell tumours. Histopathology 46, 532-539.

Sano, M., Umezawa, A., Suzuki, A., Shimoda, K., Fukuma, M., and Hata, J. (2000). Involvement of EAT/mcl-1, an anti-apoptotic bcl-2-related gene, in murine embryogenesis and human development. Exp Cell Res 259, 127-139.

Schagger, H., and Pfeiffer, K. (2000). Supercomplexes in the respiratory chains of yeast and mammalian mitochondria. EMBO J 19, 1777-1783.

Schmidt, O., Pfanner, N., and Meisinger, C. (2010). Mitochondrial protein import: from proteomics to functional mechanisms. Nat Rev Mol Cell Biol 11, 655-667.

Schwickart, M., Huang, X., Lill, J.R., Liu, J., Ferrando, R., French, D.M., Maecker, H., O'Rourke, K., Bazan, F., Eastham-Anderson, J., et al. (2010). Deubiquitinase USP9X stabilizes MCL1 and promotes tumour cell survival. Nature 463, 103-107.

Sheridan, C., Delivani, P., Cullen, S.P., and Martin, S.J. (2008). Bax- or Bak-induced mitochondrial fission can be uncoupled from cytochrome C release. Mol Cell 31, 570-585.

Shi, Y., Glynn, J.M., Guilbert, L.J., Cotter, T.G., Bissonnette, R.P., and Green, D.R. (1992). Role for c-myc in activation-induced apoptotic cell death in T cell hybridomas. Science 257, 212-214.

Sieghart, W., Losert, D., Strommer, S., Cejka, D., Schmid, K., Rasoul-Rockenschaub, S., Bodingbauer, M., Crevenna, R., Monia, B.P., Peck-Radosavljevic, M., et al. (2006). Mcl-1 overexpression in hepatocellular carcinoma: a potential target for antisense therapy. J Hepatol 44, 151-157.

Simsek, T., Kocabas, F., Zheng, J., Deberardinis, R.J., Mahmoud, A.I., Olson, E.N., Schneider, J.W., Zhang, C.C., and Sadek, H.A. (2010). The distinct metabolic profile of hematopoietic stem cells reflects their location in a hypoxic niche. Cell Stem Cell 7, 380-390.

Smirnova, E., Griparic, L., Shurland, D.L., and van der Bliek, A.M. (2001). Dynamin-related protein Drp1 is required for mitochondrial division in mammalian cells. Mol Biol Cell 12, 2245-2256.

Song, L., Coppola, D., Livingston, S., Cress, D., and Haura, E.B. (2005). Mcl-1 regulates survival and sensitivity to diverse apoptotic stimuli in human non-small cell lung cancer cells. Cancer Biol Ther 4, 267-276.

Song, Z., Chen, H., Fiket, M., Alexander, C., and Chan, D.C. (2007). OPA1 processing controls mitochondrial fusion and is regulated by mRNA splicing, membrane potential, and Yme1L. J Cell Biol 178, 749-755.

Steimer, D.A., Boyd, K., Takeuchi, O., Fisher, J.K., Zambetti, G.P., and Opferman, J.T. (2009). Selective roles for antiapoptotic MCL-1 during granulocyte development and macrophage effector function. Blood 113, 2805-2815.

Stewart, D.P., Koss, B., Bathina, M., Perciavalle, R.M., Bisanz, K., and Opferman, J.T. (2010a). Ubiquitin-independent degradation of antiapoptotic MCL-1. Mol Cell Biol 30, 3099-3110.

Stewart, M.L., Fire, E., Keating, A.E., and Walensky, L.D. (2010b). The MCL-1 BH3 helix is an exclusive MCL-1 inhibitor and apoptosis sensitizer. Nat Chem Biol 6, 595-601.

Strauss, M., Hofhaus, G., Schroder, R.R., and Kuhlbrandt, W. (2008). Dimer ribbons of ATP synthase shape the inner mitochondrial membrane. EMBO J 27, 1154-1160.

Sugioka, R., Shimizu, S., and Tsujimoto, Y. (2004). Fzo1, a protein involved in mitochondrial fusion, inhibits apoptosis. J Biol Chem 279, 52726-52734.

Tatsuta, T., and Langer, T. (2008). Quality control of mitochondria: protection against neurodegeneration and ageing. The EMBO journal 27, 306-314.

Thomas, D., Bron, P., Weimann, T., Dautant, A., Giraud, M.F., Paumard, P., Salin, B., Cavalier, A., Velours, J., and Brethes, D. (2008). Supramolecular organization of the yeast F1Fo-ATP synthase. Biol Cell 100, 591-601.

Tse, C., Shoemaker, A.R., Adickes, J., Anderson, M.G., Chen, J., Jin, S., Johnson, E.F., Marsh, K.C., Mitten, M.J., Nimmer, P., et al. (2008). ABT-263: a potent and orally bioavailable Bcl-2 family inhibitor. Cancer Res 68, 3421-3428.

Van Blerkom, J., Cox, H., and Davis, P. (2006). Regulatory roles for mitochondria in the peri-implantation mouse blastocyst: possible origins and developmental significance of differential DeltaPsim. Reproduction 131, 961-976.

Veis, D.J., Sorenson, C.M., Shutter, J.R., and Korsmeyer, S.J. (1993). Bcl-2-deficient mice demonstrate fulminant lymphoid apoptosis, polycystic kidneys, and hypopigmented hair. Cell 75, 229-240.

Velours, J., Dautant, A., Salin, B., Sagot, I., and Brethes, D. (2009). Mitochondrial F1F0-ATP synthase and organellar internal architecture. Int J Biochem Cell Biol 41, 1783-1789.

Vermeulen, L., Sprick, M.R., Kemper, K., Stassi, G., and Medema, J.P. (2008). Cancer stem cells--old concepts, new insights. Cell death and differentiation 15, 947-958.

Vogel, F., Bornhovd, C., Neupert, W., and Reichert, A.S. (2006). Dynamic subcompartmentalization of the mitochondrial inner membrane. J Cell Biol 175, 237-247.

Wagner, K.U., Claudio, E., Rucker, E.B., 3rd, Riedlinger, G., Broussard, C., Schwartzberg, P.L., Siebenlist, U., and Hennighausen, L. (2000). Conditional deletion of the Bcl-x gene from erythroid cells results in hemolytic anemia and profound splenomegaly. Development 127, 4949-4958.

Wallace, D.C. (1999). Mitochondrial diseases in man and mouse. Science 283, 1482-1488.

Wang, J.M., Chao, J.R., Chen, W., Kuo, M.L., Yen, J.J., and Yang-Yen, H.F. (1999). The antiapoptotic gene mcl-1 is up-regulated by the phosphatidylinositol 3-kinase/Akt signaling pathway through a transcription factor complex containing CREB. Mol Cell Biol 19, 6195-6206.

Warr, M.R., Mills, J.R., Nguyen, M., Lemaire-Ewing, S., Baardsnes, J., Sun, K.L., Malina, A., Young, J.C., Jeyaraju, D.V., O'Connor-McCourt, M., et al. (2011a). Mitochondrion-dependent N-terminal processing of outer membrane Mcl-1 protein removes an essential Mule/Lasu1 protein-binding site. The Journal of biological chemistry 286, 25098-25107.

Warr, M.R., and Shore, G.C. (2008). Unique biology of Mcl-1: therapeutic opportunities in cancer. Curr Mol Med 8, 138-147.

Wei, G., Twomey, D., Lamb, J., Schlis, K., Agarwal, J., Stam, R.W., Opferman, J.T., Sallan, S.E., den Boer, M.L., Pieters, R., et al. (2006). Gene expression-based chemical genomics identifies rapamycin as a modulator of MCL1 and glucocorticoid resistance. Cancer Cell 10, 331-342.

Willis, S.N., Chen, L., Dewson, G., Wei, A., Naik, E., Fletcher, J.I., Adams, J.M., and Huang, D.C. (2005). Proapoptotic Bak is sequestered by Mcl-1 and Bcl-xL, but not Bcl-2, until displaced by BH3-only proteins. Genes Dev 19, 1294-1305.

Wilson, A., Laurenti, E., Oser, G., van der Wath, R.C., Blanco-Bose, W., Jaworski, M., Offner, S., Dunant, C.F., Eshkind, L., Bockamp, E., et al. (2008). Hematopoietic stem cells reversibly switch from dormancy to self-renewal during homeostasis and repair. Cell 135, 1118-1129.

Wise, D.R., DeBerardinis, R.J., Mancuso, A., Sayed, N., Zhang, X.Y., Pfeiffer, H.K., Nissim, I., Daikhin, E., Yudkoff, M., McMahon, S.B., et al. (2008). Myc regulates a transcriptional program that stimulates mitochondrial glutaminolysis and leads to glutamine addiction. Proc Natl Acad Sci U S A 105, 18782-18787.

Wittig, I., and Schagger, H. (2009). Supramolecular organization of ATP synthase and respiratory chain in mitochondrial membranes. Biochimica et biophysica acta 1787, 672-680.

Wuilleme-Toumi, S., Robillard, N., Gomez, P., Moreau, P., Le Gouill, S., Avet-Loiseau, H., Harousseau, J.L., Amiot, M., and Bataille, R. (2005). Mcl-1 is overexpressed in multiple myeloma and associated with relapse and shorter survival. Leukemia 19, 1248-1252.

Xiang, Z., Luo, H., Payton, J.E., Cain, J., Ley, T.J., Opferman, J.T., and Tomasson, M.H. (2010). Mcl1 haploinsufficiency protects mice from Myc-induced acute myeloid leukemia. J Clin Invest 120, 2109-2118.

Yang, T., Kozopas, K.M., and Craig, R.W. (1995). The intracellular distribution and pattern of expression of Mcl-1 overlap with, but are not identical to, those of Bcl-2. J Cell Biol 128, 1173-1184.

Youle, R.J., and Strasser, A. (2008). The BCL-2 protein family: opposing activities that mediate cell death. Nat Rev Mol Cell Biol 9, 47-59.

Yuneva, M., Zamboni, N., Oefner, P., Sachidanandam, R., and Lazebnik, Y. (2007). Deficiency in glutamine but not glucose induces MYC-dependent apoptosis in human cells. J Cell Biol 178, 93-105.

Zhong, Q., Gao, W., Du, F., and Wang, X. (2005). Mule/ARF-BP1, a BH3-only E3 ubiquitin ligase, catalyzes the polyubiquitination of Mcl-1 and regulates apoptosis. Cell 121, 1085-1095.

Zhou, P., Levy, N.B., Xie, H., Qian, L., Lee, C.Y., Gascoyne, R.D., and Craig, R.W. (2001). MCL1 transgenic mice exhibit a high incidence of B-cell lymphoma manifested as a spectrum of histologic subtypes. Blood 97, 3902-3909.

Zhou, P., Qian, L., Kozopas, K.M., and Craig, R.W. (1997). Mcl-1, a Bcl-2 family member, delays the death of hematopoietic cells under a variety of apoptosis-inducing conditions. Blood 89, 630-643.

Zhuang, L., Lee, C.S., Scolyer, R.A., McCarthy, S.W., Zhang, X.D., Thompson, J.F., and Hersey, P. (2007). Mcl-1, Bcl-XL and Stat3 expression are associated with progression of melanoma whereas Bcl-2, AP-2 and MITF levels decrease during progression of melanoma. Mod Pathol 20, 416-426.

Zindy, F., Eischen, C.M., Randle, D.H., Kamijo, T., Cleveland, J.L., Sherr, C.J., and Roussel, M.F. (1998). Myc signaling via the ARF tumor suppressor regulates p53-dependent apoptosis and immortalization. Genes Dev 12, 2424-2433.

VITA

Rhonda Perciavalle was born in San Diego, CA in 1978. In June of 2003, she completed a Bachelor of Science degree in biochemistry/chemistry from the University of California, San Diego. She enrolled in the Ph.D program at the University of Tennessee Health Science Center in 2006 and joined the Opferman lab at St. Jude Children's Research Hospital in 2007. On May 5, 2012 she married Daniel Patrick. She is expected to graduate in June 2012.

Publications

1. Perciavalle, RM., Stewart, DP., Koss, B., Lynch, J., Milasta, S., Bathina, M., Temirov, J., Cleland, MM., Pelletier, S., Schuetz, D., Youle, R., Green, DR., and Opferman, JT. Anti-Apoptotic MCL-1 Localizes to the Mitochondrial Matrix and Couples Mitochondrial Fusion to Respiration. Nature Cell Biology 2012; Jun:14(6) 575-583.

2. Stewart, DP, Koss, B., Bathina, M., Perciavalle, RM., Bisanz, K., and Opferman, JT. Ubiquitin Independent Degradation of Anti-apoptotic MCL-1. Molceular Cell Biology 2010; Jun: 30(12): 3099-110.

3. Cohen, E., Bieschke J., Perciavalle, RM., Kelly, JW., Dillin, A. Opposing Activities Protect Againt Age Onset Proteotoxicity. Science 2006; 313: 1604-1610.

4. Perciavalle, RM., Opferman, JT. Delving Deeper: MCL-1's Contributions to Normal and Disease Biology. Trends in Cell Biology Reviews (In Press).

5. Koss, B., Morrison, J., Perciavalle, RM., Singh, H., Williams, RT., Opferman, JT. Requirement for Anti-Apoptotic MCL-1 in the Survival of BCR-ABL B-Lineage Acute Lymphoblastic Leukemia (In Submission).